5 Hydrostatics

The simplest state of a fluid is the state of rest. The macroscopically observable velocity vanishes and the forces developing in the fluid are described in terms of the pressure field established in response to a body force. The subject of hydrostatics encompasses two main topics: the computation of forces exerted on immersed surfaces and submerged bodies, and the study of the shapes of interfaces separating stationary, translating, or rotating fluids. Although the problem statement and mathematical formulation is straightforward in both cases, deriving solutions for all but the simplest configurations requires the use of numerical methods for solving algebraic, ordinary, and partial differential equations.

5.1 Equilibrium of pressure and body forces

Consider a parcel of a stationary fluid, as illustrated in Figure 5.1.1(a). Newton's second law of motion requires that, in the absence of macroscopically observable flow, the forces exerted on the parcel should balance to zero. In Chapter 4, we saw that two kinds of forces are exerted on a parcel: a body force due to the gravitational or another force field mediated by long-range molecular interactions, and a surface force associated with the hydrodynamic traction.

Body force

The body force due to gravity can be expressed as an integral over the volume of the parcel

C. Pozrikidis, *Fluid Dynamics*, DOI 10.1007/978-1-4899-7991-9_5

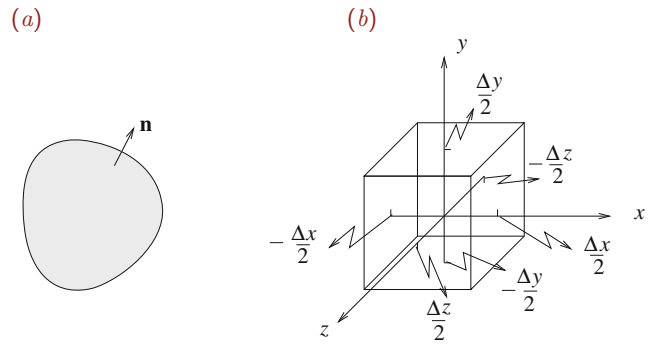

Figure 5.1.1 (a) Illustration of a parcel of a stationary fluid showing the outward unit normal vector, $\mathbf{n}$. (b) A parcel with a rectangular parallelepiped shape serves as a control volume for deriving the differential equations governing the pressure distribution in hydrostatics.

involving the possibly position-dependent fluid density, ρ, in the form

$$\mathbf{F}^{\text{body}} = \iiint_{\text{parcel}} \rho\,\mathbf{g}\,\mathrm{d}V, \tag{5.1.1}$$

where $\mathbf{g} = (g_x, g_y, g_z)$ is the acceleration of gravity vector. On the surface of the earth, the magnitude of $\mathbf{g}$ takes the approximate value $|\mathbf{g}| \equiv g = 9.80665$ m/sec^2.

Surface force

The surface force can be expressed in terms of the traction exerted on the parcel surface, $\mathbf{f}$, in the corresponding form

$$\mathbf{F}^{\text{surface}} = \iint_{\text{parcel}} \mathbf{f}\,\mathrm{d}S. \tag{5.1.2}$$

In the absence of fluid motion, the traction is due to the pressure, p, alone pushing the parcel surface toward the interior. If $\mathbf{n}$ is the unit vector normal to the parcel surface pointing outward, as illustrated in Figure 5.1.1(a), then

$$\mathbf{f} = -p\,\mathbf{n}. \tag{5.1.3}$$

The minus sign on the right-hand side accounts for the opposite orientations of the normal vector and traction due to the pressure.

Substituting (5.1.3) into (5.1.2), we derive an expression for the surface force in terms of the pressure,

$$\mathbf{F}^{\text{surface}} = -\iint_{\text{parcel}} p\,\mathbf{n}\,\mathrm{d}S. \tag{5.1.4}$$

The integral on the right-hand side can be evaluated by analytical or numerical methods.

Force equilibrium

Setting the sum of the body force given in (5.1.1) and the surface force given in (5.1.4) to zero, we obtain a vectorial equilibrium condition,

$$\iiint_{\text{parcel}} \rho\,\mathbf{g}\,\mathrm{d}V - \iint_{\text{parcel}} p\,\mathbf{n}\,\mathrm{d}S = \mathbf{0}. \tag{5.1.5}$$

The three scalar components of this equation are

$$\iiint_{\text{parcel}} \rho\,g_x\,\mathrm{d}V = \iint_{\text{parcel}} p\,n_x\,\mathrm{d}S, \qquad \iiint_{\text{parcel}} \rho\,g_y\,\mathrm{d}V = \iint_{\text{parcel}} p\,n_y\,\mathrm{d}S,$$
$$\iiint_{\text{parcel}} \rho\,g_z\,\mathrm{d}V = \iint_{\text{parcel}} p\,n_z\,\mathrm{d}S, \tag{5.1.6}$$

where the unit normal vector, $\mathbf{n} = (n_x, n_y, n_z)$, points outward from the parcel, as shown in Figure 5.1.1(a).

5.1.1 Equilibrium of an infinitesimal parcel

Next, we consider a small fluid parcel in the shape of a rectangular parallelepiped centered at the origin with six flat sides perpendicular to the x, y, or z axis and edges with length Δx, Δy, and Δz, as illustrated in Figure 5.1.1(b). Because the size of the parcel is small, density variations over the parcel volume can be neglected and the volume integrals on the left-hand side of equations (5.1.6) can be approximated with the products

$$\rho_0\,g_x\,\Delta V, \qquad \rho_0\,g_y\,\Delta V, \qquad \rho_0\,g_z\,\Delta V, \tag{5.1.7}$$

where ρ_0 is the density of the fluid at the center of the parcel located at the origin, and $\Delta V = \Delta x\,\Delta y\,\Delta z$ is the parcel volume.

Now we consider the surface integral on the left-hand side of the first equation in (5.1.6). The x component of the normal vector vanishes on all sides, except on the two sides that are perpendicular to the x axis, located at $x = \frac{1}{2}\Delta x$, and $x = -\frac{1}{2}\Delta x$, designated as the first and second side. On the first side $n_x = 1$, and on the second side $n_x = -1$. Because the parcel size is small, variations in pressure over each side can be neglected and the pressure over a side can be approximated with the value at the side center.

Subject to this approximation, the surface integral on the right-hand side of the first equation in (5.1.6) over the first or second side is, respectively,

$$p\big(x = \tfrac{1}{2}\Delta x, y = 0, z = 0\big)\,\Delta y\,\Delta z, \qquad -p\big(x = -\tfrac{1}{2}\Delta x, y = 0, z = 0\big)\,\Delta y\,\Delta z, \tag{5.1.8}$$

where the parentheses enclose the arguments of the pressure. Adding these two contributions, we obtain the net pressure force

$$F_x \equiv \Delta p_x\,\Delta y\,\Delta z, \tag{5.1.9}$$

where

$$\Delta p_x \equiv p\big(x = \tfrac{1}{2}\Delta x, y = 0, z = 0\big) - p\big(x = -\tfrac{1}{2}\Delta x, y = 0, z = 0\big). \tag{5.1.10}$$

In the limit as Δx tends to zero, the ratio of the differences in the pressure and corresponding x positions,

$$\frac{\Delta p_x}{\frac{1}{2}\Delta x - (-\frac{1}{2}\Delta x)} = \frac{\Delta p_x}{\Delta x}, \tag{5.1.11}$$

tends to the partial derivative $\partial p/\partial x$ evaluated at the origin. The expression for the net pressure force then becomes

$$F_x = \Big(\frac{\partial p}{\partial x}\Big)_{\mathbf{0}} \Delta x\, \Delta y\, \Delta z = \Big(\frac{\partial p}{\partial x}\Big)_{\mathbf{0}} \Delta V, \tag{5.1.12}$$

where the partial derivative is evaluated at the origin.

Equations of hydrostatics

Substituting (5.1.12) along with the first approximate form in (5.1.7) into the x component of the force balance (5.1.6), and simplifying by eliminating ΔV on both sides, we obtain the differential equation

$$\rho\, g_x = \frac{\partial p}{\partial x}, \tag{5.1.13}$$

where the density, ρ, and the partial derivative of the pressure are evaluated at the origin. However, since the location of the origin is arbitrary, equation (5.1.13) can be applied at every point in the fluid.

Working in a similar fashion with the second and third hydrostatic equilibrium equations in (5.1.6), we obtain the corresponding differential equations

$$\rho\, g_y = \frac{\partial p}{\partial y}, \qquad \rho\, g_z = \frac{\partial p}{\partial z}. \tag{5.1.14}$$

The three scalar equations (5.1.13) and (5.1.14) can be collected into a compact vector form,

$$\rho\, \mathbf{g} = \boldsymbol{\nabla} p, \tag{5.1.15}$$

where

$$\boldsymbol{\nabla} p = \Big(\frac{\partial p}{\partial x}, \quad \frac{\partial p}{\partial y}, \quad \frac{\partial p}{\partial z} \Big) \tag{5.1.16}$$

is the pressure gradient. In physical terms, the differential equation (5.1.15) expresses a balance between the gravitational and the pressure force in hydrostatics, that is, in the absence of fluid motion.

Derivation by the Gauss divergence theorem

The differential equilibrium equation (5.1.4) can be derived directly from the force balance (5.1.5) by applying the Gauss divergence theorem stated in equation (2.6.36),

$$\iint_{\mathcal{S}} \mathbf{h} \cdot \mathbf{n} \, \mathrm{d}S = \iiint_{\mathcal{V}} \boldsymbol{\nabla} \cdot \mathbf{h} \, \mathrm{d}V. \tag{5.1.17}$$

Selecting

$$h_x = \phi, \qquad h_y = 0, \qquad h_z = 0 \tag{5.1.18}$$

to formulate the vector function $\mathbf{h} = (\phi, 0, 0)$, we obtain

$$\iint_{\mathcal{S}} \phi \, n_x \, \mathrm{d}S = \iiint_{\mathcal{V}} \frac{\partial \phi}{\partial x} \, \mathrm{d}V, \tag{5.1.19}$$

where ϕ is an arbitrary scalar function of position. The complementary choices $\mathbf{h} = (0, \phi, 0)$ and $\mathbf{h} = (0, 0, \phi)$ yield the corresponding identities

$$\iint_{\mathcal{S}} \phi \, n_y \, \mathrm{d}S = \iiint_{\mathcal{V}} \frac{\partial f}{\partial y} \, \mathrm{d}V, \qquad \iint_{\mathcal{S}} \phi \, n_z \, \mathrm{d}S = \iiint_{\mathcal{V}} \frac{\partial f}{\partial z} \, \mathrm{d}V. \tag{5.1.20}$$

Relations (5.1.19) and (5.1.20) can be collected into a vector identity,

$$\iint_{\mathcal{S}} \phi \, \mathbf{n} \, \mathrm{d}S = \iiint_{\mathcal{V}} \boldsymbol{\nabla} \phi \, \mathrm{d}V, \tag{5.1.21}$$

where

$$\boldsymbol{\nabla} \phi = \left(\frac{\partial \phi}{\partial x}, \frac{\partial \phi}{\partial y}, \frac{\partial \phi}{\partial z} \right) \tag{5.1.22}$$

is the gradient of ϕ.

Applying (5.1.21) to the second integral on the left-hand side of (5.1.5) expressing the surface force due to the pressure, we obtain

$$\iiint_{\text{parcel}} \rho \mathbf{g} \, \mathrm{d}V - \iiint_{\text{parcel}} \boldsymbol{\nabla} p \, \mathrm{d}V = \mathbf{0}. \tag{5.1.23}$$

The differential equation (5.1.15) follows from the realization that the volume is arbitrary.

Gases and liquids

Equation (5.1.15) provides us with a basis for computing the distributions of pressure and density in a fluid, subject an additional stipulation concerning the physical properties of the fluid required by thermodynamics. Specifically, given the density field, or a relation between the density and the pressure, equation (5.1.15) allows us to compute the associated pressure and *vice versa*. To this end, we make a distinction between compressible gases and incompressible liquids.

5.1.2 Gases in hydrostatics

The density of a gas, ρ, is related to the pressure, p, and temperature, T, by an equation of state provided by thermodynamics. For an ideal gas,

$$\rho = \frac{M}{RT}\, p, \tag{5.1.24}$$

where M is the molecular mass and R is the ideal-gas constant, as discussed in Section 4.4. Substituting (5.1.24) into (5.1.15) and rearranging, we obtain a vectorial equation involving the pressure and temperature,

$$\frac{M}{RT}\,\mathbf{g} = \frac{1}{p}\,\boldsymbol{\nabla} p. \tag{5.1.25}$$

The x component of this equation reads

$$\frac{M}{RT}\, g_x = \frac{1}{p}\,\frac{\partial p}{\partial x} = \frac{\partial}{\partial x}\big(\ln \frac{p}{\pi_0}\big), \tag{5.1.26}$$

where π_0 is an unspecified reference pressure.

When the temperature of the fluid is uniform, we may integrate (5.1.26) with respect to x to obtain

$$\ln \frac{p}{\pi_0} = \frac{M}{RT}\, g_x\, x + f_x(y,z), \tag{5.1.27}$$

where $f_x(y,z)$ is an unknown function. Working in a similar fashion with the y and z components of (5.1.25) under the assumption of uniform temperature, we obtain

$$\ln \frac{p}{\pi_0} = \frac{M}{RT}\, g_y\, y + f_y(x,z), \qquad \ln \frac{p}{\pi_0} = \frac{M}{RT}\, g_z\, z + f_z(x,y), \tag{5.1.28}$$

where $f_y(z,x)$ and $f_z(x,y)$ are two unknown functions. Combining the last three equations, we obtain the pressure distribution

$$\ln \frac{p}{\pi_0} = \frac{M}{RT}\,(\, g_x\, x + g_y\, y + g_z\, z\,). \tag{5.1.29}$$

The reference pressure π_0 is determined by requiring an appropriate boundary condition.

Expressing the term in the parentheses on the right-hand side of (5.1.29) in terms of the inner product of the gravity vector, $\mathbf{g}$, and the position vector, $\mathbf{x}$, and transferring the last term to the left-hand side, we obtain the compact form

$$\ln \frac{p}{\pi_0} = \frac{M}{RT}\,\mathbf{g}\cdot\mathbf{x}, \tag{5.1.30}$$

which describes the pressure distribution in an ideal gas with uniform temperature.

Pressure distribution in the atmosphere

As an application, we consider the pressure distribution in the atmosphere regarded as an ideal gas with molar mass $M = 28.97$ kg/kmole, at temperature 25°C corresponding to absolute temperature $T = 298$ K. In Cartesian coordinates with origin at sea level, where the y axis points upward and the x and z axes are horizontal, the components of the acceleration of gravity vector are

$$g_x = 0, \qquad g_y = -g, \qquad g_z = 0, \tag{5.1.31}$$

where $g = 9.80665$ m/s^2. Equation (5.1.30) simplifies to

$$\ln \frac{p}{p_{\text{sea}}} = -\frac{Mg}{RT}\, y, \tag{5.1.32}$$

where p_{sea} is the pressure at sea level. Solving for p, we derive an exponentially decaying field,

$$p = p_{\text{sea}} \exp\big(-\frac{Mg}{RT}\, y\big). \tag{5.1.33}$$

Taking

$$p_{\text{sea}} = 1.0\,\text{atm} = 1.0133 \times 10^5\ \text{Pascal} = 1.0133 \times 10^5 \text{kg m}^{-1}\,\text{sec}^{-2}, \tag{5.1.34}$$

we find that the pressure at the elevation of $y = 1$ km$= 1,000$ m is

$$p = 1.0\ \exp\big(-\frac{28.97 \times 9.80665}{8.314 \times 10^3\ \times 298}\, 1000\big)\,\text{atm} = 0.892\,\text{atm}. \tag{5.1.35}$$

The corresponding density distribution is found by substituting the pressure distribution (5.1.33) into the right-hand side of the equation of state (5.1.24).

5.1.3 Liquids in hydrostatics

Because liquids at low and moderate pressures are nearly incompressible, their density is a physical property determined primarily by the prevailing temperature. Working as in the case of gases but treating the density as a constant, we find that the pressure distribution is given by the counterpart of equation (5.1.30),

$$p = \rho\,(g_x\, x + g_y\, y + g_z\, z) + \pi_0 \tag{5.1.36}$$

or, more concisely,

$$p = \rho\, \mathbf{g} \cdot \mathbf{x} + \pi_0, \tag{5.1.37}$$

where π_0 is a constant with units of pressure determined by an appropriate boundary condition.

Pressure distribution in a pool

As an application, we consider the pressure distribution in a liquid pool with a horizontal surface. In Cartesian coordinates where the y axis is perpendicular to the pool surface pointing in the vertical direction upward and the x and z axes are horizontal, the components of the acceleration of gravity vector are

$$g_x = 0, \qquad g_y = -g, \qquad g_z = 0, \tag{5.1.38}$$

where g is the magnitude of the acceleration of gravity. The general equation (5.1.37) then simplifies to

$$p = -\rho g y + \pi_0. \tag{5.1.39}$$

Setting the origin of the y axis at the pool surface where the liquid pressure is equal to the atmospheric pressure, p_{atm}, we find that $\pi_0 = p_{\text{atm}}$.

Manometer

The pressure distribution given in (5.1.37) also applies when a contiguous liquid occupies a convoluted domain. In practice, this property is exploited for computing the pressure difference across the two ends of a tube in terms of the difference in the levels of a liquid column placed inside the tube. A simple device serving this purpose is the U-tube manometer illustrated in Figure 5.1.2.

The pressure distribution in the liquid inside the U-tube manometer is given by equation (5.1.39). Applying this equation at the two ends of the liquid, located at $y = y_1$ and y_2, and subtracting the resulting expressions, we find that

$$\Delta p \equiv p(y_1) - p(y_2) = \rho\, g\, (y_2 - y_1). \tag{5.1.40}$$

If the tube is exposed to the atmosphere at the first end, $p(y_1) = p_{\text{atm}}$, and thus

$$p(y_2) = p_{\text{atm}} + \rho g h, \tag{5.1.41}$$

where $h \equiv y_1 - y_2$ is the readily measurable rise of the liquid column in the manometer.

Problems

5.1.1 *Hydrostatic pressure distribution*

(*a*) Derive the pressure distribution in an incompressible liquid given in equation (5.1.37).

(*b*) Derive the pressure distribution in an ideal gas occupying the semi-infinite region $y > 0$ when the temperature decreases exponentially with distance as

$$T = T_0 - \Delta T\, (1 - \mathrm{e}^{-\alpha y}), \tag{5.1.42}$$

where T_0, ΔT, and α are three specified constants. The gravity vector points in the negative direction of the y axis.

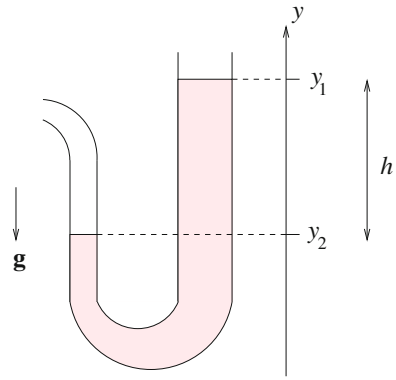

Figure 5.1.2 Illustration of a U-tube manometer. The pressure distribution in the fluid is described by the equations of hydrostatics even if the fluid has a convoluted shape, as long as it remains contiguous and uninterrupted.

5.1.2 *Function of an aircraft altimeter*

The temperature in the lower part of the troposphere extending 10 km above the surface of the earth decreases at a nearly linear rate as $T = T_0 - \alpha\, y$, where T_0 is the temperature at the surface of the earth positioned at $y = 0$, and α is the lapse rate. In North America, $\alpha = 6.5$ K/km.

(*a*) Assuming that the atmosphere behaves like an ideal gas, derive the atmospheric pressure distribution

$$p = \pi_0 \left(1 - \frac{\alpha}{T_0}\, y\right)^{\beta}, \tag{5.1.43}$$

and evaluate the dimensionless exponent $\beta \equiv Mg/(R\alpha)$, where π_0 is the pressure at sea level.

Solving (5.1.43) for the elevation y, we find that

$$y = \frac{T_0}{\alpha}\left(1 - \left(\frac{p}{\pi_0}\right)^{1/\beta}\right). \tag{5.1.44}$$

This equation is used for calibrating an aircraft altimeter, that is, for converting pressure measured with a barometer into altitude.

(*b*) Show that, as α tends to zero, in which case the temperature distribution tends to become constant, the pressure distribution (5.1.43) reduces to that shown in (5.1.33).

5.1.3 *How many molecules inside a certain volume of gas?*

How many molecules are there inside one cubic centimeter (1 milliliter) of a gas under atmospheric pressure and temperature 25°C?

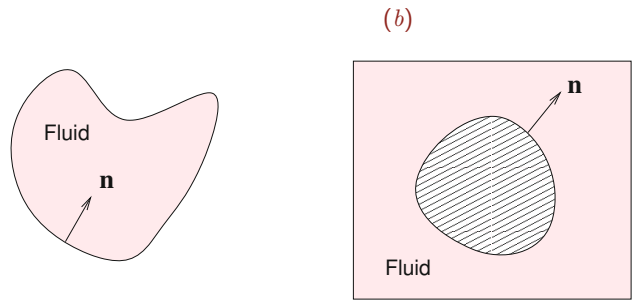

Figure 5.2.1 Illustration of a surface that (a) contains or (b) is immersed in a stationary fluid.

5.2 Force exerted on an immersed surface

To compute the hydrostatic surface force exerted on a surface that contains or is immersed in a stationary fluid, as illustrated in Figure 5.2.1, we repeat the arguments the led us to equation (5.1.4) and obtain

$$\mathbf{F}^{\text{surface}} = -\iint p\,\mathbf{n}\,\mathrm{d}S, \tag{5.2.1}$$

where $\mathbf{n}$ is the unit vector normal to the surface pointing into the fluid and the integration is performed over the surface.

To evaluate the integral on the right-hand side of (5.2.1), we must first determine the pressure distribution in the fluid, as discussed in Section 5.1, and then evaluate the integral by analytical or numerical methods.

5.2.1 *A sphere floating on a flat interface*

As an application, we consider the force exerted on a sphere floating on the flat surface of a liquid pool underneath a zero-density gas, as depicted in Figure 5.2.2. In spherical polar coordinates with origin at the center of the sphere and the x axis pointing upward, the circular contact line where the surface of the liquid meets the sphere is located at the meridional angle $\theta = \beta$.

Symmetry requires that the horizontal component of the surface force exerted on the sphere must vanish. The vertical component of the surface force is given by

$$F_x^{\text{surface}} = -\iint p\,n_x\,\mathrm{d}S, \tag{5.2.2}$$

where $n_x = \cos\theta$ is the x component of the unit normal vector. The pressure distribution is described by equation (5.1.37) with gravitational acceleration components

$$g_x = -g, \qquad g_y = 0, \qquad g_z = 0, \tag{5.2.3}$$

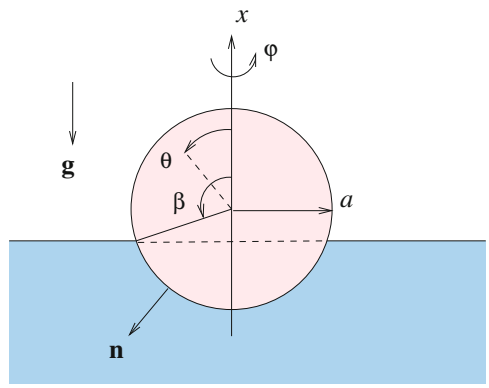

Figure 5.2.2 Illustration of a sphere floating in the flat surface of a liquid at floating angle β. The dashed line represents the horizontal circular contact line.

yielding

$$p = -\rho\, g\, x + \pi_0. \tag{5.2.4}$$

To compute the reference pressure π_0, we require that the pressure at the contact line is equal to the atmospheric pressure, $p = p_{\text{atm}}$ at $x = a\cos\beta$, and find that $p_{\text{atm}} = -\rho g\, a\cos\beta + \pi_0$, which can be rearranged to give

$$\pi_0 = \rho\, g\, a\cos\beta + p_{\text{atm}}, \tag{5.2.5}$$

where a is the sphere radius. Writing $x = a\cos\theta$, we find that the pressure distribution over the sphere is given by

$$p = -\rho\, g\, a\,(\cos\theta - \cos\beta) + p_{\text{atm}}. \tag{5.2.6}$$

Now substituting the pressure distribution (5.2.6) into the integral on the right-hand side of (5.2.2), we find that the force exerted on the sphere by the liquid is given by

$$F_x^{\text{surface}} = \iint \big(\,\rho\, g\, a\,(\cos\theta - \cos\beta) - p_{\text{atm}}\,\big)\cos\theta\,\mathrm{d}S. \tag{5.2.7}$$

The differential surface area of the sphere can be expressed in the form

$$\mathrm{d}S = (\sigma \mathrm{d}\varphi)(a\mathrm{d}\theta), \tag{5.2.8}$$

where $\sigma = a\sin\theta$ is the distance of a point on the surface of the sphere from the x axis and φ is the azimuthal angle. Substituting this expression into the right-hand side of (5.2.7) and integrating with respect to φ, we obtain

$$F_x^{\text{surface}} = 2\pi a^2 \int_\beta^\pi \big(\,\rho\, g\, a\,(\cos\theta - \cos\beta) - p_{\text{atm}}\,\big)\cos\theta\sin\theta\,\mathrm{d}\theta. \tag{5.2.9}$$

Next, we set $\sin\theta\,\mathrm{d}\theta = -\mathrm{d}\cos\theta$ and carry out the integration on the right-hand side with respect to $\cos\theta$ to find that

$$F_x^{\text{surface}} = \pi a^2 \big[\, \rho\, g\, a\, \tfrac{1}{3}\,(2 + 3\cos\beta - \cos^3\beta) + p_{\text{atm}}\,(1 - \cos^2\beta)\,\big]. \tag{5.2.10}$$

Working in a similar fashion, we find that the x component of the force due to the atmospheric pressure exerted on the non-immersed portion of the sphere subtended between the meridional angles $\theta = 0$ and β is given by

$$F_x^{\text{atm}} = -2\pi a^2 \int_0^{\beta} p_{\text{atm}} \cos\theta\, \sin\theta\, \mathrm{d}\theta = -\pi a^2\, p_{\text{atm}} (1 - \cos^2\beta). \tag{5.2.11}$$

Adding the two contributions expressed by (5.2.10) and (5.2.11), we obtain the buoyancy force exerted on the sphere,

$$F_x^{\text{buoyancy}} \equiv F_x^{\text{surface}} + F_x^{\text{atm}} = \rho g \left(\pi\, \tfrac{1}{3}\,(2 + 3\cos\beta - \cos^3\beta)\, a^3 \right). \tag{5.2.12}$$

It can be shown using elementary trigonometry that the term enclosed by the large parentheses on the right-hand side of (5.2.12) is equal to the immersed volume of the sphere underneath the flat surface of the liquid, which is equal to the volume of fluid displaced by the sphere, $V_{\text{displaced}}$. For example, if the sphere is completely immersed, $\beta = 0$, the term enclosed by the short parentheses on the right-hand side of (5.2.12) is equal to 4, and the term enclosed by the large parentheses is equal to the volume of the sphere, $V_{\text{sphere}} = \frac{4\pi}{3} a^3$.

Equation (5.2.12) states that the hydrostatic force exerted on a floating sphere is equal in magnitude and opposite in direction to the weight of the fluid displaced by the sphere. In Section 5.3, we will see that this is a more general result applicable to an arbitrarily shaped floating or immersed object.

Computation of the floating angle

The floating angle, β, is determined by the weight of the sphere: the heavier the sphere, the smaller the angle; the lighter the sphere, the larger the angle. There is a critical weight where β becomes equal to zero and the sphere is completely submerged.

To compute the floating angle corresponding to a certain weight, W, we set W equal to the buoyancy force given in (5.2.12) and rearrange to obtain a cubic equation for $\cos\beta$,

$$\cos^3\beta - 3\cos\beta + 2\,(2s - 1) = 0, \tag{5.2.13}$$

where

$$s \equiv \frac{W}{\rho g V_{\text{sphere}}} \tag{5.2.14}$$

is a dimensionless parameter and $V_{\text{sphere}} = \frac{4\pi}{3} a^3$ is the volume of the sphere. If the sphere is made of a homogeneous material with density ρ_s, then $s = \rho_s/\rho$ is the density ratio. A neutrally buoyant sphere corresponds to $s = 1$, in which case $\cos\beta = 1$ and $\beta = 0$ satisfy equation (5.2.13), as expected. When $s = \frac{1}{2}$, the floating angle is $\frac{1}{2}\pi$.

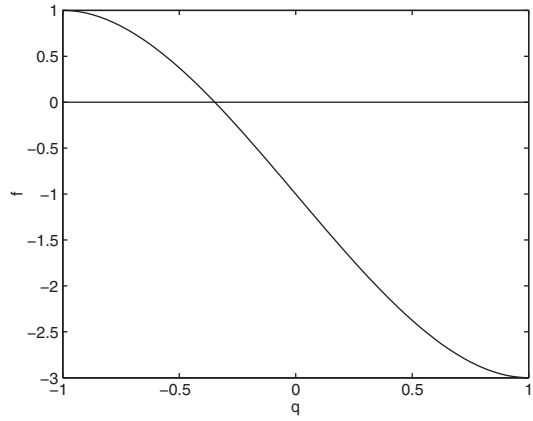

Figure 5.2.3 Graph of the function $f(q)$ defined in equation (5.2.16) whose root, Q, is desired, for $s = \frac{1}{4}$. To compute the root using Newton's method, we make an initial guess, $q^{(0)}$, and then improve the guess by moving along the tangential vector to the graph toward the q axis.

5.2.2 *Newton's method*

A variety of numerical methods are available for solving the nonlinear algebraic equation (5.2.13) for β, given s. Newton's method, also known as the Newton–Raphson method, strikes an optimal balance between conceptual simplicity and numerical efficiency. To formalize the method, we introduce the variable $q \equiv \cos\beta$, and express equation (5.2.13) in the generic form

$$f(q) = 0, \tag{5.2.15}$$

where

$$f(q) \equiv q^3 - 3\,q + 2\,(2s - 1) \tag{5.2.16}$$

is the function of interest. A graph of the function $f(q)$ for $s = 0.25$ is shown in Figure 5.2.3. The requisite value of q, denoted by Q, is located at the intersection of the graph of $f(q)$ and the q axis, satisfying $f(Q) = 0$.

To implement Newton's method, we make an initial guess for the desired root Q, denoted by $q^{(0)}$, and then generate a sequence of improvements working as follows. Near the point $q^{(0)}$, the function $f(q)$ can be approximated with a linear function that arises by expanding $f(q)$ in a Taylor series about $q^{(0)}$. Discarding all nonlinear terms, we obtain the approximate form

$$f(q) \simeq f(q^{(0)}) + \left(\frac{\mathrm{d}f}{\mathrm{d}q}\right)_{q=q^{(0)}} (q - q^{(0)}). \tag{5.2.17}$$

Setting $f(q) = 0$, solving for the q inside the parentheses on the right-hand side of (5.2.17), and denoting the solution as $q^{(1)}$, we obtain the improved value

$$q^{(1)} = q^{(0)} - \left(\frac{f}{f'}\right)_{q=q^{(0)}}, \tag{5.2.18}$$

where a prime denotes a derivative with respect to q. The process is then repeated to yield a sequence of successive approximations based on the recursive formula

$$q^{(k+1)} = q^{(k)} - \left(\frac{f}{f'}\right)_{q=q^{(k)}} \tag{5.2.19}$$

for $k = 0, 1, \ldots$. Erroneously omitting the minus sign on the right-hand side of (5.2.19) is a common source of frustration. The iterations terminate when the correction falls below a specified tolerance.

In the case of a floating sphere presently considered,

$$f' = 3\,q^2 - 3 \tag{5.2.20}$$

and Newton's formula takes the form

$$q \leftarrow q - \frac{q^3 - 3\,q + 2\,(2s-1)}{3\,q^2 - 3} = \frac{2}{3}\,\frac{q^3 - (2s-1)}{q^2 - 1}, \tag{5.2.21}$$

where the arrow stands for *replace*. The method is implemented in the following MATLAB function

```
function q = floating_sphere(s,q)

tolerance = 0.000001;
itermax = 10;
cf = 2.0*s-1.0;

error = tolerance + 1.0;
iter = 0;   % iteration counter

while (error>tolerance & iter<itermax)
  iter = iter+1;
  qsave = q;
  q2 = q*q; q3 = q2*q;
  q = 2/3 * (q3-cf)/(q2-1);
  error = abs(q-qsave)
end

return
```

The input field includes the parameter s and the initial guess. For a given s, the solution satisfying $|q| \leq 1$ is accepted; we recall that $q = \cos\beta$.

Convergence

Analysis shows that the sequence defined by (5.2.19) converges to Q as long as the initial guess $q^{(0)}$ is sufficiently close to the root, Q . The rate of convergence depends on the multiplicity of the root.

If the graph of the function $f(q)$ is not horizontal at the root, $f'(q = Q) \neq 0$, the rate of convergence is quadratic, which means that

$$q^{(k+1)} - Q \simeq \delta\,(q^{(k)} - Q)^2, \tag{5.2.22}$$

where $\delta = f''(Q)/[2f'(Q)]$ is an *a priori* unknown coefficient. Equation (5.2.22) states that the magnitude of the error in the current iteration, expressed by the left-hand side, is roughly equal to the square of the magnitude of the error in the previous iteration multiplied by a constant. Consequently, if the initial error, $q^{(0)} - Q$, is sufficiently small, the magnitude of the error, $q^{(k)} - Q$, will keep decreasing during the iterations, no matter how large the value of the coefficient δ. A prerequisite is that the initial guess is close enough to the root so that (5.2.22) applies.

If the graph of the function $f(q)$ is horizontal at the root, $(\mathrm{d}f/\mathrm{d}q)_{q=Q} = 0$, the rate of convergence is linear, which means that

$$q^{(k+1)} - Q \simeq \frac{m-1}{m}\,(q^{(k)} - Q), \tag{5.2.23}$$

where m is the multiplicity of the root; for a double root, $m = 2$. Equation (5.2.23) states that the magnitude of the error at the current iteration, $q^{(k+1)} - Q$, is roughly equal to that in the previous iteration, $q^{(k)} - Q$, multiplied by the positive coefficient $(m-1)/m$, which is less than unity for any $m > 1$. Consequently, the error $|q^{(k)} - Q|$ will keep decreasing during the iterations as long as the initial guess is close enough to the root for (5.2.23) to apply.

Problems

5.2.1 *Pycnometer*

A pycnometer is an antiquated device used to measure the specific gravity of a liquid, defined as the ratio of the density of the liquid to the density of water. In practice, this is done by reading the level of the free surface on a scale printed on a vertical tube attached to a spherical flask floating on the liquid, as illustrated in Figure 5.2.4. Pycnometer derives from the Greek word $\pi\upsilon\kappa\nu\sigma\tau\eta\tau\alpha$, which means density. Derive an equation that allows us to calibrate a pycnometer based on the known density of water.

5.2.2 *A sphere straddling the interface between two fluids*

Derive the counterpart of expression (5.2.12) for a sphere straddling the interface between a lower fluid with density ρ_2 and an upper fluid with density ρ_1.

5.2.3 *A floating cylinder*

(a) Show that the buoyancy force exerted on a floating cylinder of radius a is given by

$$F_x^{\text{buoyancy}} = \rho g a^2 \left(\pi - \beta + \tfrac{1}{2}\,\sin 2\beta\right), \tag{5.2.24}$$

where β is the floating angle defined in Figure 5.2.2.

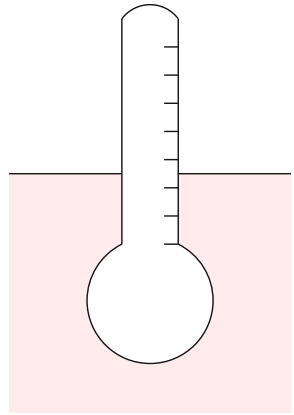

Figure 5.2.4 A pycnometer is used to measure the specific gravity of a liquid defined as the ratio between the density of the liquid to the density of water.

(*b*) Show that the floating angle of a solid cylinder satisfies the equation

$$\sin(2\beta) - 2\beta + 2\pi(1 - s) = 0, \tag{5.2.25}$$

where $s \equiv \rho_{\mathrm{B}}/\rho$ is the ratio of the density of the cylinder, ρ_{B}, to the density of the liquid, ρ.

5.2.4 *Floating sphere*

(*a*) Directory *04_nl_eq*, located inside directory *01_num_meth* of FDLIB, includes a program entitled *newton1_2* that implements Newton's method for solving one nonlinear equation. Use the program to solve equation (5.2.13) and prepare a plot the floating angle, β, against the dimensionless parameter s defined in equation (5.2.14). Discuss the convergence of the iterations in light of equations (5.2.22) and (5.2.23).

(*b*) Directory *04_nl_eq*, located inside directory *01_num_meth* of FDLIB, includes a program entitled *cubic* that computes the three roots of a cubic equation using Cardano's formula. Use the program to solve equation (5.2.13). Prepare a plot of the floating angle, β, against the dimensionless parameter, s.

5.3 Archimedes' principle

Consider the force exerted on a body with arbitrary shape immersed in a stationary fluid. Using equation (5.2.1), we find that the surface force exerted on the body is given by

$$\mathbf{F}^{\mathrm{surface}} = -\iint_{\mathrm{body}} p\,\mathbf{n}\,\mathrm{d}S, \tag{5.3.1}$$

where $\mathbf{n}$ is the unit vector normal to the body pointing into the fluid. It would appear that the computation of the integral on the right-hand side of (5.3.1) requires detailed knowledge of the shape of the body. In fact, if the fluid is incompressible, the integral can be evaluated

in a generic fashion, yielding a remarkably simple expression for the force in terms of the body volume alone.

Substituting the pressure distribution for an incompressible fluid given in (5.1.37) into the right-hand side of (5.3.1), we find that

$$\mathbf{F}^{\text{surface}} = -\iint_{\text{body}} \big(\,\rho\,(g_x x + g_y y + g_z z) + \pi_0\,\big)\,\mathbf{n}\,\mathrm{d}S. \tag{5.3.2}$$

A key observation in evaluating the surface integral is that the integrand is the product of the unit normal vector, $\mathbf{n}$, and a scalar function that is *linear* with respect to the components of the position vector, $\mathbf{x} = (x, y, z)$.

Rectangular body

To see how the evaluation of the integral can be simplified, we consider a body having the shape of a rectangular parallelepiped. The six flat sides of the body are perpendicular to the x, y, or z axis, the lengths of the edges are equal to Δx, Δy, and Δz, and the volume of the body is equal to $V_{\text{B}} = \Delta x\,\Delta y\,\Delta z$. The unit normal vector is constant over each of the six sides. For example, over the side that is perpendicular to the x axis and faces the positive direction of the x axis, $\mathbf{n} = (1, 0, 0)$. Taking into consideration this and similar simplifications, we evaluate the integral on the right-hand side of (5.3.2) without approximation, finding that

$$\mathbf{F}^{\text{surface}} = -\rho\, V_{\text{B}}\, \mathbf{g}, \tag{5.3.3}$$

which expresses Archimedes' principle, stating that *the force exerted on an immersed body by the ambient fluid is equal in magnitude and opposite in direction to the weight of the fluid displaced by the body.*

Arbitrary body

To compute the integral on the right-hand side of (5.3.2) over an arbitrarily shaped body, we may subdivide the volume of the body into small rectangular parallelepipeds and approximate the surface of the body with the collection of the faces of the parallelepipeds that are in contact with the fluid. Because of cancellations, the sum of the integrals over the faces of all elementary parallelepipeds is equal to the sum of the integrals of the faces that are wetted by the fluid. Summing all contributions, we find that the force exerted on the body is given by (5.3.3) independent of the body shape. We have found that Archimedes's principles stands true for arbitrarily shaped bodies. To confirm this intuitive result, we employ the Gauss divergence theorem.

Gauss divergence theorem

An identity stemming from the Gauss divergence theorem in three dimensions was stated in equation (5.1.21),

$$\iint_{\mathcal{S}} \phi\,\mathbf{n}\,\mathrm{d}S = \iiint_{\mathcal{V}} \boldsymbol{\nabla}\phi\,\mathrm{d}V. \tag{5.3.4}$$

Comparing (5.1.21) with (5.3.2), we set

$$\phi = \rho\,(g_x\,x + g_y\,y + g_z\,z) + \pi_0, \tag{5.3.5}$$

compute the gradient

$$\boldsymbol{\nabla}\phi = \rho\,(\,g_x,\ g_y,\ g_z\,) = \rho\,\mathbf{g}, \tag{5.3.6}$$

and find that the surface force is given by

$$\mathbf{F}^{\text{surface}} = -\iint_{\text{body}} \big[\,\rho\,(g_x\,x + g_y\,y + g_z\,z) + \pi_0\,\big]\,\mathbf{n}\,\mathrm{d}S = -\rho\,\mathbf{g}\iiint_{\text{body}} \mathrm{d}V = -\rho V_{\text{B}}\,\mathbf{g}, \tag{5.3.7}$$

which reproduces precisely equation (5.3.3).

5.3.1 Net force on a submerged body

The mass of a body with volume V_{B} made of a homogeneous material with density ρ_{B} is $m_B = \rho_{\text{B}}\,V_{\text{B}}$, and the weight of the body is

$$\mathbf{W} = \rho_{\text{B}}\,V_{\text{B}}\,\mathbf{g}, \tag{5.3.8}$$

where $\mathbf{g}$ is the gravitational acceleration. Adding to the weight the buoyancy force given in (5.3.3), we find that the net force exerted on an immersed body is

$$\mathbf{F} = \mathbf{F}^{\text{surface}} + \mathbf{W} = (\rho_{\text{B}} - \rho)\,V_{\text{B}}\,\mathbf{g}. \tag{5.3.9}$$

Since the density of a neutrally buoyant body is equal to the density of the ambient fluid, the right-hand side of (5.3.9) vanishes, yielding a zero net force.

5.3.2 Moments

The moment of the surface force about a chosen point, $\mathbf{x}_0$, is found by integrating the moment of the traction expressed in terms of the pressure,

$$\mathbf{M}^{\text{surface}} = \iint_{\text{body}} (\mathbf{x} - \mathbf{x}_0) \times (-p\,\mathbf{n})\,\mathrm{d}S, \tag{5.3.10}$$

where $\times$ denotes the outer vector product. Substituting the linear hydrostatic pressure distribution for an incompressible fluid, we obtain

$$\mathbf{M}^{\text{surface}} = -\rho \iint_{\text{body}} (\mathbf{g}\cdot\mathbf{x} + \pi_0)\,(\mathbf{x} - \mathbf{x}_0) \times \mathbf{n}\,\mathrm{d}S. \tag{5.3.11}$$

Unlike the force, the moment depends on the particular geometry of the body.

To evaluate the integral on the right-hand side of (5.3.11), we resort once again to the Gauss divergence theorem in three dimensions stated in equation (2.6.36) for an arbitrary vector field, $\mathbf{h}$,

$$\iint_{\mathcal{S}} \mathbf{h}\cdot\mathbf{n}\,\mathrm{d}S = \iiint_{\mathcal{V}} \boldsymbol{\nabla}\cdot\mathbf{h}\,\mathrm{d}V. \tag{5.3.12}$$

Setting $\mathbf{h} = \mathbf{a} \times \mathbf{w}$, where $\mathbf{a}$ is a constant vector and $\mathbf{w}$ is a differentiable function, and then discarding the arbitrary constant $\mathbf{a}$, we obtain the identity

$$\iint_{\mathcal{S}} \mathbf{n} \times \mathbf{w} \, \mathrm{d}S = \iiint_{\mathcal{V}} \boldsymbol{\nabla} \times \mathbf{w} \, \mathrm{d}V, \tag{5.3.13}$$

where $\boldsymbol{\nabla} \times \mathbf{w}$ is the curl of $\mathbf{w}$. Now setting

$$\mathbf{w} = (\mathbf{g} \cdot \mathbf{x} + \pi_0)(\mathbf{x} - \mathbf{x}_0), \tag{5.3.14}$$

we find that

$$\mathbf{M}^{\text{surface}} = \rho \iiint_{\text{body}} \boldsymbol{\nabla} \times \big((\mathbf{g} \cdot \mathbf{x} + \pi_0)(\mathbf{x} - \mathbf{x}_0) \big) \, \mathrm{d}V. \tag{5.3.15}$$

Using a vector identity, we obtain

$$\mathbf{M}^{\text{surface}} = \rho \iiint_{\text{body}} \big(\boldsymbol{\nabla}(\mathbf{g} \cdot \mathbf{x}) \times (\mathbf{x} - \mathbf{x}_0) + (\mathbf{g} \cdot \mathbf{x} + \pi_0) \, \boldsymbol{\nabla} \times \mathbf{x} \big) \, \mathrm{d}V. \tag{5.3.16}$$

Noting that $\boldsymbol{\nabla}(\mathbf{g} \cdot \mathbf{x}) = \mathbf{g}$ and $\boldsymbol{\nabla} \times \mathbf{x} = \mathbf{0}$, we obtain the final expression

$$\mathbf{M}^{\text{surface}} = \rho \, \mathbf{g} \times \iiint_{\text{body}} (\mathbf{x} - \mathbf{x}_0) \, \mathrm{d}V. \tag{5.3.17}$$

We observe that, if the point $\mathbf{x}_0$ is identified with the center of mass of a homogeneous fluid displaced by a body with volume V_{B}, given by

$$\mathbf{x}_c = \frac{1}{V_{\mathrm{B}}} \iiint_{\text{body}} \mathbf{x} \, \mathrm{d}V, \tag{5.3.18}$$

then the surface moment is zero.

The moment exerted on a homogeneous body due to gravity is given by

$$\mathbf{M}^{\text{gravity}} = -\mathbf{g} \times \iiint_{\text{body}} \rho_{\mathrm{B}} \, (\mathbf{x} - \mathbf{x}_0) \, \mathrm{d}V, \tag{5.3.19}$$

and the total moment exerted on the body is

$$\mathbf{M} = \mathbf{M}^{\text{surface}} + \mathbf{M}^{\text{gravity}} = \mathbf{g} \iiint_{\text{body}} (\rho - \rho_{\mathrm{B}}) \, (\mathbf{x} - \mathbf{x}_0) \, \mathrm{d}V, \tag{5.3.20}$$

which is zero if the point $\mathbf{x}_0$ is identified with the center of mass of a homogeneous fluid displaced by the body, or else if the density of the fluid matches the density of the body.

Equilibrium of an immersed body

The buoyancy force vector passes through the *center of mass of the fluid* displaced by the body, whereas the body weight vector passes through the *center of mass of the body.* If the

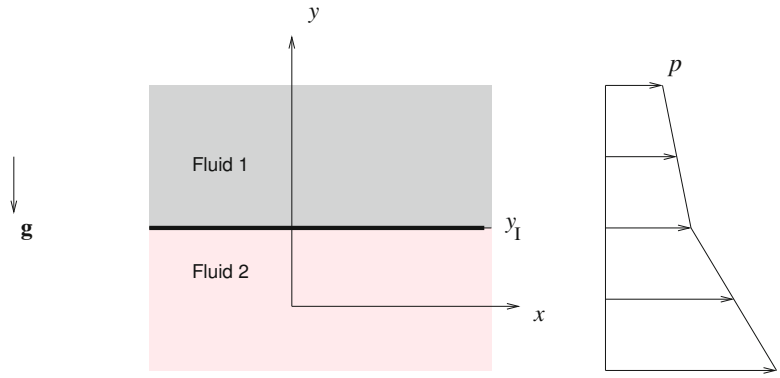

Figure 5.4.1 Illustration of an infinite horizontal interface located at $y = y_I$, separating two stationary fluids. The pressure distribution is shown on the right.

former lies above the latter, the body is in a state of stable equilibrium and will remain stationary. In the opposite case, the body will rotate spontaneously to reach a stable configuration.

Problem

5.3.1 *Applications of the Gauss divergence theorem*

(*a*) Apply (5.1.21) for a constant function f and discuss the results.

(*b*) Show that the center of gravity of a homogeneous body can be computed in terms of a surface integral as

$$\mathbf{x}_c = \frac{1}{2V_B} \iint_{\text{body}} (x^2 + y^2 + z^2)\, \mathbf{n}\, \mathrm{d}S. \tag{5.3.21}$$

5.4 Interfacial shapes

Consider two superposed stationary incompressible fluids separated by an infinite horizontal interface located at $y = y_I$, as illustrated in Figure 5.4.1. The acceleration of gravity points against the y axis. The upper fluid is labeled 1 and the lower fluid is labeled 2.

Using the general expression for the pressure distribution in an incompressible liquid, given in equation (5.1.37), and setting $g_x = 0$, $g_y = -g$, and $g_z = 0$, we find that the pressure distributions in the two fluids are given by

$$p^{(1)}(y) = -\rho_1 g y + \pi_1, \qquad p^{(2)}(y) = -\rho_2 g y + \pi_2. \tag{5.4.1}$$

The constants π_1 and π_2 are related by the condition for the jump in the traction across an interface with uniform surface tension stated in equation (4.5.16).

Since in this case the curvature of the interface vanishes, $\kappa = 0$, condition (4.5.16) requires that the pressure is continuous across the interface,

$$p^{(1)}(y = y_{\rm I}) = p^{(2)}(y = y_{\rm I}). \tag{5.4.2}$$

Substituting the pressure distributions given in (5.4.1) into (5.4.2), we obtain

$$-\rho_1\, g\, y_{\rm I} + \pi_1 = -\rho_2\, g\, y_{\rm I} + \pi_2, \tag{5.4.3}$$

which can be rearranged to give

$$\pi_2 = \pi_1 + (\rho_2 - \rho_1)\, g\, y_{\rm I}. \tag{5.4.4}$$

One of the two reference pressures, π_1 and π_2, is determined by requiring an appropriate boundary condition far from the interface, and the other follows from (5.4.4). For example, if the pressure on the upper side of the interface is equal to the atmospheric pressure $p_{\rm atm}$, then

$$\pi_1 = p_{\rm atm} + \rho_1\, g\, y_{\rm I}, \qquad \pi_2 = p_{\rm atm} + \rho_2\, g\, y_{\rm I}. \tag{5.4.5}$$

5.4.1 Curved interfaces

In practice, the flat interface depicted in Figure 5.4.1 terminates at a side wall, as illustrated in Figure 5.4.2. Additional examples of terminated interfaces are depicted in Figure 5.5.1, illustrating a semi-infinite interface ending at an inclined plate, in Figure 5.6.1, illustrating an interface confined between two parallel plates, and in Figure 5.7.1, illustrating the interface of a drop attached to a horizontal plane.

Contact line

The line where two fluids meet on a solid surface is called the contact line. In the case of a two-dimensional or axisymmetric interface, the contact line is represented by a contact point, which is the trace of the contact line in the xy or an azimuthal plane, marked by a circular symbol in Figures 5.5.1, 5.6.1, and 5.7.1.

Contact angle

The angle subtended between (a) the line that is normal to the contact line and tangential to the solid surface, and (b) the line that is normal to the contact line and tangential to the interface, measured by convention on the side of fluid labeled 2, as illustrated in Figure 5.4.2, is called the contact angle.

The static contact angle is a physical constant determined by the prevailing physical conditions and physical properties of the solid and fluids. If fluid 1 wets the solid better than fluid 2, then the contact angle is less than $\frac{1}{2}\pi$ but higher than the minimum possible value of 0. If fluid 2 wets the solid better than fluid 1, the contact angle is higher than $\frac{1}{2}\pi$ but less than the maximum possible value of π.

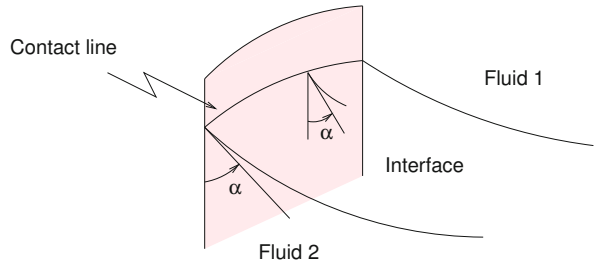

Figure 5.4.2 Illustration of an interface terminating at a contact line on a surface. By convention, the contact angle, α, is measured on the side of the fluid labeled 2.

If the side-wall illustrated in Figure 5.4.2 is vertical and the static contact angle is equal to $\frac{1}{2}\pi$, the interface remains flat all the way up to the contact line. Under more general conditions, the interface assumes a curved shape established spontaneously to satisfy a physical requirement on the contact angle.

5.4.2 The Laplace-Young equation for a two-dimensional interface

To derive an equation governing the shape of a two-dimensional curved interface separating two immiscible fluids, we substitute the pressure distributions (5.4.1) into the interfacial condition (4.5.16),

$$p^{(2)} - p^{(1)} = \gamma\,\kappa, \tag{5.4.6}$$

finding

$$-\rho_2\,g\,y + \pi_2 + \rho_1\,g\,y - \pi_1 = \gamma\,\kappa, \tag{5.4.7}$$

where κ is the interfacial curvature and y is the elevation of the interface. Rearranging, we obtain the Laplace–Young equation governing the shape of a two-dimensional interface in hydrostatics,

$$\kappa = -\frac{\Delta\rho\,g}{\gamma}\,y + B, \tag{5.4.8}$$

where $\Delta\rho \equiv \rho_2 - \rho_1$ is the density difference and

$$B \equiv \frac{\pi_2 - \pi_1}{\gamma} \tag{5.4.9}$$

is a constant with units of inverse length. In applications, the constant B is determined by enforcing an appropriate boundary condition or global constraint.

The Laplace–Young equation (5.4.8) essentially requires that the curvature of an interface is a linear function of the elevation from a reference state, y. An obvious solution is found by assuming that the elevation y is constant along the interface, $y = b$, and then setting $B = \Delta\rho\,gb/\gamma$, finding that $\kappa = 0$. However, the flat shape of the interface computed in

this fashion will not necessarily satisfy the boundary condition on the static contact angle; consequently, the obvious solution will not be admissible. The shape of the interface must be found so that equation (5.4.8) and a prescribed boundary condition on the contact angle are both satisfied.

Capillary length

Assuming that the fluids separated by an interface are stably stratified, that is, $\rho_2 > \rho_1$ or $\Delta\rho \equiv \rho_2 - \rho_1 > 0$, we introduce the capillary length defined as

$$\lambda \equiv \left(\frac{\gamma}{\Delta\rho\, g} \right)^{1/2}. \tag{5.4.10}$$

For an air-water interface at 20° Celsius, $\gamma = 73$ dynes/cm $= 73 \times 10^{-3}$ kg/sec^2, $\rho_1 = 0.0$ kg/m^3, $\rho_2 = 1000.0$ kg/m^3, yielding a capillary length of 2.72 mm. Equation (5.4.8) may now be recast into the compact form

$$\kappa = -\frac{y}{\lambda^2} + B. \tag{5.4.11}$$

All three terms in this equation have units of inverse length.

Arbitrary orientation

Implicit in (5.4.8) is the assumption that the acceleration of gravity vector, $\mathbf{g}$, points against the y axis. The general expression for an arbitrary orientation of the gravitational acceleration with respect to the working coordinates is

$$\kappa = \frac{\Delta\rho}{\gamma}\, \mathbf{g} \cdot \mathbf{x} + B, \tag{5.4.12}$$

where the point $\mathbf{x}$ lies at the interface, the pressure distributions in the two fluids are given by

$$p^{(1)}(\mathbf{x}) = \rho_1 \mathbf{g} \cdot \mathbf{x} + \pi_1, \qquad p^{(2)}(\mathbf{x}) = \rho_2\, \mathbf{g} \cdot \mathbf{x} + \pi_2, \tag{5.4.13}$$

and the constant B is given in (5.4.9).

5.4.3 Three-dimensional and axisymmetric interfaces

The equations derived in Section 5.4.2 for a two-dimensional interface also apply for an axisymmetric or a genuinely three-dimensional interface, provided that the curvature in the xy plane is replaced by twice the mean curvature, $2\kappa_m$. The counterpart of the Laplace–Young equation (5.4.10) is

$$2\,\kappa_m = -\frac{y}{\lambda^2} + B, \tag{5.4.14}$$

where the constant B is given in (5.4.9). We recall that the mean curvature is the average of two conjugate curvatures at any point on the interface.

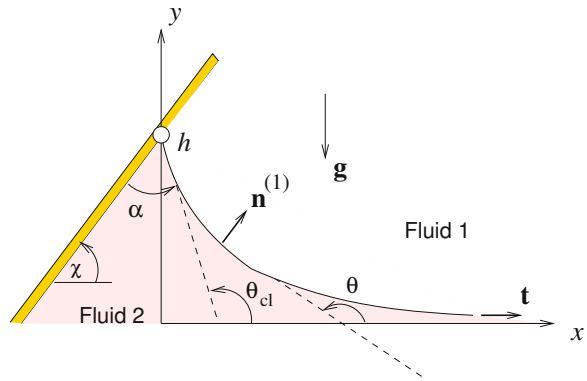

Figure 5.5.1 Illustration of a semi-infinite interface attached to an inclined plate. Far from the plate, the interface becomes horizontal.

When gravitational effects are not important, the first term on the right-hand side of (5.4.14) is insignificant. Consequently, the interface adjusts to obtain a uniform mean-curvature shape, such as that assumed by a thin soap film attached to a wire frame.

Numerical solutions of the unsimplified Laplace–Young equation for a variety of interfacial configurations are discussed in the remainder of this chapter.

Problem

5.4.1 *Pressure in a layer*

Derive expressions for the pressure distribution across a horizontal liquid layer of thickness h sandwiched between two semi-infinite fluids.

5.4.2 *Constant mean curvature*

Compile a list of five geometrical shapes with constant mean curvature.

5.5 A semi-infinite interface attached to an inclined plate

We begin the study of two-dimensional interfacial shapes by considering a semi-infinite interface attached to a flat plate that is inclined by an angle χ with respect to the horizontal plane, as illustrated in Figure 5.5.1. Far from the plate, as x tends to infinity, the interface tends to become horizontal. The contact angle subtended between the inclined plate and the tangent to the interface at the contact point is required to have a prescribed value, α.

It is convenient to set the origin of the y axis at the position of the flat interface far from the plate, and describe the interface by a function

$$y = f(x). \tag{5.5.1}$$

As x tends to infinity, the function $f(x)$ decays to zero to yield a flat interface. Since the interfacial curvature tends to zero far from the plate, the constant B on the right-hand side of the governing Laplace–Young equation (5.4.10) must be zero, yielding the simpler form

$$\kappa = -\frac{f}{\lambda^2}. \tag{5.5.2}$$

The curvature is given by expressions (4.3.28) and (4.3.30) as

$$\kappa = -\frac{f''}{(1+f'^2)^{3/2}} = \frac{1}{f'}\Big(\frac{1}{\sqrt{1+f'^2}}\Big)' = \frac{1}{f'}\frac{\mathrm{d}|\cos\theta|}{\mathrm{d}x} = -\Big(\frac{f'}{\sqrt{1+f'^2}}\Big)', \tag{5.5.3}$$

where $f' = \tan\theta$, as shown in Figure 5.5.1, and a prime denotes a derivative with respect to x. Substituting the last expression into (5.5.2) and integrating with respect to x, we find that

$$\Big(\frac{f'}{\sqrt{1+f'^2}}\Big)_{\mathrm{cl}} = \sin\theta_{\mathrm{cl}} = \frac{1}{\lambda^2}\int_0^\infty f(x)\,\mathrm{d}x, \tag{5.5.4}$$

where the subscript cl denotes evaluation at the contact line,

$$\theta_{\mathrm{cl}} = \alpha + \chi. \tag{5.5.5}$$

The integral on the right-hand side of (5.5.4) is the area of fluid 2 confined between the meniscus above the flat interface and the vertical line passing through the contact line. The weight of the corresponding fluid, reduced by the buoyancy force, is balance by the vertical component of the capillary force.

Substituting the second and third expressions in (5.5.3) into (5.5.2), and rearranging, we derive a nonlinear differential equation governing the interfacial shape,

$$\frac{\mathrm{d}}{\mathrm{d}x}\Big(\frac{1}{\sqrt{1+f'^2}}\Big) = \frac{\mathrm{d}|\cos\theta|}{\mathrm{d}x} = -\frac{ff'}{\lambda^2} = -\frac{1}{2}\frac{(f^2)'}{\lambda^2}. \tag{5.5.6}$$

Integrating once with respect to x, we obtain

$$\frac{1}{\sqrt{1+f'^2}} = |\cos\theta| = -\frac{1}{2}\frac{f^2}{\lambda^2} + C, \tag{5.5.7}$$

where C is a dimensionless integration constant. Requiring that f decays to zero as x tends to infinity, and correspondingly θ tends to π, we obtain $C = 1$.

Capillary rise

At the contact line located at $x = 0$, the slope angle θ takes the value given in (5.5.5). Evaluating equation (5.5.7) at $x = 0$ with $C = 1$ and rearranging, we obtain an expression for the positive or negative capillary rise, $h \equiv f(0)$,

$$\frac{1}{2}\frac{h^2}{\lambda^2} = 1 - |\cos(\alpha+\chi)|, \tag{5.5.8}$$

which shows that the maximum possible value of $|h|$ occurs when $\alpha + \chi$ is a multiple of $\frac{1}{2}\pi$, and is equal to $\sqrt{2}\lambda$.

Numerical formulation

To compute the shape of the interface, we apply (5.5.7) with $C = 1$ and rearrange to obtain a first-order ordinary differential equation,

$$\frac{\mathrm{d}f}{\mathrm{d}x} = \pm\Big(\frac{4}{(2-\phi^2)^2} - 1\Big)^{1/2} = \pm\frac{\phi}{2-\phi^2}\sqrt{4-\phi^2}, \tag{5.5.9}$$

where $\phi \equiv f/\lambda$ is a dimensionless function. The plus or minus sign on the right-hand side must be selected according to the expected interface shape.

The preceding analysis assumes that the interface has a monotonic shape, which is true if the angle θ_{cl} lies in the range $(\frac{1}{2}\pi, \frac{3}{2}\pi)$. Outside this range, the capillary rise is given by equation (5.5.8) with the minus sign replaced by a plus sign on the right-hand side.

When the shape of the interface is non-monotonic, the interface becomes vertical at a point, the function $f(x)$ is multi valued, and the integration of (5.5.9) requires careful consideration. To bypass this subtlety, we regard the x coordinate along the interface as a function of the independent variable f, and recast (5.5.9) into the form

$$\frac{\mathrm{d}x}{\mathrm{d}f} = \pm\frac{2-\phi^2}{\phi}\,\frac{1}{\sqrt{4-\phi^2}}. \tag{5.5.10}$$

The solution of (5.5.10) must be found for $|f| < |h|$, where $|h|$ is the capillary rise computed from equation (5.5.8).

5.5.1 Numerical method

A numerical solution of (5.5.10) can be computed according to the following steps:

1. Compute the angle θ_{cl} from equation (5.5.5).
2. Compute the capillary rise h using the formulas

$$\frac{h}{\sqrt{2}\,\lambda} = \begin{cases} (1+|\cos\theta_{\mathrm{cl}}|)^{1/2} & \text{if} \quad 0 < \theta_{\mathrm{cl}} < \frac{1}{2}\pi, \\ (1-|\cos\theta_{\mathrm{cl}}|)^{1/2} & \text{if} \quad \frac{1}{2}\pi < \theta_{\mathrm{cl}} < \pi, \\ -(1-|\cos\theta_{\mathrm{cl}}|)^{1/2} & \text{if} \quad \pi < \theta_{\mathrm{cl}} < \frac{3}{2}\pi, \\ -(1+|\cos\theta_{\mathrm{cl}}|)^{1/2} & \text{if} \quad \frac{3}{2}\pi < \theta_{\mathrm{cl}} < 2\pi. \end{cases} \tag{5.5.11}$$

3. Integrate the differential equation (5.5.10) from $f = h$ to 0 subject to the initial condition $x(f = h) = 0$ using, for example, the explicit Euler method or the modified Euler method discussed in Section 1.5. If h is negative, use a negative spatial step.

To implement the explicit Euler method, we select a small positive or negative integration step, $\Delta f = h/N$, where N defines the level of numerical discretization, evaluate equation

(5.5.10) at the point f, and approximate the derivative on the left-hand side with the finite difference, setting

$$\frac{\mathrm{d}x}{\mathrm{d}f} \simeq \frac{x(f+\Delta f)-x(f)}{\Delta f}. \tag{5.5.12}$$

Rearranging, we obtain

$$x(f+\Delta f) = x(f) + \Delta f\, \frac{2-\phi^2}{\phi}\, \frac{1}{\sqrt{4-\phi^2}}. \tag{5.5.13}$$

The repetitive application of this formula starting from $f = h$ where $x = 0$ generates a sequence of points distributed over the interface.

Modified Euler method (RK2)

To implement the modified Euler method, we replace formula (5.5.13) with a slightly more involved formula,

$$x(f+\Delta f) = x(f) + \Delta f\, \tfrac{1}{2} \left(\frac{2-\phi^2}{\phi}\, \frac{1}{\sqrt{4-\phi^2}} + \frac{2-\phi_{\mathrm{tmp}}^2}{\phi_{\mathrm{tmp}}}\, \frac{1}{\sqrt{4-\phi_{\mathrm{tmp}}^2}} \right), \tag{5.5.14}$$

where $\phi_{\mathrm{tmp}} = \phi + \Delta\phi$ and $\Delta\phi = \Delta f/\lambda$.

The modified Euler method is implemented in the following MATLAB code entitled *men_2d_plate* residing in directory *03_hydrostat* of FDLIB. The program scans tilting angles, while holding the contact angle α constant, and displays the interfacial profile in animation, as follows:

```
%---
% data
%---

gac = 1.0;   % acceleration of gravity
rhop = 1.0;   % pool density
rhoa = 0.0;   % ambient fluid density
gamma = 1.0;   % surface tension
chi = 0.01*pi;   % plate inclination
alpha = 0.01*pi;   % contact angle
ndiv = 2*64;   % interface divisions

%---
% prepare
%---

drho = rhop-rhoa;

if(drho<0)
  disp 'The density of the pool must be higher than'
```

```
  disp 'the density of the ambient fluid'
  return
end

capls = gamma/(gac*abs(drho));
capl = sqrt(capls);
dchi = 0.05;

Irepeat = 1;

%========
while (Irepeat==1)
%========

%--------------------------------
% angle theta at the contact line
%--------------------------------

thcl = alpha+chi;
cst = cos(thcl);

%----------------------------------------
% compute the magnitude of meniscus rise h
%----------------------------------------

if((thcl>0.5*pi)&(thcl<1.5*pi))
  h = sqrt(2.0*capls*(1.0-abs(cst)));
else
  h = sqrt(2.0*capls*(1.0+abs(cst)));
end

%---
% sign of meniscus rise
%---

if(thcl<pi)
  h = abs(h);   % meniscus goes up
else
  h =-abs(h);   % meniscus goes down
end

%---
% plate position at y=0
%---

xpl = -h/tan(chi);

%----------------------------------------
% integrate meniscus equation dx/df = G(f)
```

```
% from f=h to f=0 using the modified Euler
% method with constant step
%-----------------------------------------

df = h/ndiv;   % note that df can be positive or negative
dfh = 0.5*df;

y(1) = h;
x(1) = 0.0;   % starting point

for i=1:ndiv-1
  fred = y(i)/capl;
  freds = fred*fred;
  xp = (2.0-freds)/sqrt(4.0-freds)/fred;
  xsv = x(i);   % save
  xpsv = xp;   % save
  y(i+1) = y(i)-df;
  x(i+1) = x(i)+xp*df;
  fred = y(i+1)/capl;
  freds = fred*fred;
  xp = (2.0-freds)/(fred*sqrt(4.0-freds));
  x(i+1) = xsv+(xpsv+xp)*dfh;
end

%---
% plotting
%---

plot(x,y)
hold on
patch([xpl, 0, x, x(ndiv), (-2-h)/tan(chi)] ...
  ,[0, h, y,-2, -2],'y');
plot([-1 3 3 -1 -1],[-2 -2 2 2 -2])
plot([-10 10],[-10*tan(chi)+h, 10*tan(chi)+h] ...
  ,'r','LineWidth',3);
 plot([xpl, 10],[0, 0],'c--','LineWidth',1);
hold off
axis equal
 xlabel('x','fontsize',15);  ylabel('y','fontsize',15);
axis([-1 3 -2 2])
pause(0.1)

%---
% tilt the plate
%---

chi = chi + dchi;

if(chi > 0.99*pi | chi<0.01*pi)
```

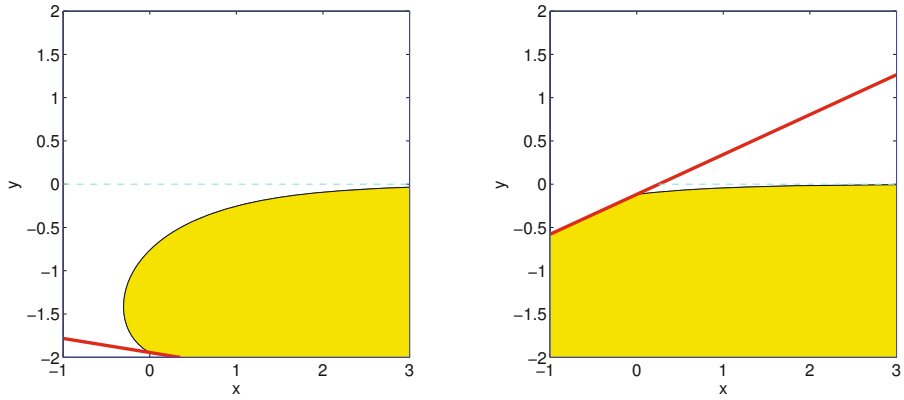

Figure 5.5.2 A semi-infinite meniscus attached to an inclined plate generated by the FDLIB code *men_2d_plate*. The plate inclination angles χ are different, but the contact angle α is the same in both cases.

```
  dchi = -dchi;
end

%====
end
%====
```

The graphics display generated by the code for two plate inclination angles and a fixed contact angle is shown in Figure 5.5.2.

5.5.2 *A floating cylinder*

The flat-plate solution derived in this section can be used to derive a trigonometric equation governing the floating angle, β, and position of the center of a floating circular cylinder of radius a, as shown in Figure 5.5.3. In the case of a flat interface, the cylinder center is located at $y_c = -a\cos\beta$.

In the chosen system of Cartesian coordinates, the undisturbed interface far from the floating cylinder is located at $y = 0$. The contact point on the right side of the cylinder is located at

$$x_{\rm cl} = a\sin\beta, \qquad y_{\rm cl} = y_c + a\cos\beta, \tag{5.5.15}$$

and the local inclination angle is $\chi = \pi - \beta$. Setting $h = y_{\rm cl}$ and substituting the expression for $y_{\rm cl}$ into (5.5.8), we obtain

$$\tfrac{1}{2}\left(\frac{y_{\rm cl}}{\lambda}\right)^2 = 1 - |\cos(\alpha - \beta + \pi)| = 2\sin^2\frac{\alpha-\beta}{2}, \tag{5.5.16}$$

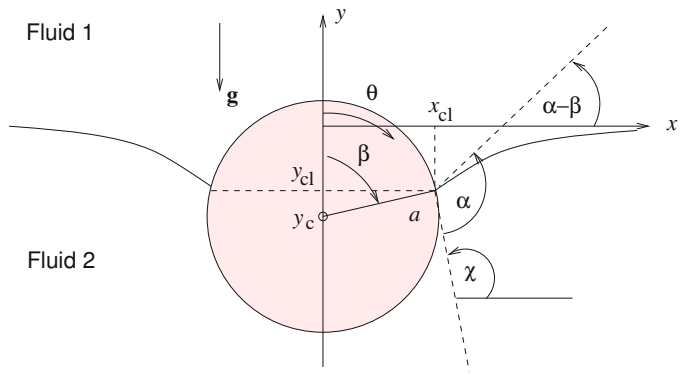

Figure 5.5.3 Illustration of a cylinder floating at the interface between two immiscible fluids. A curved meniscus is established on either side of the cylinder.

yielding

$$y_{\rm cl} = -2\,\lambda\,\sin\frac{\alpha-\beta}{2}. \tag{5.5.17}$$

The hydrostatic pressure distributions in the upper and lower fluid are given by

$$p^{(1)}(y) = -\rho_1 g y + \pi_0, \qquad p^{(2)}(y) = -\rho_2 g y + \pi_0, \tag{5.5.18}$$

where ρ_1 is the density of the upper fluid, ρ_2 is the density of the lower fluid, g is the gravitational acceleration, and π_0 is an inconsequential constant. The buoyancy force exerted by the fluids on the cylinder is given by

$$F_y^{\rm buoyancy} = -2\int_0^{\beta} p^{(1)}\,n_y\,a\,{\rm d}\theta - 2\int_{\beta}^{\pi} p^{(2)}\,n_y\,a\,{\rm d}\theta, \tag{5.5.19}$$

where θ is the polar angle defined in Figure 5.5.3, $n_y = \cos\theta$ is the y component of the outward unit vector, and the factor of 2 accouns for both sides of the cylinder. Substituting the pressure distributions (5.5.18) and setting $y = y_c + a\cos\theta$, we obtain

$$F_y^{\rm buoyancy} = 2ga\left(\rho_1\int_0^{\beta}(y_c + a\cos\theta)\,\cos\theta\,{\rm d}\theta + \rho_2\int_{\beta}^{\pi}(y_c + a\cos\theta)\,\cos\theta\,{\rm d}\theta\right). \tag{5.5.20}$$

Performing the integration, we find that

$$F_y^{\rm buoyancy} = ag\left(-2\,y_c\,\Delta\rho\sin\beta + a\,\Delta\rho\,\tfrac{1}{2}\left(\pi - 2\beta - \sin(2\beta)\right) + \pi a\overline{\rho}\right), \tag{5.5.21}$$

where $\Delta\rho = \rho_2 - \rho_1$ and

$$\overline{\rho} = \tfrac{1}{2}\,(\rho_1 + \rho_2) \tag{5.5.22}$$

is the mean density of the fluids.

The y component of the capillary force per unit length of the cylinder, acting on both sides of the cylinder, is given by

$$F_y^{\text{capillary}} = 2\gamma \sin(\alpha - \beta). \tag{5.5.23}$$

Balancing the weight of the cylinder, the buoyancy force, and the capillary force, we obtain the equilibrium equation

$$\pi a^2 \rho_b - F_y^{\text{buoyancy}} = F_y^{\text{capillary}}, \tag{5.5.24}$$

where ρ_b is the cylinder (body) density.

Making substitutions, setting $y_c = y_{\text{cl}} - a\cos\beta$, using (5.5.17), and simplifying, we obtain a trigonometric equation for β,

$$8\lambda \sin\frac{\alpha-\beta}{2} \sin\beta + \pi(1+\tau) - 2\beta + \sin(2\beta) + 4\lambda^2 \sin(\alpha-\beta) = 0, \tag{5.5.25}$$

which is also a quadratic equation for the dimensionless variable

$$\lambda \equiv \frac{\lambda}{a} \equiv \frac{1}{\sqrt{\text{Bo}}}, \tag{5.5.26}$$

where $\text{Bo} \equiv (a/\lambda)^2$ is a Bond number, and

$$\tau = 2\,\frac{\overline{\rho} - \rho_b}{\Delta\rho} \tag{5.5.27}$$

is a dimensionless density parameter. Given α and τ, equation (5.5.25) can be solved readily for β using Newton's method.

Problems

5.5.1 *Floating cylinder*

Show that the buoyancy force exerted on the floating cylinder is given by the alternative expression

$$F_y^{\text{buoyancy}} = -2a\,(x_c + a\cos\beta)\,\Delta\rho g \sin\beta + \tfrac{1}{2}\Delta\rho\, g\,(A_2 - A_1) + \overline{\rho} g A, \tag{5.5.28}$$

where A_1 and A_2 are the cylinder areas above and below the horizontal plane passing through the rectilinear contact lines on either side of the cylinder, and $A = \pi a^2$ is the cylinder cross-sectional area. Derive the expressions

$$A_1 = a^2\left(\beta - \tfrac{1}{2}\sin(2\beta)\right), \qquad A_2 = a^2\left(\pi - \beta + \tfrac{1}{2}\sin(2\beta)\right). \tag{5.5.29}$$

5.5.2 *Semi-infinite meniscus*

Run the code *men_2d_plate* to generate a family of shapes corresponding to a fixed plate inclination angle, β, and various contact angles, α. Generate another family of shapes corresponding to a fixed contact angle and various plate inclination angles. Discuss the behavior of the capillary rise in each case.

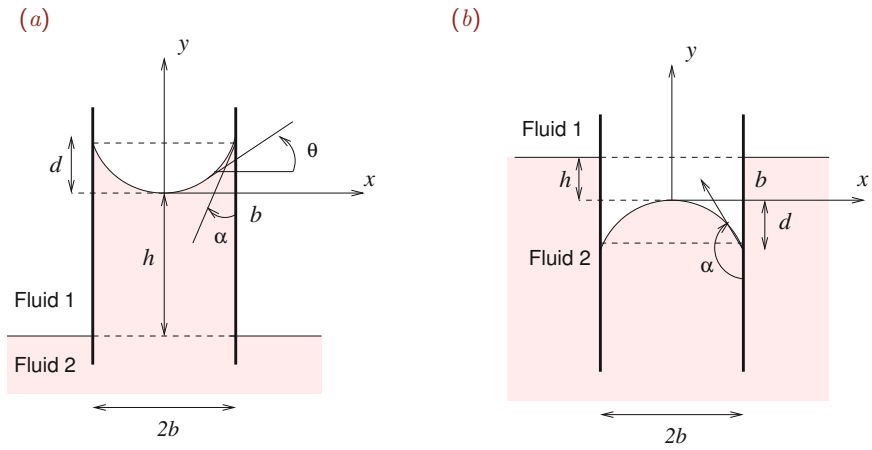

Figure 5.6.1 Illustration of a meniscus between two parallel vertical plates for contact angle (a) $\alpha < \frac{1}{2}\pi$ and (b) $\alpha > \frac{1}{2}\pi$. In the second case, the meniscus submerges and the capillary rise h is negative.

5.6 A meniscus between two parallel plates

Consider a two-dimensional interface between two fluids subtended between two parallel vertical plates, as illustrated in Figure 5.6.1(a). It is reasonable to assume that the two contact points are at the same elevation and the interface is symmetric with respect to the mid-plane located at $x = 0$.

It is convenient to set the origin of the Cartesian axes at the interface midway between the plates and describe the position of the interface by a function

$$y = f(x). \tag{5.6.1}$$

Outside and far from the plates, the interface assumes a horizontal shape located at $y = -h$, where h is the positive or negative capillary rise of the meniscus midway between the plates.

The lower fluid is labeled as fluid 2 and the upper fluid is labeled as fluid 1. The pressure distributions in the two fluids are given by

$$p^{(1)}(y) = -\rho_1 g y + \pi_1, \qquad p^{(2)}(y) = -\rho_2 g y + \pi_2, \tag{5.6.2}$$

where π_1 and π_2 are two reference pressures. Our objective is to compute the capillary rise, h, along with the unknown shape of the meniscus by solving the Laplace–Young equation (5.4.10),

$$\kappa = -\frac{f}{\lambda^2} + B, \tag{5.6.3}$$

where $B \equiv (\pi_2 - \pi_1)/\gamma$ and $\lambda^2 \equiv \gamma/(\Delta\rho\, g)$ is the square of the capillary length. We have assumed that $\Delta\rho \equiv \rho_2 - \rho_1 > 0$, so that the fluids are stably stratified.

Evaluating equation (5.6.3) at a point outside and far from the plates where the curvature of the interface tends to vanish and the interfacial elevation tends to $-h$, we obtain

$$B = -\frac{h}{\lambda^2}. \tag{5.6.4}$$

The Laplace–Young equation (5.6.3) then becomes

$$\kappa = -\frac{f+h}{\lambda^2}, \tag{5.6.5}$$

where $f + h$ is the unknown elevation of the curved interface between the plates measured with respect to the flat interface outside the plates.

The curvature is given by equations (4.3.28) and (4.3.30), repeated below for convenience,

$$\kappa = -\frac{f''}{(1+f'^2)^{3/2}} = \frac{1}{f'}\left(\frac{1}{\sqrt{1+f'^2}}\right)' = -\left(\frac{f'}{\sqrt{1+f'^2}}\right)' \tag{5.6.6}$$

and

$$\kappa = \frac{1}{\tan\theta}\frac{\mathrm{d}\cos\theta}{\mathrm{d}x} = -\frac{\mathrm{d}\sin\theta}{\mathrm{d}x}, \tag{5.6.7}$$

where $f' = \tan\theta$, the slope angle θ is defined in Figure 5.6.1, and a prime denotes a derivative with respect to x.

Mid-plane curvature and capillary rise

Our choice of Cartesian axes requires that $f = 0$ at the mid-plane, $x = 0$. Equation (5.6.3) then gives

$$\kappa(0) = B. \tag{5.6.8}$$

Because the interface is symmetric with respect to $x = 0$, $f' = 0$ at $x = 0$, the first expression in (5.6.6) yields

$$\kappa(0) = -f''(0). \tag{5.6.9}$$

Combining equations (5.6.8) and (5.6.9), we find that

$$B = -f''(0), \tag{5.6.10}$$

and thus

$$\frac{h}{\lambda^2} = -\kappa(0) = f''(0), \tag{5.6.11}$$

which shows that the capillary rise is determined by the curvature of the interface at the mid-plane, and *vice versa*. If the capillary rise is zero, the curvature of the interface at the mid-plane is also zero, and *vice versa*.

Meniscus height

Substituting the first expression for the curvature in terms of the slope angle θ given in (5.6.7) into (5.6.5), and recalling that $\tan\theta = f'$, we obtain

$$\frac{\mathrm{d}\cos\theta}{\mathrm{d}x} = -\frac{f+h}{\lambda^2}\,f' = -\frac{1}{\lambda^2}\left(\tfrac{1}{2}\,(f^2)' + hf'\right). \tag{5.6.12}$$

Integrating with respect to x from 0 to b, and noting that

$$\theta_b = \tfrac{1}{2}\pi - \alpha, \qquad \cos\theta_b = \sin\alpha, \tag{5.6.13}$$

we obtain a quadratic equation for the meniscus height, $d \equiv f(b)$,

$$1 - \sin\alpha = \frac{1}{\lambda^2}\left(\tfrac{1}{2}\,d + h\right)d, \tag{5.6.14}$$

where $\theta_b = \theta(x=0)$.

Vertical force balance

Substituting into (5.6.5) the second expression for the curvature in terms of the slope angle θ given in (5.6.7), and integrating with respect to x from 0 to b, we obtain

$$\cos\alpha = \frac{1}{\lambda^2}\int_0^b (f+h)\,\mathrm{d}x. \tag{5.6.15}$$

In fact, this equation expresses a balance of the weight of fluid between the plates above or below the flat interface, the buoyancy force, and the capillary force at the rectilinear contact lines.

Differential equations

To compute the shape of the interface, we substitute the first expression for the curvature given in (5.6.6) into the Laplace–Young equation (5.6.5), and rearrange to derive a second-order ordinary differential equation involving the capillary rise h as an unknown,

$$f'' = \frac{1}{\lambda^2}\,(f+h)\,(1+f'^2)^{3/2}. \tag{5.6.16}$$

The solution must be found in the interval $0 < x < b$ subject to the boundary conditions

$$f(0) = 0, \qquad f'(0) = 0, \qquad f'(b) = \tan(\frac{1}{2}\pi - \alpha) = \cot\alpha. \tag{5.6.17}$$

The third condition specifies the prescribed value of the contact angle. It is important to bear in mind that h is an implicit function of the shape function f by way of equation (5.6.11).

When $\alpha = \frac{1}{2}\,\pi$, all three boundary (5.6.17) are homogeneous and the obvious solution describes a flat, non-elevated and non-submerged interface, $h = 0$ and $f = 0$.

Canonical form

To compute the meniscus shape under general conditions, we recast the second-order differential equation (5.6.16) involving the unspecified parameter h into the canonical form of a system of three first-order differential equations. The word *canonical* derives from the Greek work $\kappa\alpha\nu o\nu\iota\kappa o\varsigma$, which means *normal*. This is done by introducing three new variables,

$$y_1 \equiv f, \qquad y_2 \equiv f', \qquad y_3 \equiv h. \tag{5.6.18}$$

Given these definitions, and noting that $y_2' = f''$, we resolve equation (5.6.16) into three first-order component equations,

$$\frac{\mathrm{d}y_1}{\mathrm{d}x} = y_2, \qquad \frac{\mathrm{d}y_2}{\mathrm{d}x} = \frac{1}{\lambda^2}\,(y_1 + y_3)\,(1 + y_2^2)^{3/2}, \qquad \frac{\mathrm{d}y_3}{\mathrm{d}x} = 0. \tag{5.6.19}$$

The third equation simply states that $y_3 \equiv h$ is a constant. In terms of the new variables, the boundary conditions (5.6.17) become

$$y_1(0) = 0, \qquad y_2(0) = 0, \qquad y_2(b) = \cot\alpha. \tag{5.6.20}$$

If the value of $y_3(0) = h$ were known, we would be able to integrate the system (5.6.19) from $x = 0$ to b using, for example, the explicit Euler or the modified Euler method discussed in Sections 1.5 and 5.5.

Explicit Euler method

To implement the explicit Euler method, we recast the system (5.6.19) into the general symbolic form

$$\frac{\mathrm{d}y_1}{\mathrm{d}x} = f_1(y_1, y_2, y_3, x), \qquad \frac{\mathrm{d}y_2}{\mathrm{d}x} = f_2(y_1, y_2, y_3, x), \qquad \frac{\mathrm{d}y_3}{\mathrm{d}x} = f_3(y_1, y_2, y_3, x), \tag{5.6.21}$$

where

$$f_1 \equiv y_2, \qquad f_2 = \frac{1}{\lambda^2}\,(y_1 + y_3)\,(1 + y_2^2)^{3/2} \qquad f_3 \equiv 0 \tag{5.6.22}$$

are the phase-space velocities.

Next, we evaluate equations (5.6.21) at a point, x, choose a small spatial step, Δx, and approximate the derivatives on the left-hand sides with finite differences writing, for example,

$$\frac{\mathrm{d}y_1}{\mathrm{d}x} = \frac{y_1(x + \Delta x) - y_1(x)}{\Delta x}. \tag{5.6.23}$$

Solving for $y_1(x + \Delta x)$ and repeating for the second and third equation, we obtain

$$\begin{bmatrix} y_1(x + \Delta x) \\ y_2(x + \Delta x) \\ y_3(x + \Delta x) \end{bmatrix} = \begin{bmatrix} y_1(x) \\ y_2(x) \\ y_3(x) \end{bmatrix} + \begin{bmatrix} f_1(y_1(x), y_2(x), y_3(x), x) \\ f_2(y_1(x), y_2(x), y_3(x), x) \\ f_3(y_1(x), y_2(x), y_3(x), x) \end{bmatrix} \Delta x. \tag{5.6.24}$$

In vector notation,

$$\mathbf{y}(x+\Delta x) = \mathbf{y}(x) + \mathbf{f}\big(\mathbf{y}(x), x\big)\,\Delta x, \tag{5.6.25}$$

where $\mathbf{y} \equiv (y_1, y_2, y_3)$ is the solution vector and $\mathbf{f} \equiv (f_1, f_2, f_3)$ is the corresponding phase-space velocity vector. The repetitive application of formula (5.6.25) starting from $x = 0$ allows us to generate a sequence of points along the meniscus.

Modified Euler method

To implement the modified Euler method, we replace formula (5.6.25) with a predictor formula,

$$\mathbf{y}^{\text{tmp}} = \mathbf{y}(x) + \mathbf{f}(\mathbf{y}(x), x)\,\Delta x, \tag{5.6.26}$$

followed by a corrector formula,

$$\mathbf{y}(x+\Delta x) = \mathbf{x}(x) + \tfrac{1}{2}\,[\,\mathbf{f}(\mathbf{y}(x), x) + \mathbf{f}(\mathbf{y}^{\text{tmp}}, x+\Delta x)\,]\,\Delta x,$$

where the superscript "tmp" denotes a preliminary value computed by the explicit Euler method. The first equation generates a provisional (temporary) value, and the second equation advances the solution using the initial and provisional values.

The modified Euler method is implemented in the following MATLAB code entitled *men_2d_ode*, located in directory *men_2d* inside directory *03_hydrostat* of FDLIB:

```
function [x,y1,y2] = men_2d_ode (npts,capls,b,h)

%-----------------------------------------
% Integrate ODEs by the modified Euler method
% Integration interval:  (0, b)
% Initial condition y1(0) = 0, y2(0) = 0
%-----------------------------------------

%----------------------
% prepare and initialize
%----------------------

dx = b/npts;   % uniform x step
x(1) = 0.0; y1(1) = 0.0; y2(1) = 0.0;

%---------------------------------------
% integrate by the modified Euler method
%---------------------------------------

for i=1:npts

  if(i==1)
    y1p = 0.0     % value at mid-plane
```

```
    y2p = h/capls   % value at mid-plane
  else
    y1p = y2(i);
    y2p = (y1(i)+h)*sqrt( (1.0+y2(i)*y2(i))^3 )/capls;
  end

  y1sv = y1(i); y2sv = y2(i);   % save
  y1psv = y1p; y2psv = y2p;
  x(i+1) = x(i) + dx;
  y1(i+1) = y1(i) + y1p*dx;
  y2(i+1) = y2(i) + y2p*dx;

  y1p = y2(i+1);     % second velocity evaluation
  y2p = (y1(i+1)+h)*sqrt((1.0+y2(i+1)^2)^3 )/capls;
  y1(i+1) = y1sv + 0.5*(y1psv+y1p)*dx;
  y2(i+1) = y2sv + 0.5*(y2psv+y2p)*dx;

end

%-----
% done
%-----

return
```

Note that the capillary rise, h, is specified in the input field.

The shooting method

Because the value of h is *a priori* unknown, the starting vector $\mathbf{y}(0)$ is not available and the solution of (5.6.19) must be found by iteration. The shooting method prescribes the obvious:

1. Guess a value for $y_3(0) = h$.
2. Compute the solution of (5.6.19).
3. Check whether the third condition in (5.6.20) is fulfilled within a specified tolerance; if not, repeat the computation with an improved guess.

To improve the guess in a systematic fashion that guarantees rapid convergence, we note that the value of $x_2(b)$ computed by solving equations (5.6.19) depends on the guessed value, $y_3(0) = h$. To signify this dependence, we extend the list of arguments of y_2, writing $y_2(b; h)$. The third boundary condition in (5.6.20) requires that

$$q_2(b\,; h) - \cot\alpha = 0, \tag{5.6.27}$$

which means that h is a root of an objective function defined as

$$Q(h) \equiv y_2(b\,; h) - \cot\alpha. \tag{5.6.28}$$

The problem has been reduced to computing the solution of the algebraic equation $Q(h) = 0$, where the left-hand side is evaluated by integrating equations (5.6.19) with a specified value of h.

Secant updates

The secant method provides us with a simple algorithm for solving the targeted nonlinear algebraic equation, $Q(h) = 0$, according to the following steps:

1. Select a value for h that approximates the root, $h^{(1)}$, and compute $Q(h^{(1)})$ by integrating system (5.6.19).
2. Select another value for h that approximates the root, $h^{(2)}$, and compute $Q(h^{(2)})$ by integrating (5.6.19).
3. Approximate the graph of the function $Q(h)$ with a straight line passing through the points computed in Steps 1 and 2. The slope of the approximating straight line is
$$s^{(2)} = \frac{Q(h^{(2)}) - Q(h^{(1)})}{h^{(2)} - h^{(1)}}. \tag{5.6.29}$$
4. Identify the improved value $h^{(3)}$ with the root of the linear function that describes the approximating straight line. Elementary algebra shows that the root is given by
$$h^{(3)} = h^{(2)} - \frac{Q(h^{(2)})}{s^{(2)}}. \tag{5.6.30}$$
5. Repeat the computation with the pairs $h^{(2)}$ and $h^{(3)}$ until convergence.

A reasonable guess for h can be obtained by assuming that the meniscus has a circular shape of radius R, which is positive when the interface is concave upward and negative when the interface is concave downward. Using elementary trigonometry, we find that the prescribed boundary condition on the contact angle will be satisfied when $\cos\alpha = b/R$. Rearranging, we derive the approximation
$$\kappa \simeq -\frac{1}{R} = -\frac{1}{b}\cos\alpha. \tag{5.6.31}$$
Using equation (5.6.11) we obtain the desired educated guess,
$$h \simeq \frac{\lambda^2}{b}\cos\alpha. \tag{5.6.32}$$
Equation (5.6.32) reveals that the maximum possible value of $|h|$ for a circular interface is λ^2/b.

The shooting method is implemented in the following MATLAB function entitled *men_2d*, located in directory *03_hydrostat* of FDLIB:

```
function [Iflag,x,y1,hmen] = men_2d ...
...
    (b,gac,gamma,rhop,rhoa ...
    ,alpha,npts,epsilon,maxiter,tol)

%-----------------------------------------
% Hydrostatic shape of a 2D meniscus between
% two vertical parallel plates computed
% by the shooting method
%-----------------------------------------

Iflag = 0;   % flag for success

%-----
% prepare
%----

drho = rhop-rhoa;   % density difference

% square of the capillary length:
  capls = gamma/(gac*abs(drho));

%----------------------
% initial guess for h
% computed by assuming a circular interface
%----------------------

h(1) = capls*cos(alpha)/b;

if(abs(alpha-0.5*pi)<0.0000001)
  cota = 0.0;
else
  cota = 1.0/tan(alpha);
end

%---
% compute the first solution of the odes
% to start-up the secant method
%---

Ic = 1;   % counter
[x,y1,y2] = men_2d_ode(npts,capls,b,h(Ic));

error(Ic) = y2(npts+1)-cota;

%-------------------------
% second start-up solution
%-------------------------
```

```
Ic = 2;
h(2) = h(1)+epsilon;
[x,y1,y2] = men_2d_ode(npts,capls,b,h(Ic));

error(Ic) = y2(npts+1)-cota;

%---------------------------------------
% iterate using the secant method
% until convergence
%---------------------------------------

for iter=1:maxiter

  Ic = Ic+1;

%---
% secant updating
%---

  Icb = Ic-2; Ica = Ic-1;
  dedh = (error(Ica)-error(Icb))/(h(Ica)-h(Icb));
  h(Ic) = h(Ica)-error(Ica)/dedh;

  [x,y1,y2] = men_2d_ode(npts,capls,b,h(Ic));

  error(Ic) = y2(npts+1)-cota;

  if(abs(error(Ic))<tol)
    break
  end

%---
end
%---

if(iter==maxiter)
  disp('men_2d:  ODE solver failed')
  Iflag=1;
  return
end

hmen = h(Ic);

%---
% done
%---

return
```

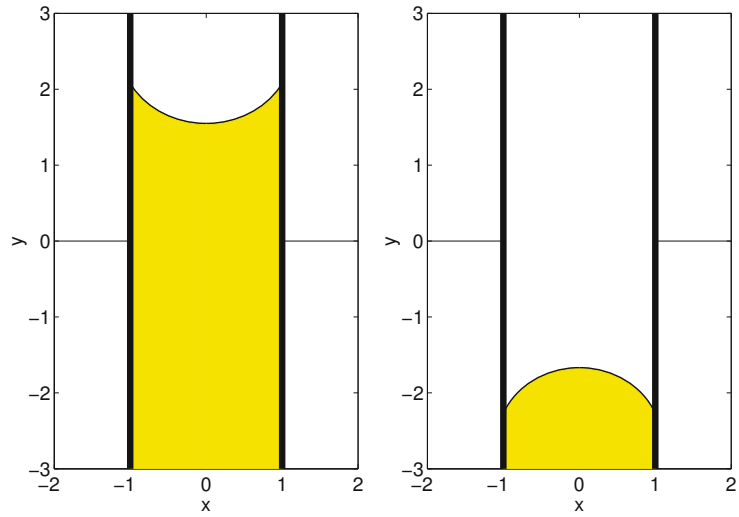

Figure 5.6.2 Shape of a meniscus inside a circular capillary tube generated by the FDLIB code *men_2d*.

Results of computations for a contact angle that is lower than $\frac{1}{2}\pi$ and a contact angle that is higher than $\frac{1}{2}\pi$ are shown in Figure 5.6.2. In the second case, the meniscus submerges below the level of the liquid outside the plates. Scaling all lengths by the plate half-separation, b, we find that the shape of the meniscus depends on the contact angle, α, and on the ratio λ/b. As λ/b increases, the meniscus tends to obtain a circular shape.

PROBLEM

5.6.1 *Meniscus between plates*

(a) Run the code *men_2d* to generate a family of shapes corresponding to fixed plate separation and various contact angles. Discuss the behavior of the capillary rise.

(b) Generate another family of shapes corresponding to fixed contact angle and various plate separations. Discuss the behavior of the capillary rise.

5.7 A two-dimensional drop on a horizontal plane

In the next application, we study the shape of a two-dimensional liquid drop or gas bubble surrounded by a stationary ambient fluid, resting above or hanging below a horizontal plane, as shown in Figure 5.7.1. The drop or bubble fluid is labeled 2 and the surrounding fluid is labeled 1.

The resting drop shown in Figure 5.7.1(a) is called a *sessile* drop, while the hanging drop shown in Figure 5.7.1(b) is called a *pendant* drop.

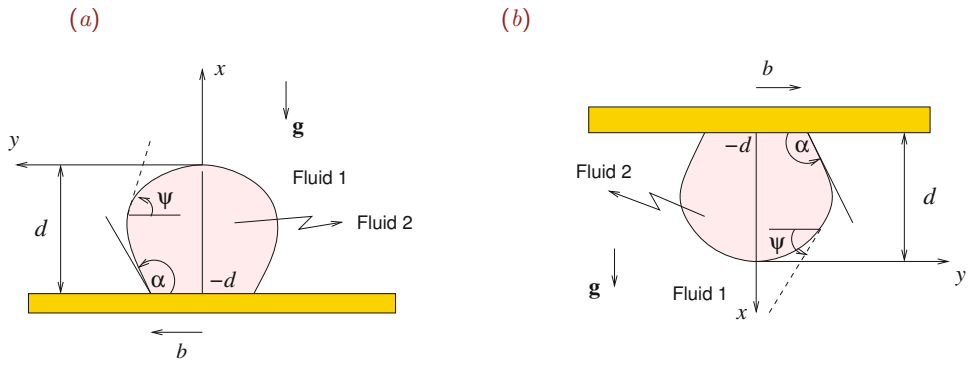

Figure 5.7.1 Illustration of a two-dimensional (a) sessile liquid drop or gas bubble resting on a horizontal plane and (b) pendant liquid drop or gas bubble hanging below a horizontal plane.

Our objective is to compute the shape of the interface for specified surface tension, γ, contact angle, α, and drop area, A_{D}. The forthcoming analysis also applies for a gas bubble regarded as a zero-density drop, $\rho_2 = 0$.

Working coordinates

It is convenient to work in Cartesian coordinates with origin located at the extreme point of the interface, as shown in Figure 5.7.1 for a sessile or pendant drop. The x axis points normal to the interface into the ambient fluid. The pressure distribution in the two fluids is given by

$$p^{(1)}(x) = -s_1 \rho_1 g x + \pi_1, \qquad p^{(2)}(x) = -s_1 \rho_2 g x + \pi_2, \tag{5.7.1}$$

where π_1 and π_2 are two reference pressures. The coefficient s_1 is equal to 1 for a sessile drop or -1 for a pendant drop, reflecting the orientation of the gravity with respect to the positive direction of the x axis.

The shape of the interface is governed by the Laplace–Young equation determining the jump in pressure across the interface due to surface tension in terms of the curvature,

$$\kappa = -s_1 \frac{\Delta\rho\, g}{\gamma} x + B, \tag{5.7.2}$$

where $\Delta\rho = \rho_2 - \rho_1$ and $B \equiv (\pi_2 - \pi_1)/\gamma$ is an *a priori* unknown constant with dimensions of inverse length. In terms of the square of the capillary length, $\lambda^2 \equiv \gamma/(|\Delta\rho|\, g)$, equation (5.7.2) takes the compact form

$$\kappa = -s_1 s_2 \frac{x}{\lambda^2} + B, \tag{5.7.3}$$

where the coefficient s_2 is equal to 1 if $\rho_2 > \rho_1$ or -1 if $\rho_2 < \rho_1$.

Evaluating equation (5.7.2) at the origin, $x = 0$, we find that the constant B is equal to the unknown curvature of the interface at the plane of symmetry located at $y = 0$,

$$B = \kappa_0, \tag{5.7.4}$$

where $\kappa_0 \equiv \kappa(x = 0)$.

Describing the interface by a function,

$$y = f(x), \tag{5.7.5}$$

we obtain the following expressions for the curvature given in (4.3.28),

$$\kappa = -\frac{f''}{(1+f'^2)^{3/2}} = \frac{1}{f'}\Big(\frac{1}{\sqrt{1+f'^2}}\Big)' = -\Big(\frac{f'}{\sqrt{1+f'^2}}\Big)', \tag{5.7.6}$$

where a prime denotes a derivative with respect to x.

Drop height

Substituting the last expression for the curvature given in (5.7.6) into the Young–Laplace equation (5.7.3), we obtain

$$-\Big(\frac{f'}{\sqrt{1+f'^2}}\Big)' = -s_1 s_2 \frac{x}{\lambda^2} + B. \tag{5.7.7}$$

Integrating with respect to x across the height of the drop, from $x = -d$ to 0, as shown in Figure 5.7.1, we obtain

$$1 - \cos\alpha = 2\,\sin^2\frac{\alpha}{2} = s_1 s_2 \,\tfrac{1}{2}\,\frac{d^2}{\lambda^2} + Bd. \tag{5.7.8}$$

When $s_1 s_2 = 1$ and the top of the drop is nearly flat due to strong gravitational effects, $Bd \simeq 0$, we find that

$$d \simeq 2\,\lambda\,\sin\frac{\alpha}{2}, \tag{5.7.9}$$

which is consistent with the capillary height of a semi-infinite meniscus attached to a flat plate.

Vertical force balance

Substituting into (5.7.3) the second expression for the curvature given in (5.7.6), and multiplying both sides by f', we obtain

$$\Big(\frac{1}{\sqrt{1+f'^2}}\Big)' = -s_1 s_2 \frac{1}{\lambda^2}\,\big[\,(xf)' - f\,\big] + Bf'. \tag{5.7.10}$$

Integrating with respect to x across the height of the drop from $x = -d$ to 0, we obtain

$$\sin\alpha = s_1 s_2 \frac{1}{\lambda^2}\,\big(\,d\,b - \tfrac{1}{2}\,A_{\mathrm{D}}\,\big) + B\,b, \tag{5.7.11}$$

where

$$A_{\mathrm{D}} = 2\int_{-d}^{0} f(x)\,\mathrm{d}x \tag{5.7.12}$$

is the drop area, b is half the length of the drop base, and d is the drop height, as shown in Figure 5.7.1. Equation (5.7.11) can be used to compute one of b, d, and $B = \kappa_0$ from two of the others.

In fact, equation (5.7.11) expresses a force balance. To demonstrate this directly, we observe that the additional force exerted on a longitudinal strip of the substrate covering the base of the drop is

$$\Delta F_x = -(2\,bw)\left(p^{(2)} - p^{(1)}\right)_{x=-d} = -(2\,bw)\left(s_1\Delta\rho\, gd + B\gamma\right), \tag{5.7.13}$$

where and w is the width the strip. Adding to this force the capillary force exerted on the substrate at the contact line due to surface tension, we obtain the total force,

$$F_x = \Delta F_x + 2w\gamma\sin\alpha = -s_1\Delta\rho\, g\,2\,bwd - \gamma\,2w\left(Bb - \sin\alpha\right). \tag{5.7.14}$$

The first term on the right-hand side is the weight of of a cylindrical slab of fluid with length $2b$, width w, and height d, reduced by the buoyancy force. The net force is precisely equal to the weight of the drop reduced by the buoyancy force,

$$F_x = -s_1\Delta\rho\, gA_{\mathrm{D}}w, \tag{5.7.15}$$

yielding the relation

$$s_1 s_2\left(A_{\mathrm{D}} - 2bd\right) = 2\,\lambda^2\left(Bb - \sin\alpha\right), \tag{5.7.16}$$

as given in (5.7.11).

Parametric representation

One important difference between the problem presently considered and those discussed previously in this chapter, is that, neither the range of x nor the range of y is known over the span of the drop interface at the outset.

To circumvent this difficulty, we describe the shape of the interface in parametric form in terms of the slope angle ψ defined in Figure 5.7.1, increasing from zero at the origin to α at the contact point. Our objective is to compute two scalar functions of ψ such that the x and y coordinates of a point at the interface are described by the functions

$$x = X(\psi), \qquad y = Y(\psi) \tag{5.7.17}$$

for $0 \le \psi \le \alpha$. One important advantage of the adopted parametrization is that the boundary condition for the contact angle at the contact point is satisfied automatically and can be removed from further discussion. To compute the functions $X(\psi)$ and $Y(\psi)$, we

require two ordinary differential equations and a suitable number of boundary conditions or global constraints.

Ordinary differential equations

The first differential equation is the definition of the chosen parameter ψ in terms of the interface slope,

$$\cot\psi = -\frac{\mathrm{d}Y}{\mathrm{d}X}. \tag{5.7.18}$$

The second differential equation must originate from the Young–Laplace equation. Referring to expressions (5.7.6) for the curvature, we set $f' = \mathrm{d}Y/\mathrm{d}X$ and find that

$$\kappa = -\frac{1}{\cot\psi}\frac{\mathrm{d}}{\mathrm{d}X}\left(\frac{1}{\sqrt{1+\cot^2\psi}}\right) = -\frac{1}{\cot\psi}\frac{\mathrm{d}\sin\psi}{\mathrm{d}X} = -\sin\psi\,\frac{\mathrm{d}\psi}{\mathrm{d}X} = \frac{\mathrm{d}\cos\psi}{\mathrm{d}X}. \tag{5.7.19}$$

Substituting the penultimate expression into the left-hand side of (5.7.3), we obtain

$$\sin\psi\,\frac{\mathrm{d}\psi}{\mathrm{d}X} = -\frac{\mathrm{d}\cos\psi}{\mathrm{d}X} = s_1 s_2\,\frac{X}{\lambda^2} - B, \tag{5.7.20}$$

which can be rearranged to give the desired parametric dependence

$$\frac{\mathrm{d}X}{\mathrm{d}\psi} = \frac{\sin\psi}{Q}, \tag{5.7.21}$$

where

$$Q \equiv s_1 s_2\,\frac{X}{\lambda^2} - B. \tag{5.7.22}$$

To derive a corresponding parametric dependence for Y, we recast (5.7.18) into the form

$$\frac{\mathrm{d}Y}{\mathrm{d}\psi} = -\cot\psi\,\frac{\mathrm{d}X}{\mathrm{d}\psi}. \tag{5.7.23}$$

Substituting (5.7.21) into (5.7.23), we obtain

$$\frac{\mathrm{d}Y}{\mathrm{d}\psi} = -\frac{\cos\psi}{Q}. \tag{5.7.24}$$

Equations (5.7.21) and (5.7.24) provide us with the desired system of two first-order differential equations involving an unspecified parameter, B. The boundary conditions require that $X(0) = 0$ and $Y(0) = 0$. The constraint on the drop area requires that

$$2\int_{-d}^{0} Y\,\mathrm{d}x = A_{\mathrm{D}}, \tag{5.7.25}$$

where $x = -d$ describes the position of the plane.

Shooting method

Because the value of the constant B is *a priori* unknown, the solution must be found by iteration. The shooting method combined with the secant method for improving the guess provides us with an efficient algorithm. The numerical procedure involves the following steps:

1. Guess a value for B.
2. Integrate the system of equations (5.7.21) and (5.7.24).
3. Compute the integral on the right-hand side of (5.7.25) using the trapezoidal rule and then evaluate the objective function

$$Q \equiv 2 \int_{-d}^{0} y \, \mathrm{d}x - A_{\mathrm{D}}. \tag{5.7.26}$$

4. Improve the guess for B with the goal of driving the objective function Q to zero using, for example, the secant method discussed in Section 5.6.

Since the constant B is equal to the unknown curvature of the interface at the mid-plane located at $y = 0$, a reasonable guess can be obtained by assuming that the interface is a section of a circle, and then computing the radius of the circle, ϱ, according to specified values of the contact angle and drop area. Using elementary trigonometry, we find that

$$\varrho = \left(\frac{2A_{\mathrm{D}}}{2\,\alpha - \sin 2\alpha} \right)^{1/2} \tag{5.7.27}$$

and set $B = 1/\varrho$.

Fourth-order Runge–Kutta method

The fourth-order Runge–Kutta method (RK4) is an improvement of the modified Euler method discussed earlier in this section, involving three exploratory steps and one final step.

The following MATLAB function entitled *drop_2d_ode*, located in directory *drop_2d* inside subdirectory *03_hydrostat* of FDLIB, implements the method for solving the system of equations (5.7.21) and (5.7.24) and simultaneously computing the drop area:

```
function [x,y,area] = drop_2d_ode ...
  ...
  (npts ...
  ,capls ...
  ,Isp ...
  ,dpsi ...
  ,B ...
  )
```

```
%---------------------------------------
% Integrate two ODEs by RK4 with uniform
% step size for the angle psi
%---------------------------------------

%--------
% prepare
%--------

dpsih = 0.5*dpsi;

%----------------
% top of the drop
%----------------

psi = 0.0; x(1) = 0.0; y(1) = 0.0;

%-----------
% integrate
%----------

for i=1:npts

  if(i==1)
    xp = 0.0; yp = 1.0/B;
  else
    Q = Isp*x(i)/capls-B;
    xp = sin(psi)/Q;
    yp =-cos(psi)/Q;
  end
  xp1 = xp; yp1 = yp;

  psi = psi +dpsih;
  x(i+1) = x(i)+xp*dpsih;
  y(i+1) = y(i)+yp*dpsih;

  Q = Isp*x(i+1)/capls-B;
  xp = sin(psi)/Q;
  yp =-cos(psi)/Q;
  xp2 = xp; yp2 = yp;

  x(i+1) = x(i)+xp*dpsih;
  y(i+1) = y(i)+yp*dpsih;

  Q = Isp*x(i+1)/capls-B;
  xp = sin(psi)/Q;
  yp =-cos(psi)/Q;
  xp3 = xp; yp3 = yp;
```

```
  psi = psi +dpsih;
  x(i+1) = x(i)+xp*dpsi;
  y(i+1) = y(i)+yp*dpsi;

  Q = Isp*x(i+1)/capls-B;
  xp = sin(psi)/Q;
  yp =-cos(psi)/Q;
  xp4 = xp; yp4 = yp;

  x(i+1) = x(i) + (xp1+2*xp2+2*xp3+xp4)*dpsi/6.0;
  y(i+1) = y(i) + (yp1+2*yp2+2*yp3+yp4)*dpsi/6.0;

end

%----------------------------------------
% compute the area of the integrated shape
% by the trapezoidal rule
%----------------------------------------

area = 0.0;
for i=1:npts
  area= area+(y(i+1)+y(i))*abs(x(i+1)-x(i));
end

area = 0.5*area;   % to account for trapezoidal weights

%---
% double the area to get the full shape
%---

area = 2.0*area

%-----
% done
%-----

return
```

The following MATLAB function entitled *drop_2d*, located in directory *03_hydrostat* of FDLIB, implements the secant method:

```
function [a,Bfinal,x,y] = drop_2d ...
  ...
  (Jsp,gac,gamma,rhod,rhoa,area...
  ,alpha,npts,epsilon,maxiter,tol)

%-----------------------------------------
% Hydrostatic shape of a two-dimensional
% sessile drop resting on a horizontal plane,
```

```
% or pendant drop hanging underneath
% a horizontal plane, for a specified
% specified area and contact angle
%
% Jsp = 1 for a sessile drop
% Jsp = -1 for a pendant drop
%-------------------------------------------

%--------
% prepare
%--------

Iflag=0;   % signals failure

drho = rhod-rhoa;   % density difference
% square of the capillary length:
capls = gamma/(gac*abs(drho));

Isp = 1;   % Isp is an orientation index

if(drho<0)
  Isp = -Isp;
end

if(Jsp==-1)
  Isp = -Isp;
end

%----------------------------------
% to start, assume that the drop shape
% is a truncated circle
% and compute the circle radius "a"
% in terms of the drop area and contact angle
%----------------------------------

a = sqrt(area/(alpha-0.5*sin(2.0*alpha)));
B(1) = 1.0/a;

%---
% compute the initial solution of the odes
% to start-up the secant method
%---

dpsi = alpha/npts;
Ic = 1;   % counter

[x,y,area_sh] = drop_2d_ode ...
  ...
  (npts ...
```

```
  ,capls ...
  ,Isp ...
  ,dpsi ...
  ,B(Ic) ...
  );

error(Ic) = area_sh - area;
err = abs(error(Ic));

%-------------------------
% second start-up solution
%-------------------------

Ic=2;
B(2) = B(1)+epsilon;

[x,y,area_sh] = drop_2d_ode ...
  ...
  (npts ...
  ,capls ...
  ,Isp ...
  ,dpsi ...
  ,B(Ic) ...
  );

error(Ic) = area_sh - area;
err = abs(error(Ic));

%---------------------------------------
% iterate on B using the secant method
% until convergence
%---------------------------------------

for iter=1:maxiter

  Ic = Ic+1;

%---
% secant updating
%---

  Icb = Ic-2;
  Ica = Ic-1;
  dedc = (error(Ica)-error(Icb))/(B(Ica)-B(Icb));
  B(Ic) = B(Ica)-error(Ica)/dedc;

  [x,y,area_sh] = drop_2d_ode ...
    ...
    (npts ...
```

```
    ,capls ...
    ,Isp ...
    ,dpsi ...
    ,B(Ic) ...
    );

  error(Ic) = area_sh - area;
  err = abs(error(Ic));
  if(err<tol) break; end

%---
end
%---

if(iter==maxiter)
  disp('drop_2d:  ODE solver failed')
  Iflag=1; return
end

Bfinal = B(Ic);

%---
% done
%---

return
```

Families of drop shapes computed using the code are shown in Figure 5.7.2. Gravity squeezes the sessile drop toward the wall and pulls the pendant drop away from the wall.

Problems

5.7.1 *Radius of a circular drop*

Derive formula (5.7.27) for the radius of a circular drop.

5.7.2 *Two-dimensional drop on a horizontal plane*

Run the code *drop_2d* to generate a family of interfacial shapes corresponding to a fixed value of the drop area and various contact angles. Discuss the computed interfacial shapes.

5.8 A two-dimensional drop on an inclined plane

We proceed to consider the more challenging problem of a two-dimensional drop resting above or hanging underneath an inclined plane, as shown in Figure 5.8.1. In the working Cartesian coordinates defined in this figure, the origin of the x axis is set at the inclined plane at the location of the front or rear contact point.

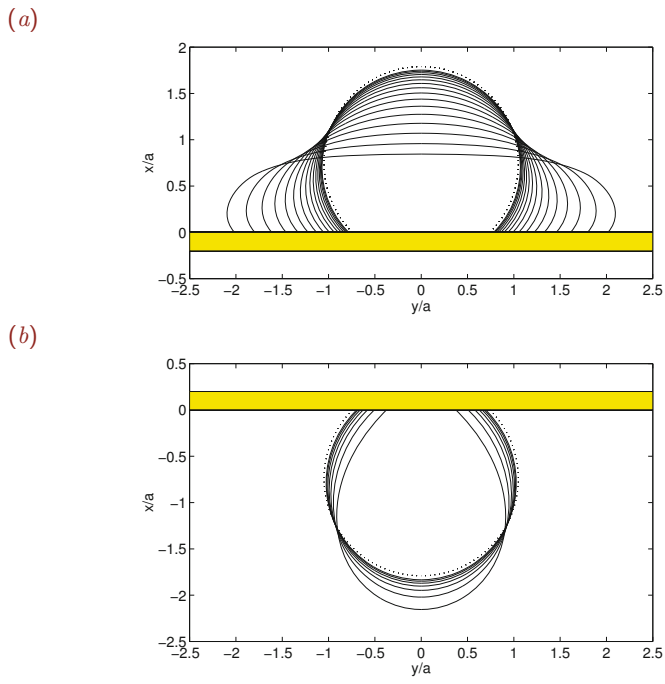

Figure 5.7.2 Shapes of (a) sessile and (b) pendant two-dimensional drops for contact angle $\alpha = \frac{3\pi}{4}$ and different surface tensions computed using the FDLIB code *drop_2d*. The dotted lines trace the approximate circular shape established for small drops or high surface tension. The x and y coordinates have been scaled by the equivalent drop radius, a, defined in terms of the drop area as $A_D = \pi a^2$.

In the case of the sessile drop, depicted in Figure 5.8.1(a), the contact angle at the first contact point, α_1, is larger than the contact angle at the second contact point, α_2. In the case of the pendant drop, shown in Figure 5.8.1(b), the first contact angle, α_1, is smaller than the second contact angle, α_2.

In the inclined system of coordinates depicted in Figure 5.8.1(a, b), the Cartesian components of the acceleration of gravity vector are given by

$$g_x = -g\,\cos\beta, \qquad g_y = -g\,\sin\beta, \tag{5.8.1}$$

where β is the plane inclination angle ranging from 0 to 2π.

The pressure distributions in the ambient fluid and inside the drop are given by

$$p^{(1)}(x,y) = -\rho_1 g\,(x\,\cos\beta + y\,\sin\beta) + \pi_1 \tag{5.8.2}$$

and

$$p^{(2)}(x,y) = -\rho_2 g\,(x\,\cos\beta + y\,\sin\beta) + \pi_2, \tag{5.8.3}$$

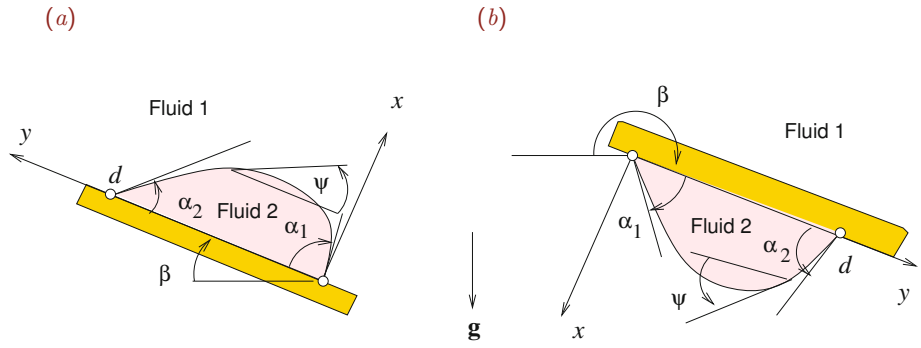

Figure 5.8.1 Illustration of a two-dimensional liquid drop (a) resting above and (b) hanging underneath an inclined plane.

where π_1 and π_2 are two reference pressures. Substituting these expressions into the interfacial balance (4.5.16), we obtain

$$-\rho_2\, g\,(X\cos\beta + Y\sin\beta) + \pi_2 + \rho_1\, g\,(X\cos\beta + Y\sin\beta) + \pi_1 = \gamma\,\kappa, \tag{5.8.4}$$

where (X, Y) are interfacial coordinates. Rearranging, we obtain the Laplace–Young equation

$$\kappa = -s_1\,\frac{\Delta\rho\, g}{\gamma}(X\,\cos\beta + Y\,\sin\beta) + C, \tag{5.8.5}$$

where $\Delta\rho \equiv \rho_2 - \rho_1$ and $C \equiv (\pi_2 - \pi_1)/\gamma$. Physically, the constant C represents the curvature of the interface at the first contact point where $X = 0$ and $Y = 0$.

Parametric representation

The interface will be described parametrically in terms of the slope angle, ψ, varying from $-\alpha_1$ at the first contact point, to α_2 at the second contact point, as shown in Figure 5.8.1. Regarding X and Y as functions of ψ and working as in Section 5.7 for a drop attached to a horizontal plane, we derive the differential equations

$$\frac{\mathrm{d}X}{\mathrm{d}\psi} = \frac{\sin\psi}{Q}, \qquad \frac{\mathrm{d}Y}{\mathrm{d}\psi} = -\frac{\cos\psi}{Q}, \tag{5.8.6}$$

where

$$Q \equiv s\,\frac{X\cos\beta + Y\sin\beta}{\lambda^2} - C, \tag{5.8.7}$$

and the coefficient s is equal to 1 if $\rho_2 > \rho_1$ or -1 if $\rho_2 < \rho_1$.

The first contact line boundary condition sets the origin of the Cartesian axes at the inclined plane,

$$X(-\alpha_1) = 0, \qquad Y(-\alpha_1) = 0. \tag{5.8.8}$$

The second contact line boundary condition requires that

$$X(\alpha_2) = 0. \tag{5.8.9}$$

The constraint on the drop area, A_{D}, requires that

$$\int_0^d X \, \mathrm{d}y = A_{\mathrm{D}}, \tag{5.8.10}$$

where $y = d$ marks the position of the second contact line.

5.8.1 First contact angle specified

Given the drop area, A_{D}, we may specify the first contact angle, α_1, and compute the second contact angle, α_2, and the constant C to satisfy conditions (5.8.9) and (5.8.10). A shooting method can be implemented for this purpose according to the following steps:

1. Guess values for C and α_2.
2. Integrate the system of equations (5.8.6) with the initial conditions given in (5.8.8).
3. Compute the integral on the right-hand side of (5.8.10) using the trapezoidal rule.
4. Evaluate the two components of an objective function,

$$F(1) \equiv X(\alpha_2), \qquad F(2) \equiv \int_0^d X \, \mathrm{d}y - A_{\mathrm{D}}. \tag{5.8.11}$$

5. Improve the values of C and α_2 to drive the two components of the objective function, $F(1)$ and $F(2)$ to zero,

$$F(1) = 0, \qquad F(2) = 0, \tag{5.8.12}$$

   and return to Step 2.

The following MATLAB function entitled *drop_2di1_ode*, located in directory *drop_2di1* inside directory *03_hydrostat* of FDLIB, solves the system of equations (5.8.6) and computes the first and second components of the objective function, **F**:

```
function F = drop_2di1_ode(solution)

%--------------------------------------------
% Two-dimensional drop on an inclined plane.
% Integrate ODEs by RK4 with uniform
% step size for the slope angle psi
%
% SYMBOLS:
% -------
%
% dpsi:  increments in psi
% C: shooting parameter
```

```
% solution(1) = C
% solution(2) = alpha_2
%-------------------------------------------

global area capls Isp npts beta alpha1 alpha2 x y

%--------
% dispense variables
%--------

C = solution(1);
alpha2 = solution(2);

%--------
% prepare
%--------

csb = cos(beta);
snb = sin(beta);
dpsi = (alpha1+alpha2)/npts;
dpsih = 0.5*dpsi;

%----------------
% first contact point
%----------------

psi = -alpha1; x(1) = 0.0; y(1) = 0.0;

%----------
% integrate
%----------

for i=1:npts

  Q = Isp*(csb*x(i)+snb*y(i))/capls-C;
  xp = sin(psi)/Q; yp =-cos(psi)/Q;
  xp1 = xp; yp1 = yp;

  psi = psi +dpsih;
  x(i+1) = x(i)+xp*dpsih;
  y(i+1) = y(i)+yp*dpsih;

  Q = Isp*(csb*x(i+1)+snb*y(i+1))/capls-C;
  xp = sin(psi)/Q; yp =-cos(psi)/Q;
  xp2 = xp; yp2 = yp;

  x(i+1) = x(i)+xp*dpsih;
  y(i+1) = y(i)+yp*dpsih;
```

```
  Q = Isp*(csb*x(i+1)+snb*y(i+1))/capls-C;
  xp = sin(psi)/Q; yp =-cos(psi)/Q;
  xp3 = xp; yp3 = yp;

  psi = psi +dpsih;
  x(i+1) = x(i)+xp*dpsi;
  y(i+1) = y(i)+yp*dpsi;

  Q = Isp*(csb*x(i+1)+snb*y(i+1))/capls-C;
  xp = sin(psi)/Q; yp =-cos(psi)/Q;
  xp4 = xp; yp4 = yp;

  x(i+1) = x(i) + (xp1+2*xp2+2*xp3+xp4)*dpsi/6.0;
  y(i+1) = y(i) + (yp1+2*yp2+2*yp3+yp4)*dpsi/6.0;

end

F(1) = x(npts+1);

%----------------------------------------
% compute the area of the integrated shape
% by the trapezoidal rule
%----------------------------------------

ar = 0.0;

for i=1:npts
  ar = ar+(x(i+1)+x(i))*(y(i+1)-y(i));
end
ar = 0.5*ar;   % to account for trapezoidal weights

F(2) = ar-area;

%-----
% done
%-----

return
```

The improvement in the values of C and α_2 in Step 5 of the algorithm can be done using Newton's method for solving a system of two nonlinear equations (5.8.12).[1] The method is implemented in the following FDLIB function entitled *drop_2di1_newton2*, located in directory *drop_2di1* inside directory *03_hydrostat* of FDLIB:

```
function [x,f,Iflag] = drop_2di1_newton2 ...
...
```

[1] Pozrikidis, C. (2008) *Numerical Computation in Science and Engineering.* Second Edition, Oxford University Press.

```
  (Niter ...
  ,eps ...
  ,x ...
  )

%========
% Solve two nonlinear equations by Newton's method
%
% SYMBOLS:
% --------
%
% x:  solution vector
% eps:  small number for computing the Jacobian
%         by numerical differentiation
% Dx:  correction vector
% tol:  accuracy
% Iflag:  will set equal to 1 if something is wrong
%========

tol = 0.0000001;   % tolerance
relax = 1.0;

%-----------
% initialize
%-----------

Iflag = 1;

%---------------------
% start the iterations
%---------------------

for Iter=1:Niter

  f = drop_2di1_ode(x);

%---------------------
% compute the Jacobian
% by numerical differentiation
%---------------------

for j=1:2
  x(j) = x(j)+eps;   % perturb
  f1 = drop_2di1_ode(x);
  x(j) = x(j)-eps;   % reset
  for i=1:2
    Jac(i,j) = (f1(i)-f(i))/eps;
  end
end
```

```
%---
% solve the equation:  Jac .  Dx = - f
% for the correction vector Dx by Cramer's rule
%---

b1 = -f(1);
b2 = -f(2);
Det = Jac(1,1)*Jac(2,2)-Jac(1,2)*Jac(2,1);
dx(1) = (b1*Jac(2,2)-Jac(1,2)*b2)/Det;
dx(2) = (b2*Jac(1,1)-Jac(2,1)*b1)/Det;

%--------
% correct
%--------

x(1) = x(1) + relax*dx(1);
x(2) = x(2) + relax*dx(2);

%-------
% escape
%-------

Iescape = 1;
if(abs(dx(1)) > tol) Iescape = 0; end
if(abs(dx(2)) > tol) Iescape = 0; end

if(Iescape==1)
  Iflag = 0;
  f = drop_2di_ode(x);
  return
end

%----
end   % of iterations
%----

%-----
% done
%-----

return
```

The overall procedure is implemented in the following MATLAB code entitled *drop_2di1*, located in directory *drop_2di1* inside directory *03_hydrostat* of FDLIB:

```
%-----------------------------------------------------
% Hydrostatic shape of a two-dimensional
% sessile drop resting on an inclined plane
```

```
% or a pendant drop hanging underneath a inclined plane,
% for a specified area and first contact angle
%-------------------------------------------------------

global area capls Isp npts beta alpha1 alpha2 x y

gac = 1.0;   % acceleration of gravity
rhod = 1.0;   % density of the drop
rhoa = 0.0;   % density of the ambient fluid

area = pi;   % drop area
beta = 0.125*pi;   % inclination angle
alpha1 = 0.35*pi;   % first contact angle
npts = 64;   % number of interfacial markers

%---
% prepare
%---

drho = rhod-rhoa;   % density difference

Isp = 1.0;     % orientation index

if(drho<0)
  Isp = -Isp;
end

csb = cos(beta);
snb = sin(beta);

ROT = [csb, snb; -snb, csb];   % rotation matrix for graphics

%---
% initial guess for a circular interface
%---

a = sqrt(area/(alpha1-0.5*sin(2.0*alpha1)));
Crc = 1.0/a;
solution = [Crc alpha1];

%---
% loop over surface tension and animate
%---

for repeat=1:100

  gamma = 10.0-repeat*0.10;
  capls = gamma/(gac*abs(drho));   % square of the cap length
```

```
%---
% newton's method for two equations
%---

  Niter = 10;   % maximum number of iterations
  eps = 0.001;   % step for numerical differentiation

  [solution,F,Iflag] = drop_2di1_newton2 ...
    ...
    (Niter ...
    ,eps ...
    ,solution ...
    );

  if(Iflag==1) break; end

%---
% dispense the solution
%---

  C = solution(1)
  alpha2 = solution(2)

  xplot = -y;
  yplot = x;

  for i=1:npts+1
    xx = [xplot(i), yplot(i)];
    xx = ROT*xx';
    xplot(i) = xx(1);
    yplot(i) = xx(2);
  end

  plot(xplot,yplot,'-')

  hold on
   plot(csb*[0.2,-2.5],snb*[-0.2,2.5],'r','LineWidth',3)
  axis equal
  hold off
  pause(0.1)

  if(alpha2<0.05*pi) break; end
  if(alpha2>0.95*pi) break; end

end
```

The shapes of a sessile and a pendant drop for $\alpha_1 = 0.45\pi$ computed using the code are shown in Figure 5.8.2.

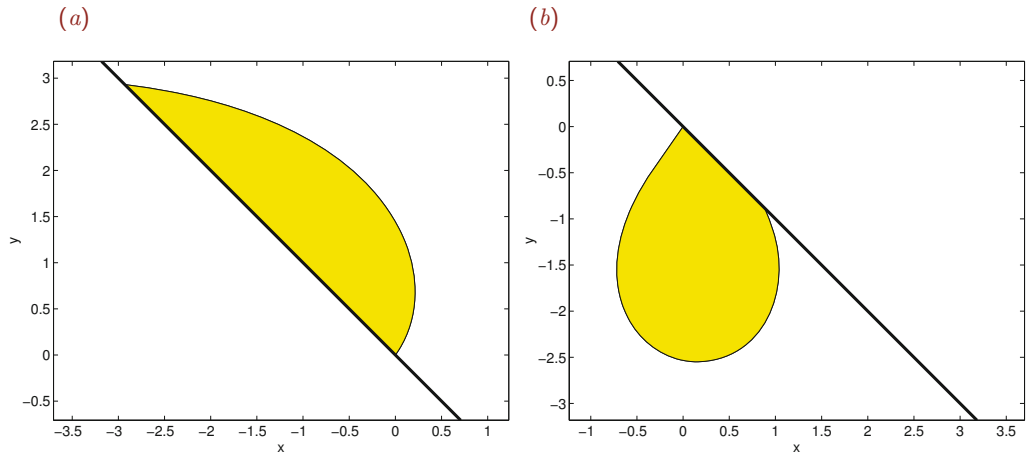

Figure 5.8.2 Interfacial shapes of (a) a sessile two-dimensional drop for inclination angle $\beta = 0.25\,\pi$, and (b) pendant two-dimensional drop for inclination angle $\beta = 1.25\,\pi$, generated by the FDLIB code *drop_2di1*.

Those who can afford access to MATLAB toolboxes may use the internal MATLAB function *fsolve* for solving the two nonlinear equations instead of the custom-made function *drop_2di1_newton2*. Bear in mind that some programmers consider the usage of a *global* statement an anathema.

5.8.2 Specified contact points

Consider a physical experiment where a droplet is placed on a horizontal plane and adjusts to a symmetric equilibrium shape corresponding to a specified static contact angle at both contact points, α. The distance between the two contact points is denoted by d, as shown in Figure 5.8.1.

The plane is now rotated and the drop deforms while both contact points remain pinned at the plane. Instead, the first and second contact angles, α_1 and α_2, deviate from the reference value α in response to the changing orientation of the acceleration of gravity vector with respect to the inclination of the plane. In the physical world, the contact points will remain stationary only if the two contact angles are confined inside a contact angle hysteresis window bounded by the advancing and receding contact lines.

For each plane inclination angle, the three unknowns, C, α_1, and α_2, must be found as part of the solution to satisfy (a) the requirement on the drop area expressed by (5.8.10), and (b) the two second contact point conditions

$$X(\alpha_2) = 0, \qquad Y(\alpha_2) = d. \tag{5.8.13}$$

A shooting method can be implemented according to the following steps:

1. Guess values for C, α_1, and α_2.
2. Integrate the system of equations (5.8.6) with initial conditions provided in (5.8.8).
3. Compute the integral on the right-hand side of (5.8.10) using the trapezoidal rule.
4. Evaluate the three components of the objective function

$$F(1) = X(\alpha_2), \qquad F(2) = Y(\alpha_2) - d, \qquad F(3) \equiv \int_0^d X \, \mathrm{d}y - A_{\mathrm{D}}. \tag{5.8.14}$$

5. Improve the values of C, α_1, and α_2, to drive the three components of the objective function, $F(1)$, $F(2)$, and $F(3)$, to zero

$$F(1) = 0, \qquad F(2) = 0, \qquad F(3) = 0, \tag{5.8.15}$$

and return to Step 2.

The following MATLAB function entitled *drop_2di2_ode*, located in directory *drop_2di* inside directory *03_hydrostat* of FDLIB, solves the system of equations (5.8.6) and computes the three components of the objective function, **F**:

```
function F = drop_2di2_ode (solution)

%-------------------------------------------
% Two-dimensional drop on an inclined plane.
%
% Integrate ODEs by the RK4 method with uniform
% step size for the slope angle psi
%
% SYMBOLS:
% -------
%
% dpsi:  increments in psi
% C: shooting parameter
%-------------------------------------------

global area capls Isp npts beta alpha1 alpha2 d x y

%--------
% dispense variables
%--------

C = solution(1);
alpha1 = solution(2);
alpha2 = solution(3);

%--------
% prepare
%--------
```

```
csb = cos(beta);
snb = sin(beta);
dpsi = (alpha1+alpha2)/npts;
dpsih = 0.5*dpsi;

%----------------
% first contact point
%----------------

psi = -alpha1; x(1) = 0.0; y(1) = 0.0;

%----------
% integrate
%----------

for i=1:npts

  Q = Isp*(csb*x(i)+snb*y(i))/capls-C;
  xp = sin(psi)/Q; yp =-cos(psi)/Q;
  xp1 = xp; yp1 = yp;

  psi = psi +dpsih;
  x(i+1) = x(i)+xp*dpsih;
  y(i+1) = y(i)+yp*dpsih;

  Q = Isp*(csb*x(i+1)+snb*y(i+1))/capls-C;
  xp = sin(psi)/Q; yp =-cos(psi)/Q;
  xp2 = xp; yp2 = yp;

  x(i+1) = x(i)+xp*dpsih;
  y(i+1) = y(i)+yp*dpsih;

  Q = Isp*(csb*x(i+1)+snb*y(i+1))/capls-C;
  xp = sin(psi)/Q; yp =-cos(psi)/Q;
  xp3 = xp; yp3 = yp;

  psi = psi +dpsih;
  x(i+1) = x(i)+xp*dpsi;
  y(i+1) = y(i)+yp*dpsi;

  Q = Isp*(csb*x(i+1)+snb*y(i+1))/capls-C;
  xp = sin(psi)/Q; yp = -cos(psi)/Q;
  xp4 = xp; yp4 = yp;

  x(i+1) = x(i) + (xp1+2*xp2+2*xp3+xp4)*dpsi/6.0;
  y(i+1) = y(i) + (yp1+2*yp2+2*yp3+yp4)*dpsi/6.0;

end
```

```
F(1) = x(npts+1);
F(2) = y(npts+1)-d;

%----------------------------------------
% compute the are of the integrated shape
% by the trapezoidal rule
%----------------------------------------

ar = 0.0;
for i=1:npts
  ar = ar+(x(i+1)+x(i))*(y(i+1)-y(i));
end
ar = 0.5*ar; % to account for trapezoidal weights

F(3) = ar-area;

%-----
% done
%-----

return
```

The improvement in the values of C, α_1, and α_2 in Step 5 of the algorithm can be done using Newton's method for solving a system of three nonlinear equations (5.8.12).[2] The method is implemented in the following FDLIB function entitled *drop_2di2_newton3*, located in directory *drop_2di1* inside directory *03_hydrostat* of FDLIB:

```
function [x,f,Iflag] = drop_2di2_newton3 ...
...
  (Niter ...
  ,eps ...
  ,x ...
  )

%-----------------------------------------------
% Newton's method for three nonlinear equations
%
% SYMBOLS:
% --------
%
% eps:  small interval for computing the Jacobian
% by numerical differentiation
% Dx:  correction vector
% tol:  accuracy
% Iflag:  will set equal to 1 if something is wrong
%-------------------------------------------------
```

[2] Pozrikidis, C. (2008) *Numerical Computation in Science and Engineering.* Second Edition, Oxford University Press.

```
tol = 0.0000001;

%-----------
% initialize
%-----------

Iflag = 1;

%---------------------
% start the iterations
%---------------------

for Iter=1:Niter

f = drop_2di2_ode(x);

%---------------------
% compute the Jacobian
% by numerical differentiation
%---------------------

for j=1:3
  x(j) = x(j)+eps;   % perturb
  f1 = drop_2di2_ode(x);
  x(j) = x(j)-eps;   % reset
  for i=1:3
    Jac(i,j) = (f1(i)-f(i))/eps;
  end
end

%---
% solve the equation:  Jac .  Dx = - f
% for the correction vector Dx
% by Cramer's rule
%---

A11 = Jac(1,1); A12 = Jac(1,2); A13 = Jac(1,3);
A21 = Jac(2,1); A22 = Jac(2,2); A23 = Jac(2,3);
A31 = Jac(3,1); A32 = Jac(3,2); A33 = Jac(3,3);

B1 = -f(1);
B2 = -f(2);
B3 = -f(3);

Det = A11*( A22*A33-A23*A32 ) ...
- A12*( A21*A33-A23*A31 ) ...
+ A13*( A21*A32-A22*A31 );
```

```
Det1 = B1*( A22*A33-A23*A32 ) ...
- A12*( B2*A33-A23*B3 ) ...
+ A13*( B2*A32-A22*B3 );

Det2 = A11*( B2 *A33-A23*B3 ) ...
- B1*( A21*A33-A23*A31 ) ...
+ A13*( A21* B3-B2 *A31 );

Det3 = A11*( A22* B3-A32* B2 ) ...
- A12*( A21* B3-A31* B2 ) ...
+ B1*( A21*A32-A22*A31 );

dx(1) = Det1/Det;
dx(2) = Det2/Det;
dx(3) = Det3/Det;

%--------
% correct
%--------

x(1) = x(1)+dx(1);
x(2) = x(2)+dx(2);
x(3) = x(3)+dx(3);

%-------
% escape
%-------

Iescape = 1;
if(abs(dx(1)) > tol) Iescape = 0; end
if(abs(dx(2)) > tol) Iescape = 0; end
if(abs(dx(3)) > tol) Iescape = 0; end

if(Iescape==1)
  Iflag = 0;
  f = drop_2di2_ode(x);
  return
end

%----
end   % of iterations
%----

%-----
% done
%-----

return
```

The overall method is implemented in the following MATLAB code entitled *drop_2di2*, located in directory *drop_2di* inside directory *03_hydrostat* of FDLIB:

```
%-------------------------------------------------------
% Hydrostatic shape of a two-dimensional
% sessile drop resting on an inclined plane
% or a pendant drop hanging underneath a inclined plane,
% for a specified area and first contact points
%
% This code animates interfacial profiles on a
% continuously rotated plane.
%-------------------------------------------------------

global area capls Isp npts beta alpha1 alpha2 d x y

Jsp = -1;   % pendant
Jsp = 1;   % sessile

gac = 1.0;   % acceleration of gravity
gamma = 2.0;   % surface tension
rhod = 1.0;   % density of the drop
rhoa = 0.0;   % density of the ambient fluid
area = pi;   % drop area

alpha = 0.75*pi;   % contact angle on a plane
npts = 32;   % number of interfacial markers

epsilon = 0.01;   % for the shooting method
maxiter = 16;   % on a horizontal plane
tol = 0.000000001;   % for the shooting method

%---
% compute the drop shape on a horizontal plane
% rcrc:  radius of the circular drop
%---

rcrc = sqrt(area/(alpha-0.5*sin(2.0*alpha)));
B = 1.0/rcrc;

[B,x,y] = drop_2d ...
  ...
  (Jsp,gac,gamma,rhod,rhoa,area ...
  ,alpha,npts,epsilon,maxiter,tol ...
  ,B);

%---
% shift to reset the origin at the wall
%---
```

```
shiftx = x(npts+1);
x = x-shiftx;

%---
% position of the contact line
%---

d = 2*y(npts+1);

%---
% prepare to rotate
%---

drho = rhod-rhoa;   % density difference
Isp = 1.0;   % Isp is an orientation index
if(drho<0) Isp = -1.0; end
capls = gamma/(gac*abs(drho));   % square of the capillary length
npts = 2*npts;
C = B-shiftx/capls;
alpha1 = alpha;
alpha2 = alpha;

%------------
% start rotating
%------------

for repeat=1:1024

  beta = 0.002*(repeat-1.0)*pi;
  csb = cos(beta); snb = sin(beta);
  ROT = [csb, snb; -snb, csb];   % rotation matrix for graphics

  solution = [C alpha1 alpha2];

  Niter = 10;   % number of iterations
  eps = 0.001;   % step for numerical differentiation

  [solution,F,Iflag] = drop_2di2_newton3 ...
    ...
    (Niter ...
    ,eps ...
    ,solution ...
    );

%---
% distribute the solution
%---

  C = solution(1)
```

```
  alpha1 = solution(2)
  alpha2 = solution(3)

% ---
% plot
% ---

  xplot = -y; yplot = y;

  for i=1:npts+1
    xx = [xplot(i), yplot(i)];
    xx = ROT*xx';
    xplot(i) = xx(1);
    yplot(i) = xx(2);
  end

  plot(xplot,yplot,'-')
  hold on
  plot(csb*[0.5,-2.0],snb*[-0.5,2.0],'r','LineWidth',3)
  axis equal
  xlabel('x','fontsize',15)
  ylabel('y','fontsize',15)
  hold off
  pause(0.1)

end
```

Problems

5.8.1 *Two-dimensional drop on a horizontal or inclined plane*

Derive a relation between the constant B introduced in (5.7.2) and the constant C introduced in (5.8.5) for a horizontal plane, $\beta = 0$.

5.8.2 *Two-dimensional drop on an inclined plane*

Write a code that computes interfacial shapes for a fixed drop area and contact points, and unspecified contact lines.

5.9 Axisymmetric meniscus inside a tube

To compute the shape of an axisymmetric interface, we work as in the case of a two-dimensional interface discussed previously in this chapter, with some minor differences. Added considerations include possible subtleties in the computation of the mean curvature and a more pronounced sensitivity to numerical parameters. The new features will be illustrated with reference to the axisymmetric versions of the two-dimensional configurations studied in Sections 5.6 and 5.7.

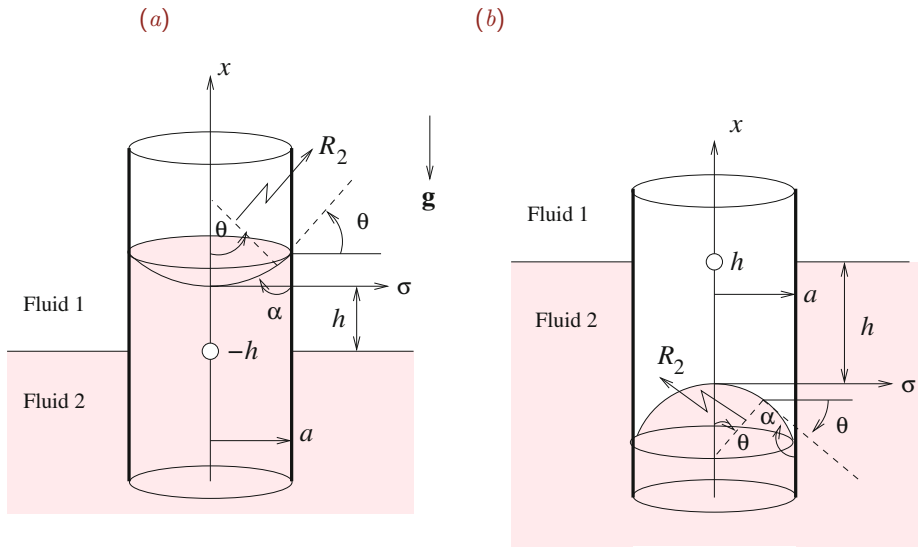

Figure 5.9.1 Illustration of an axisymmetric meniscus inside a vertical circular tube for (a) contact angle α less than $\frac{1}{2}\pi$, and (b) α greater than $\frac{1}{2}\pi/2$.

In this section, we consider the shape of an axisymmetric meniscus inside a vertical cylindrical tube of radius a, as illustrated in Figure 5.9.1. The axisymmetric meniscus is the counterpart of the two-dimensional meniscus between two vertical plates shown in Figure 5.6.1.

In cylindrical polar coordinates, (x, σ), the axisymmetric meniscus can be described by a function,

$$x = f(\sigma), \tag{5.9.1}$$

where the ordered pair (σ, x) comprise Cartesian coordinates in an azimuthal plane with origin positioned such that $f(0) = 0$, as shown in Figure 5.9.1. Regularity requires that $f'(0) = 0$, and the condition on the contact angle requires that

$$f'(a) = \cot\alpha. \tag{5.9.2}$$

Outside the tube, the interface assumes a flat horizontal shape with vanishing curvature located at $x = -h$, where h is positive in Figure 5.9.1(a) and negative in Figure 5.9.1(b).

The pressure distributions in the two fluids are given by

$$p^{(1)}(y) = -\rho_1 g y + \pi_1, \qquad p^{(2)}(y) = -\rho_2 g y + \pi_2, \tag{5.9.3}$$

where π_1 and π_2 are two reference pressures.

Laplace–Young equation

Our main objective is to compute the capillary rise, h, along with the unknown meniscus shape by solving the Laplace–Young equation (5.4.14). In the present problem, this equation takes the specific form

$$2\,\kappa_m = -\frac{\Delta\rho\, g}{\gamma}\, x + B, \tag{5.9.4}$$

where κ_m is the mean curvature, $B \equiv (\pi_2 - \pi_1)/\gamma$ is a constant, and $\Delta\rho \equiv \rho_2 - \rho_1$.

Evaluating equation (5.9.4) at a point outside and far from the tube where the mean curvature of the interface tends to vanish and the interfacial elevation tends to $-h$, we obtain the relation

$$B = -\frac{h}{\lambda^2}, \tag{5.9.5}$$

where h is the capillary rise and $\lambda^2 \equiv \gamma/(\Delta\rho\, g)$ is the square of the capillary length, under the assumption that $\Delta\rho \equiv \rho_2 - \rho_1 > 0$.

Combining the last two equations, we obtain the governing equation

$$2\,\kappa_m = -\frac{f + h}{\lambda^2}, \tag{5.9.6}$$

involving the *a priori* unknown capillary rise, h. The numerator of the fraction on the right-hand side, $f + h$, is the elevation of the meniscus with respect to the flat interface outside the tube.

Mean curvature

The mean curvature is given by formulas (4.4.33) and (4.4.34), repeated below for convenience,

$$2\,\kappa_m = -\frac{1}{\sigma}\left(\sigma\,\frac{f'}{\sqrt{1+f'^2}}\right)' = -\frac{f''}{(1+f'^2)^{3/2}} - \frac{1}{\sigma}\,\frac{f'}{\sqrt{1+f'^2}} \tag{5.9.7}$$

and

$$2\,\kappa_m = \frac{1}{f'}\left(\frac{1}{\sqrt{1+f'^2}}\right)' - \frac{1}{\sigma}\,\frac{f'}{\sqrt{1+f'^2}}, \tag{5.9.8}$$

where a prime denotes a derivative with respect to σ.

Applying equation (5.9.6) at the origin, $x = 0$, where $f' = 0$, we find that

$$\frac{h}{\lambda^2} = -2\kappa_m^0 = 2f''(0) \tag{5.9.9}$$

where $\kappa_m^0 = \kappa_m(0)$ is the centerline mean curvature.

Meniscus height

Substituting the expression for the mean curvature given in (5.9.8) into the left-hand side of the Laplace–Young equation (5.9.6), multiplying by f', and rearranging, we obtain

$$\Big(\frac{1}{\sqrt{1+f'^2}}\Big)' - \frac{1}{\sigma}\,\frac{f'^2}{\sqrt{1+f'^2}} = -\frac{1}{\lambda^2}\,\big[\,\tfrac{1}{2}\,(f^2)' + hf'\,\big]. \tag{5.9.10}$$

Integrating with respect to σ across the tube radius from $\sigma = 0$ to a, we obtain

$$1 - \sin\alpha = \frac{1}{\lambda^2}\,\big(\,\tfrac{1}{2}\,d + h\,\big)\,d - \mathcal{J}, \tag{5.9.11}$$

where

$$\mathcal{J} \equiv \int_0^a \frac{1}{\sigma}\,\frac{f'^2}{\sqrt{1+f'^2}}\mathrm{d}\sigma. \tag{5.9.12}$$

The appearance of the integral $\mathcal{J}$, associated with the second principal curvature, distinguishes the axisymmetric from the two-dimensional meniscus discussed in Section 5.6.

Vertical force balance

Substituting the first expression for the mean curvature given in (5.9.7) into the left-hand side of the Laplace–Young equation (5.9.6), and multiplying both sides by σ, we obtain

$$\Big(\sigma\,\frac{f'}{\sqrt{1+f'^2}}\Big)' = \frac{f+h}{\lambda^2}\,\sigma. \tag{5.9.13}$$

Integrating with respect to σ from 0 to a and noting that $f'(a) = \cot\alpha$, we obtain

$$a\,\cos\alpha = \frac{1}{\lambda^2}\int_0^b (f+h)\,\sigma\,\mathrm{d}x. \tag{5.9.14}$$

This equation expresses a balance between the weight of the fluid inside the tube above or below the flat interface, the buoyancy force, and the capillary force at the circular contact line.

Differential equations

Substituting the second expression for the mean curvature given in (5.9.7) into the left-hand side of the Laplace–Young equation (5.9.6), and rearranging, we derive a second-order differential equation,

$$f'' = (1+f'^2)\,\Big(\,-\frac{f'}{\sigma} + \sqrt{1+f'^2}\,\frac{f+h}{\lambda^2}\,\Big). \tag{5.9.15}$$

An equivalent first-order system is

$$\frac{\mathrm{d}f}{\mathrm{d}\sigma} = q, \qquad \frac{\mathrm{d}q}{\mathrm{d}\sigma} = (1+q^2)\,\Big(\,-\frac{q}{\sigma} + \sqrt{1+q^2}\,\frac{f+h}{\lambda^2}\,\Big). \tag{5.9.16}$$

The first equation defines the slope function q, and the second equation enforces the Laplace–Young equation.

Parametric representation

It is expedient to describe the shape of the interface in parametric form in terms of the slope angle θ, varying from 0 at the centerline of the tube to the value $\frac{1}{2}\pi - \alpha$ at the inner wall of the tube, defined by

$$f' = \tan\theta, \tag{5.9.17}$$

where α is the contact angle, as shown in Figure 5.9.1. The axial and radial positions of a point at the interface are described by the functions

$$x = X(\theta), \qquad \sigma = \Sigma(\theta). \tag{5.9.18}$$

In terms of the slope angle, the mean curvature is given by the expressions

$$2\,\kappa_m = \frac{1}{\tan\theta}\frac{\mathrm{d}}{\mathrm{d}\sigma}\left(\frac{1}{\sqrt{1+\tan^2\theta}}\right) - \frac{\sin\theta}{\sigma} = \frac{1}{\tan\theta}\frac{\mathrm{d}\cos\theta}{\mathrm{d}\sigma} - \frac{\sin\theta}{\sigma} \tag{5.9.19}$$

and

$$2\,\kappa_m = -\cos\theta\,\frac{\mathrm{d}\theta}{\mathrm{d}\sigma} - \frac{\sin\theta}{\sigma}. \tag{5.9.20}$$

In the case of a raised meniscus depicted in Figure 5.9.1(a), the angle θ is positive and the second principal radius of curvature is negative, $R_2 < 0$. In the case of a submerged meniscus depicted in Figure 5.9.1(b), θ is negative and $R_2 > 0$.

Substituting expression (5.9.20) into the left-hand side of the Laplace–Young equation (5.9.6) and rearranging, we obtain the differential equation

$$\frac{\mathrm{d}\Sigma}{\mathrm{d}\theta} = \frac{\cos\theta}{Q}, \tag{5.9.21}$$

where

$$Q \equiv \frac{X+h}{\lambda^2} - \frac{\sin\theta}{\Sigma}. \tag{5.9.22}$$

Equation (5.9.21) governs the parametric representation of the radial position, $\sigma = \Sigma(\theta)$, in terms of the slope angle, θ. To derive a corresponding equation for the axial position X, we combine the definition

$$f' = \tan\theta = \frac{\mathrm{d}X}{\mathrm{d}\Sigma} \tag{5.9.23}$$

with equation (5.9.21), and obtain

$$\frac{\mathrm{d}X}{\mathrm{d}\theta} = \frac{\sin\theta}{Q}. \tag{5.9.24}$$

The boundary conditions require that $\Sigma = 0$ and $X = 0$ at $\theta = 0$, and $\Sigma = a$ at $\theta = \frac{1}{2}\pi - \alpha$.

Evaluation at the origin

An apparent difficulty is encountered when we attempt to evaluate the function Q defined in (5.9.22) at $\theta = 0$, corresponding to the centerline, $\Sigma = 0$, as the second fraction on the right-hand side becomes undefined.

However, using the l'Hôpital rule, we find that, as θ tends to zero, this ratio reduces to the derivative $\mathrm{d}\theta/\mathrm{d}\Sigma$. Substituting this asymptotic limit into (5.9.22) and the result into (5.9.21) and (5.9.24), we derive the regularized initial conditions

$$\left(\frac{\mathrm{d}\Sigma}{\mathrm{d}\theta}\right)_{\theta=0} = 2\,\frac{\lambda^2}{h}, \qquad \left(\frac{\mathrm{d}X}{\mathrm{d}\theta}\right)_{\theta=0} = 0, \tag{5.9.25}$$

which are used to start up the integration.

Computer code

The following MATLAB function entitled *men_ax_ode*, located in directory *men_ax* inside subdirectory *03_hydrostat* of FDLIB, integrates the differential equations using the modified Euler method subject to a given value for h provided in the input:

```
function [x,s] = men_ax_ode (npts,capls,a,dthet,h)

%-------------------------------------------
% Integrate the ODEs for an axisymmetric meniscus
% by the modified Euler method
%
% npts:  number of integration intervals
% cpls:  square of the capillary length
%-------------------------------------------

%--------
% prepare
%--------

dtheth = 0.5*dthet;

%-----------
% centerline
%-----------

thet = 0.0; s(1) = 0.0; x(1) = 0.0;

%---
for i=1:npts
%---
```

```
if(i==1)
  sp = 2.0*capls/h;
  xp = 0.0D0;
else
  cs = cos(thet);
  sn = sin(thet);
  Q = (x(i)+h)/capls-sn/s(i);
  xp = sn/Q;
  sp = cs/Q;
end

xsv = x(i); % save
ssv = s(i); % save
xpsv = xp;
spsv = sp;

thet = thet+dthet;
x(i+1) = x(i)+xp*dthet;
s(i+1) = s(i)+sp*dthet;

cs = cos(thet);
sn = sin(thet);
Q = (x(i+1)+h)/capls-sn/s(i+1);
xp = sn/Q;
sp = cs/Q;

x(i+1) = xsv + (xpsv+xp)*dtheth;
s(i+1) = ssv + (spsv+sp)*dtheth;

%---
end
%---

%-----
% done
%-----

return
```

Solution by iteration

Since the value of the capillary rise, h, is *a priori* unknown, the solution must be found by iteration. A shooting method for computing h can be implemented according to the following steps:

1. Guess a value for h.
2. Solve equations (5.9.21) and (5.9.24) subject to the initial conditions $\Sigma = 0$ and $X = 0$ at $\theta = 0$.

3. Check whether the condition $\Sigma = a$ at $\theta = \frac{1}{2}\pi - \alpha$ is satisfied. If not, improve the guess using, for example, the secant method discussed in Section 5.7.

A reasonable guess for h at Step 1 can be obtained by assuming that the meniscus has a spherical shape consistent with the prescribed contact angle, α. Using elementary trigonometry, we find that

$$h \simeq 2\,\frac{\lambda^2}{a}\,\cos\alpha. \tag{5.9.26}$$

Note that, when $\alpha > \frac{1}{2}\pi$, the predicted rise is negative, in agreement with physical intuition.

The improvement in Step 3 can be made using the secant method discussed in Section 5.6.1 for the corresponding problem in two dimensions.

The algorithm is implemented in the following MATLAB function entitled *men_ax* located in directory *03_hydrostat* of FDLIB:

```
function [Iflag,x,s,hout] = men_ax ...
...
  (a,gac,gamma,rhop,rhoa ...
  ,alpha,npts ...
  ,epsilon,maxiter,tol ...
  ,hin ...
  )

%-----------------------------------
% shape of an axisymmetric meniscus
% inside a tube of radius computed
% by a shooting method for h
%
% hin:  initial guess for h
%-----------------------------------

Iflag = 0;   % flag for success

%----
% prepare
%----

drho = rhop-rhoa ;   % density difference
%         square of the capillary length:
capls = gamma/(gac*abs(drho));

npts1 = npts+1;

dthet = (0.5*pi-alpha)/npts;

%---------------------
```

```
% initial guess for h
%---------------------

h(1) = hin;

%---
% compute the first solution of the odes
% to start-up the secant method
%---

Ic = 1;   % counter
[x,s] = men_ax_ode(npts,capls,a,dthet,h(Ic));

error(Ic) = s(npts1)-a;

%-------------------------
% second start-up solution
%-------------------------

Ic = 2;
h(2) = h(1)+epsilon;
[x,s] = men_ax_ode(npts,capls,a,dthet,h(Ic));

error(Ic) = s(npts1)-a;

%---------------------------------------
% iterate using the secant method
% until convergence
%---------------------------------------

for iter=1:maxiter

  Ic = Ic+1;

%---
% secant updating
%---

  Icb = Ic-2;
  Ica = Ic-1;

  dedh = (error(Ica)-error(Icb))/(h(Ica)-h(Icb));
  h(Ic) = h(Ica) - error(Ica)/dedh;

  [x,s] = men_ax_ode(npts,capls,a,dthet,h(Ic));

  error(Ic) = s(npts1)-a;

  if(abs(error(Ic))<tol)
```

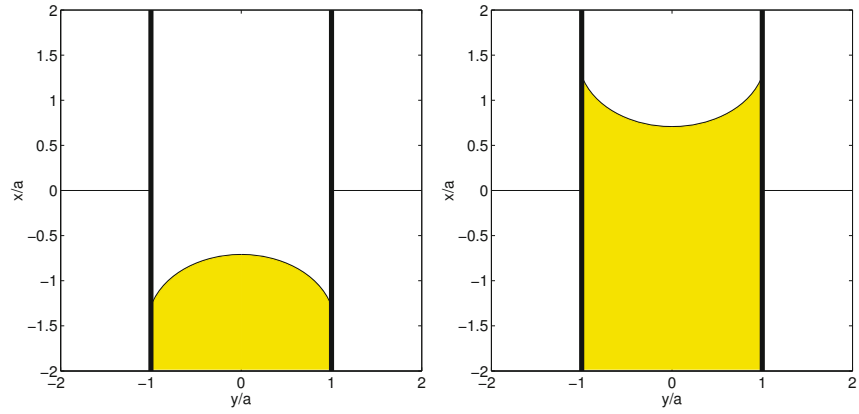

Figure 5.9.2 Shape of a meniscus inside a vertical tube generated by the FDLIB code *men_ax* for two contact angles.

```
    break
  end

%---
end
%---

if(iter==maxiter)
  disp('men_ax:  ODE solver failed')
  Iflag=1;
  return
end

hout = h(Ic);

%---
% done
%---

return
```

Results of computations for a contact angle that is lower than $\frac{1}{2}\pi$ and a contact angle that is higher than $\frac{1}{2}\pi$ are shown in Figure 5.9.2. In the second case, the meniscus submerges below the level of the liquid outside the tube.

Scaling all lengths by the tube radius, a, we find that the shape of the meniscus depends on the contact angle, α, and ratio λ/a. As λ/a increases, the meniscus tends to obtain a spherical shape.

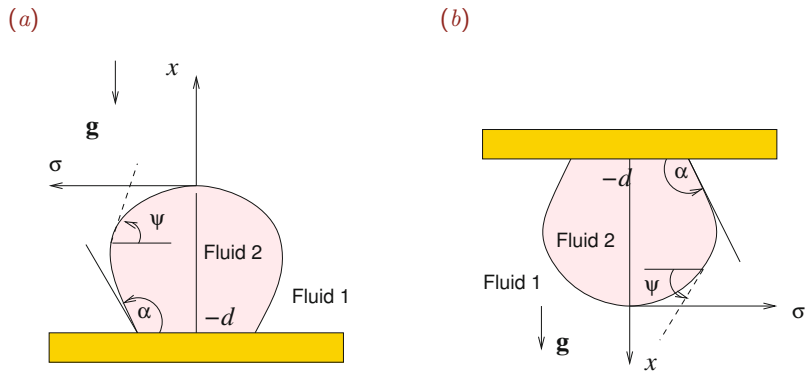

Figure 5.10.1 Illustration of (a) an axisymmetric sessile liquid drop resting on a horizontal plane and (b) an axisymmetric pendant liquid drop hanging under a horizontal plate.

Problem

5.9.1 *Axisymmetric meniscus*

Run the code *men_ax* to generate a family of shapes corresponding to a fixed tube radius and various contact angles. Generate another family of shapes corresponding to a contact angle and various tube radii. Discuss the behavior of the capillary rise in each case.

5.10 Axisymmetric drop on a horizontal plane

Consider an axisymmetric drop of a fluid labeled 2 resting above or hanging underneath a horizontal plane, as shown in Figure 5.10.1. The drop is surrounded by an ambient fluid labeled 1. The resting drop shown in Figure 5.10.1(a) is a *sessile* drop, while the hanging drop shown in Figure 5.10.1(b) is a *pendant* drop.

Our objective is to compute the shape of the interface for specified surface tension, γ, contact angle, α, and drop volume, $V_{\rm D}$. The forthcoming analysis also applies for a gas bubble regarded as a zero-density drop, $\rho_2 = 0$.

The pressure distribution in the two fluids is given by the familiar expressions

$$p^{(1)}(x) = -s_1\rho_1 g x + \pi_1, \qquad p^{(2)}(x) = -s_1\rho_2 g x + \pi_2, \tag{5.10.1}$$

where π_1 and π_2 are two reference pressures. The coefficient s_1 is equal to 1 for a sessile drop or -1 for a pendant drop, reflecting the orientation of gravity with respect to the positive direction of the x axis. The shape of the interface is governed by the Laplace–Young equation stated in (5.4.14),

$$2\,\kappa_m = -s_1\,\frac{\Delta\rho\, g}{\gamma}\,x + B, \tag{5.10.2}$$

where κ_m is the mean curvature of the interface, $\Delta\rho = \rho_2 - \rho_1$, and $B \equiv (\pi_2 - \pi_1)/\gamma$ is an *a priori* constant with units of inverse length. In terms of the square of the capillary length, $\lambda^2 \equiv \gamma/(|\Delta\rho|\, g)$, equation (5.10.2) takes the compact form

$$2\,\kappa_m = -s_1 s_2\,\frac{x}{\lambda^2} + B, \tag{5.10.3}$$

where the coefficient s_2 is equal to 1 if $\rho_2 > \rho_1$ or -1 if $\rho_2 < \rho_1$.

Applying equation (5.10.2) at the origin, we find that the constant B is equal to twice the mean curvature of the interface at the centerline,

$$B = 2\,\kappa_m^0, \tag{5.10.4}$$

where we have denoted $\kappa_m^0 = \kappa_m(0)$.

Mean curvature

In Section 4.3, we saw that, if the position of the drop surface is described by a function

$$\sigma = w(x), \tag{5.10.5}$$

then the mean curvature is given by the expressions

$$2\,\kappa_m = -\frac{w''}{(1+w'^2)^{3/2}} + \frac{1}{w}\,\frac{1}{\sqrt{1+w'^2}} = -\Big(\frac{w'}{\sqrt{1+w'^2}}\Big)' + \frac{1}{w}\,\frac{1}{\sqrt{1+w'^2}} \tag{5.10.6}$$

and

$$2\,\kappa_m = \frac{1}{ww'}\Big(\frac{w}{\sqrt{1+w'^2}}\Big)', \tag{5.10.7}$$

where a prime denotes a derivative with respect to x.

Drop height

Substituting the second expression for the mean curvature given in (5.10.6) into the Young–Laplace equation (5.10.3), we obtain

$$-\Big(\frac{w'}{\sqrt{1+w'^2}}\Big)' + \frac{1}{w}\,\frac{1}{\sqrt{1+w'^2}} = -s_1 s_2\,\frac{x}{\lambda^2} + B. \tag{5.10.8}$$

Integrating with respect to x across the height of the drop from $x = -d$ to 0, we obtain

$$1 - \cos\alpha = 2\,\sin^2\frac{\alpha}{2} = s_1 s_2\,\tfrac{1}{2}\,\frac{d^2}{\lambda^2} + B\,d - \mathcal{J}, \tag{5.10.9}$$

where

$$\mathcal{J} \equiv \int_{-d}^{0} \frac{1}{w}\,\frac{\mathrm{d}x}{\sqrt{1+w'^2}} = \int_{-d}^{0} \frac{\sin\psi}{\sigma}\,\mathrm{d}x, \tag{5.10.10}$$

and the slope angle, ψ, is defined by the equation

$$w' = -\cot\psi, \tag{5.10.11}$$

as shown in Figure 5.10.1. The appearance of the integral $\mathcal{J}$ associated with the second principal curvature distinguishes the axisymmetric from the two-dimensional drop discussed in Section 5.7.

When $s_1 s_2 = 1$, the top of the drop is nearly flat due to dominant gravitational effects, $Bd \simeq 0$. Under these conditions, the integral $\mathcal{J}$ can be approximated by integrating around the sides of the drop where $w \simeq b$. Using the two-dimensional meniscus equation (5.5.10), we obtain

$$w' \simeq \frac{1}{\phi}\,\frac{2-\phi^2}{\sqrt{4-\phi^2}} \tag{5.10.12}$$

and approximate

$$\mathcal{J} \simeq \frac{\lambda}{2\,b}\int_0^{d/\lambda} \phi\,\sqrt{4-\phi^2}\,\mathrm{d}\phi = \tfrac{1}{6}\,\frac{\lambda}{b}\,\Big(8-\Big(4-\frac{d^2}{\lambda^2}\Big)^{3/2}\Big), \tag{5.10.13}$$

where $\xi \equiv x + d$ is the distance of the interface from the support and $\phi = \xi/\lambda$. For a nearly flat drop, equation (5.10.9) then gives

$$2\,\sin^2\frac{\alpha}{2} \simeq \tfrac{1}{2}\,\frac{d^2}{\lambda^2} + \tfrac{1}{6}\,\frac{\lambda}{b}\,\Big[8-\Big(4-\frac{d^2}{\lambda^2}\Big)^{3/2}\Big], \tag{5.10.14}$$

which provides us with a relation between the drop height, b, and the radius of the base, b. When the ratio d/λ is small, we obtain

$$d \simeq 2\,\lambda\,\sin\frac{\alpha}{2}, \tag{5.10.15}$$

consistent with the elevation of a semi-infinite meniscus attached to a vertical plate.

Vertical force balance

Substituting the expression for the curvature given in (5.10.7) into the Young–Laplace equation (5.10.3), and rearranging, we obtain

$$\Big(\frac{w}{\sqrt{1+w'^2}}\Big)' = -s_1 s_2\,\tfrac{1}{2}\,\frac{1}{\lambda^2}\,\big[\,(xw^2)' - w^2\,\big] + B\,\tfrac{1}{2}\,(w^2)'. \tag{5.10.16}$$

Integrating with respect to x across the height of the drop from $x = -d$ to 0, we obtain

$$b\,\sin\alpha = s_1 s_2\,\tfrac{1}{2}\,\frac{1}{\lambda^2}\,\Big(\,d\,b^2 - \frac{1}{\pi}\,V_{\mathrm{D}}\,\Big) + \tfrac{1}{2}\,B\,b^2, \tag{5.10.17}$$

where

$$V_{\mathrm{D}} = \pi\int_{-d}^{0} w^2(x)\,\mathrm{d}x \tag{5.10.18}$$

is the drop volume and d is the drop height, as shown in Figure 5.10.1. Given α and V_{D}, equation (5.10.17) can be used to compute b, d, or $B = 2\kappa_m^0$, from knowledge of two others.

In fact, equation (5.10.17) expresses a force balance. To demonstrate this, we note that the additional force exerted on the plane due to the drop is

$$\Delta F_x = -(\pi b^2)\,(p^{(2)} - p^{(1)})_{x=-d} = -(\pi b^2)\,\big(\,s_1 \Delta\rho\, g d + B\gamma\,\big). \tag{5.10.19}$$

Adding to this force the capillary force around the circular contact line, we obtain the total vertical force

$$F_x = \Delta F_x + 2\pi b\gamma \sin\alpha = -s_1 \Delta\rho\, g\, \pi b^2 d - \gamma\, \pi b\,\big(\,Bb - 2\sin\alpha\,\big). \tag{5.10.20}$$

The first term on the right-hand side is the weight of of a cylindrical column of fluid with radius b and height d reduced by the buoyancy force. This force is precisely equal to the weight of the drop reduced by the buoyancy force,

$$F_x = -s_1 \Delta\rho\, g V_{\mathrm{D}}, \tag{5.10.21}$$

yielding the relation

$$s_1 s_2\,(V_{\mathrm{D}} - \pi d\, b^2) = \pi b\, \lambda^2\,\big(\,Bb - 2\sin\alpha\,\big), \tag{5.10.22}$$

which is precisely equation (5.10.17).

Parametric representation

Working as in Section 5.7 for a two-dimensional drop, we describe the interface parametrically in terms of the slope angle ψ defined in Figure 5.10.1 as

$$x = X(\psi), \qquad \sigma = \Sigma(\psi), \tag{5.10.23}$$

where

$$\cot\psi = -\frac{\mathrm{d}\Sigma}{\mathrm{d}X}. \tag{5.10.24}$$

Substituting these expressions into (5.10.7), we obtain

$$2\,\kappa_m = -\frac{1}{\cot\psi}\frac{\mathrm{d}}{\mathrm{d}X}\Big(\frac{1}{(1+\cot^2\psi)^{1/2}}\Big) + \frac{\sin\psi}{\Sigma} = -\frac{1}{\cot\psi}\frac{\mathrm{d}\sin\psi}{\mathrm{d}X} + \frac{\sin\psi}{\Sigma} \tag{5.10.25}$$

and

$$2\,\kappa_m = -\sin\psi\,\frac{\mathrm{d}\psi}{\mathrm{d}X} + \frac{\sin\psi}{\Sigma} = \frac{\mathrm{d}\cos\psi}{\mathrm{d}X} + \frac{\sin\psi}{\Sigma}. \tag{5.10.26}$$

Substituting these expressions into the Young–Laplace equation (5.10.2), we obtain

$$\sin\psi\,\frac{\mathrm{d}\psi}{\mathrm{d}X} - \frac{\sin\psi}{\Sigma} = -\frac{\mathrm{d}\cos\psi}{\mathrm{d}X} - \frac{\sin\psi}{\Sigma} = s_1\,\frac{\Delta\rho\, g}{\gamma}\,X - B. \tag{5.10.27}$$

Rearranging, we obtain

$$\sin\psi \frac{\mathrm{d}\psi}{\mathrm{d}X} = s_1 \frac{\Delta\rho\, g}{\gamma} X - B + \frac{\sin\psi}{\Sigma}, \tag{5.10.28}$$

which provides us with the differential equations

$$\frac{\mathrm{d}X}{\mathrm{d}\psi} = \frac{\sin\psi}{Q}, \qquad \frac{\mathrm{d}\Sigma}{\mathrm{d}\psi} = -\frac{\cos\psi}{Q}, \tag{5.10.29}$$

where

$$Q \equiv \frac{\sin\psi}{\Sigma} + s_1 s_2 \frac{X}{\lambda^2} - B. \tag{5.10.30}$$

We observe that the shape of a bubble on a flat plate, $s_1 = 1$ and $s_2 = -1$, is similar to that of a drop underneath a flat plate, $s_1 = -1$ and $s_2 = 1$.

Since the origin of the x axis is set at the *a priori* unknown highest elevation of the interface where $\psi = 0$,

$$X(0) = 0, \qquad \Sigma(0) = 0. \tag{5.10.31}$$

The constraint on the drop volume, V_D, takes the form

$$\pi \int_{-d}^{0} \Sigma^2 \,\mathrm{d}x = V_\mathrm{D}, \tag{5.10.32}$$

where $x = -d$ describes the position of the plane, as shown in Figure 5.10.1. At the axis of symmetry located at $\sigma = 0$, equations (5.10.29) are replaced by the regularized equations

$$\left(\frac{\mathrm{d}\Sigma}{\mathrm{d}\psi}\right)_{\psi=0} = \frac{2}{B}, \qquad \left(\frac{\mathrm{d}X}{\mathrm{d}\psi}\right)_{\psi=0} = 0, \tag{5.10.33}$$

arising from Taylor series expansions.

Equations (5.10.29) can be solved by the shooting method discussed in Section 5.7 for the corresponding problem in two dimensions. A reasonable guess for the constant B can be obtained by assuming that the interface is a section of a sphere, and then computing the radius of the sphere, ϱ, to satisfy the constraints on the contact angle and drop volume. Using elementary trigonometry, we find that

$$\varrho = \left(\frac{3\, V_\mathrm{D}/\pi}{2 + \cos^3\alpha - 3\cos\alpha}\right)^{1/3}, \tag{5.10.34}$$

and set $B = 2/\varrho$.

A numerical method for solving the boundary-value problem is implemented in a code entitled *drop_ax*, located in directory *03_hydrostat* of FDLIB, not listed in the text. The algorithm incorporates minor modifications of the code *drop_2d* listed in Section 5.7.

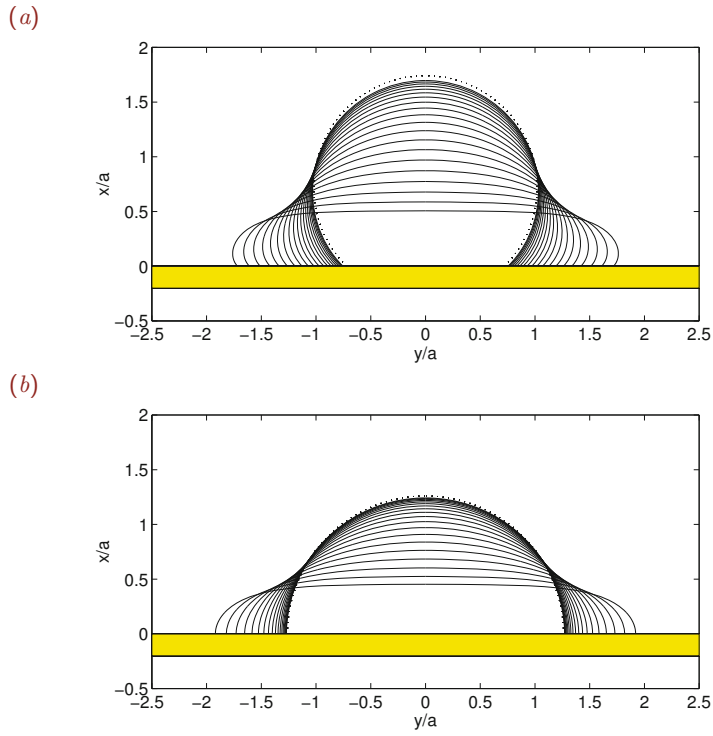

Figure 5.10.2 Shapes of (a) a sessile and (b) a pendant drops for contact angle $\alpha = \frac{3}{4}\pi$ and $\alpha = \frac{1}{4}\pi$ computed by code *drop_ax* of FDLIB. The dotted lines show the approximate spherical shape arising for small drops or large surface tension.

Drop shapes computed using this code are shown in Figure 5.10.2 where the x and y coordinates are scaled by the equivalent drop radius, a, defined by the equation $V_D = 4\pi a^3/3$. Gravity squeezes the sessile drop toward the wall and pulls the pendant drop away from the wall.

Solution space

The numerical method described earlier in this section fails when the drop develops a re-entrant shape near the base. The reason is that, when this occurs, the functions $X(\psi)$ and $\Sigma(\psi)$ cease to be single valued.

To address this difficulty, we integrate the parametric differential equations from $\psi = 0$ up to a specified maximum value $\psi_{\max} < \alpha$, and then continue the integration regarding the radial distance as a function of the axial position, $\sigma = w(x)$. To perform the integration with respect to x, we substitute the expression for the mean curvature given in (5.10.6) into

the Laplace–Young equation and obtain

$$-\frac{w''}{(1+w'^2)^{3/2}}+\frac{1}{\sigma}\,\frac{1}{\sqrt{1+w'^2}}=-\frac{\Delta\rho\,g}{\gamma}\,x+B, \tag{5.10.35}$$

where a prime denotes a derivative with respect to x. Rearranging, we derive the second-order differential equation,

$$w''=(1+w'^2)\left(\frac{1}{w}+\sqrt{1+w'^2}\,(s_1 s_2\frac{x}{\lambda^2}-B)\right), \tag{5.10.36}$$

which can be resolved into a system of two first-order equations,

$$\frac{\mathrm{d}w}{\mathrm{d}x}=q,\qquad \frac{\mathrm{d}q}{\mathrm{d}x}=(1+q^2)\left(\frac{1}{w}+\sqrt{1+q'^2}\,\left(s_1 s_2\frac{x}{\lambda^2}-B\right)\right). \tag{5.10.37}$$

Initial conditions are provided by the values computed at the end of the integration domain with respect to ψ.

The following MATLAB function entitled *drop_ax1_ode*, located in directory *drop_ax* inside directory *03_hydrostat* of FDLIB, integrates successively the two sets of differential equations:

```
function [x,s,Ntot,vlm,slope] = drop_ax1_ode ...
...
(npts1 ...    % number of steps using the psi parametrization
,capls ...    % square of the capillary length
,Isp ...
,psi_max ...
,B ...
,ratio ...    % grading of psi integration intervals
,Next ...    % determines the x position of the drop base
,npts2 ...    % number of steps using the x parametrization
)

%-------------------------------------------
% Integrate ODEs using RK4
% Return the interfacial profile (x, s)
% total number of divisions (Ntot)
% volume of the drop (vlm)
% slope at the base (slope)
%-------------------------------------------

%==============
% first section
%==============

%---------
% set the step size vector dpsi
% so that it increases geometrically
```

```
% by the factor "ratio"
%---------

if(ratio==1)
  alp = 1.0;
  factor = 1.0/npts1;
else
  texp = 1/(npts1-1);
  alp = ratio^texp1;
  factor = (1.0-alp)/(1.0-alp^npts1);
end

dpsi(1) = psi_max*factor;

for i=2:npts1
  dpsi(i) = dpsi(i-1)*alp;
end

%----------------
% top of the drop
%----------------

psi = 0.0;
x(1) = 0.0;
s(1) = 0.0;

%----------
% integrate
%----------

for i=1:npts1

  dpsih(i) = 0.5*dpsi(i);

  if(i==1)
    xp = 0.0;
    sp = 2.0/B;
  else
    Q = sin(psi)/s(i)+Isp*x(i)/capls-B;
    xp = sin(psi)/Q;
    sp =-cos(psi)/Q;
  end

  xp1 = xp;
  sp1 = sp;

  psi = psi +dpsih(i);
  x(i+1) = x(i)+xp*dpsih(i);
  s(i+1) = s(i)+sp*dpsih(i);
```

```
  Q = sin(psi)/s(i+1)+Isp*x(i+1)/capls-B;
  xp = sin(psi)/Q;
  sp =-cos(psi)/Q;
  xp2 = xp;
  sp2 = sp;

  x(i+1) = x(i)+xp*dpsih(i);
  s(i+1) = s(i)+sp*dpsih(i);

  Q = sin(psi)/s(i+1)+Isp*x(i+1)/capls-B;
  xp = sin(psi)/Q;
  sp =-cos(psi)/Q;
  xp3 = xp;
  sp3 = sp;

  psi = psi +dpsih(i);
  x(i+1) = x(i)+xp*dpsi(i);
  s(i+1) = s(i)+sp*dpsi(i);

  Q = sin(psi)/s(i+1)+Isp*x(i+1)/capls-B;
  xp = sin(psi)/Q;
  sp =-cos(psi)/Q;
  xp4 = xp;
  sp4 = sp;

  x(i+1) = x(i) + (xp1+2*xp2+2*xp3+xp4)*dpsi(i)/6.0;
  s(i+1) = s(i) + (sp1+2*sp2+2*sp3+sp4)*dpsi(i)/6.0;

end

Ntot = npts1;

%==============
% continue the integration with a uniform step "dx"
% using the x parametrization up to x = Next*x(npts1+1)
%==============

dx = Next*x(npts1+1)/npts2;

%---
% initial slope
%---

Q = sin(psi)/s(npts1+1)+Isp*x(npts1+1)/capls-B;
xp = sin(psi)/Q;
sp =-cos(psi)/Q;
q(npts1+1) = xp/sp;   % dx/dsigma
```

```
%---
% integrate
%---

for i=npts1+1:npts1+npts2+2

  dsdx = q(i);
  tmp = 1+q(i)*q(i);
  dqdx = tmp*( 1/s(i)+sqrt(tmp)*(Isp*x(i)/capls-B) );
  dsdx1 = dsdx;
  dqdx1 = dqdx;

  x(i+1) = x(i)+0.5*dx;
  s(i+1) = s(i)+0.5*dx*dsdx;
  q(i+1) = q(i)+0.5*dx*dqdx;

  dsdx = q(i+1);
  tmp = 1+q(i+1)*q(i+1);
  dqdx = tmp*( 1/s(i+1)+sqrt(tmp)*(Isp*x(i+1)/capls-B) );
  dsdx2 = dsdx;
  dqdx2 = dqdx;

  x(i+1) = x(i)+0.5*dx;
  s(i+1) = s(i)+0.5*dx*dsdx;
  q(i+1) = q(i)+0.5*dx*dqdx;

  dsdx = q(i+1);
  tmp = 1+q(i+1)*q(i+1);
  dqdx = tmp*( 1/s(i+1)+sqrt(tmp)*(Isp*x(i+1)/capls-B) );
  dsdx3 = dsdx;
  dqdx3 = dqdx;

  x(i+1) = x(i)+dx;
  s(i+1) = s(i)+dx*dsdx;
  q(i+1) = q(i)+dx*dqdx;

  dsdx = q(i+1);
  tmp = 1+q(i+1)*q(i+1);
  dqdx = tmp*( 1/s(i+1)+sqrt(tmp)*(Isp*x(i+1)/capls-B) );
  dsdx4 = dsdx;
  dqdx4 = dqdx;

  s(i+1) = s(i)+dx*(dsdx1+2.0*dsdx2+2.0*dsdx3+dsdx4)/6.0;
  q(i+1) = q(i)+dx*(dqdx1+2.0*dqdx2+2.0*dqdx3+dqdx4)/6.0;

  Ntot = Ntot+1;
  if(s(i+1)<0) break; end

end
```

```
slope = q(i+1);

%-----------------------------------------
% compute the volume of the integrated shape
% by the trapezoidal rule
%-----------------------------------------

vlm = 0.0;
for i=1:Ntot
  vlm = vlm+(s(i+1)*s(i+1)+s(i)*s(i))*abs(x(i+1)-x(i));
end
vlm = 0.5*vlm;   % to account for trapezoidal weights
vlm = pi*vlm;

%-----
% done
%-----

return
```

Families of shapes parametrized by the constant B can be generated by specifying the capillary length, λ, and then computing the numerical parameter `Next` to ensure a specified drop volume. The constant B determines the contact angle implicitly, while the parameter `Next` determines the location of the drop base explicitly. Finding the proper value of `Next` can be done using the secant method.

The numerical procedure is implemented in the following MATLAB function entitled *drop_ax1*, located in directory *drop_ax* inside directory *03_hydrostat* of FDLIB:

```
%----
% Solution branches of a sessile or pendant drop
%----

a = 1.0;   % drop radius
Isp = -1;   % pendant drop
psi_max = 0.25*pi;
npts1 = 24;
npts2 = 48;
ratio = 0.9;
maxiter = 10;   % for secant iterations
tol = 0.0000001;   % for secant iterations

%---
% prepare
%---

volume = 1.0*4*pi*a^3/3;
```

```
%---
% family parameters
%---

capls = 2.0;
Nloop = 2*2*2*2*2*2*128;
Bmin = 1.00;
Bmax = 4.0;
DB = 0.0020;
Nplot = 32;   % will plot after Nplot shapes

%---
% prepare to plot
%---

  figure(1)
  hold on
  xlabel('y/a','fontsize',15)
  ylabel('x/a','fontsize',15)
  set(gca,'fontsize',15)
  axis equal
  box on

  xwall(1) =-1.8; ywall(1) = 0;
  xwall(2) = 1.8; ywall(2) = 0;

  if(Isp==1)
    patch([xwall xwall(2) xwall(1)], ...
    [ywall ywall(2)-0.2 ywall(1)-0.2],'g')
  else
    patch([xwall xwall(2) xwall(1)], ...
    [ywall ywall(2)+0.2 ywall(1)+0.2],'g')
  end

  plot(xwall,ywall,'k')

%---
% prepare to loop
%---

B = Bmin;
Next(1) = 2.0;
Iplot = Nplot;

%============
for Iloop=1:Nloop   % loop over B
%============

  B = B+DB;
```

```
  Ic = 1;     % counter

  [ x,s,Ntot,vlm,slope ] = drop_ax1_ode ...
  ...
  (npts1 ...
  ,capls ...
  ,Isp ...
  ,psi_max ...
  ,B ...
  ,ratio ...
  ,Next(1) ...
  ,npts2 ...
  );

  error(Ic) = vlm-volume;

  Ic = 2;
  Next(Ic) = Next(Ic-1)+0.10;

  [x,s,Ntot,vlm,slope] = drop_ax1_ode ...
  ...
  (npts1 ...
  ,capls ...
  ,Isp ...
  ,psi_max ...
  ,B ...
  ,ratio ...
  ,Next(2) ...
  ,npts2 ...
  );

  error(Ic) = vlm-volume;

%---------------------------------------
% iterate on Next using the secant method
% until convergence
%---------------------------------------

Iconverged = 0;

  for iter=1:maxiter

    Ic = Ic+1;

%---
% secant updating
%---

    Icb = Ic-2;
```

```
    Ica = Ic-1;
    dedc = (error(Ica)-error(Icb))/(Next(Ica)-Next(Icb));
    Next(Ic) = Next(Ica)-error(Ica)/dedc;

    [x,s,Ntot,vlm,slope] = drop_ax1_ode ...
    ...
    (npts1 ...
    ,capls ...
    ,Isp ...
    ,psi_max ...
    ,B ...
    ,ratio ...
    ,Next(Ic) ...
    ,npts2 ...
    );

    error(Ic) = vlm-volume;
    err = abs(error(Ic));

    if(err<tol)
      Iconverged = 1;
      break;
    end

%----
  end
%----

  Next(1) = Next(Ic);

  if(Iplot==Nplot)
    figure(1)
    x = x-x(Ntot+1);   % shift the profile
    plot( s,Isp*x,'k-')
    plot(-s,Isp*x,'k-')
    Iplot = 0;
  end

  Iplot = Iplot+1;

  if(B>Bmax) break; end

%============
end
%============
```

A family of shapes generated by the code is shown in Figure 5.10.2. We observe interesting compact, light-bulb, and hourglass interfacial contours. However, not all of these shapes are stable and therefore expected to occur in practice.

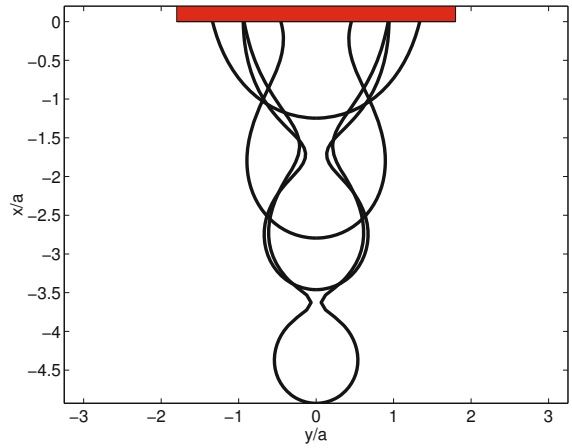

Figure 5.10.2 A family of axisymmetric drop shapes corresponding to a fixed capillary length and varying contact angle.

Problems

5.10.1 *Drop on a plane*

(a) Derive the regularized expressions (5.10.33) departing from equations (5.10.29) and (5.10.30). (b) Derive formula (5.10.34).

5.10.2 *Axisymmetric drops*

Run the code *drop_ax* to generate a family of shapes corresponding to a fixed value drop volume and various contact angles. Generate another family of shapes corresponding to a fixed contact angle and various drop volumes.

5.11 A sphere straddling an interface

In Section 5.2.1, we discussed the equilibrium position of a spherical particle floating on a flat interface. The flat interfacial shape is established under specific conditions, or else when the capillary length, λ, is much smaller than the particle size. A more sophisticated analysis is required under more general circumstances.

Shown in Figure 5.11.1 is a floating sphere of radius a straddling an axisymmetrically deformed and otherwise flat interface. The origin of the x axis is set at the position of the flat interface far from the sphere. The center of the sphere is located at $x = x_c$ and the circular contact line is located at the axial and radial positions

$$x_{\rm cl} = x_c + a\cos\beta, \qquad \sigma_{\rm cl} = a\sin\beta, \tag{5.11.1}$$

where the floating angle, β, varies in the range $[0, \pi]$. In the case of a flat interface, $x_{\rm cl} = 0$ and $x_c = -a\cos\beta$.

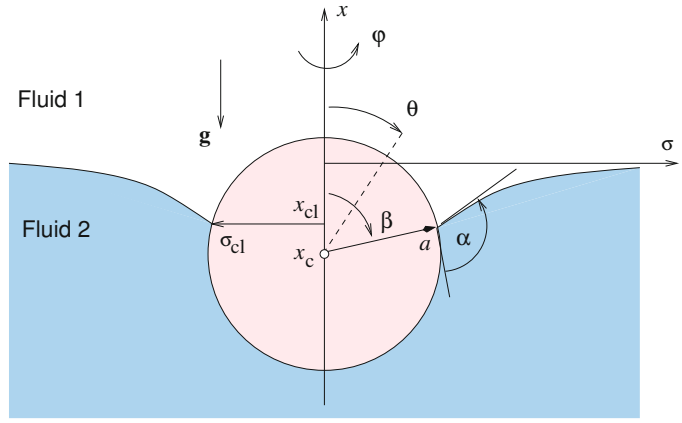

Figure 5.11.1 Illustration of a sphere straddling a curved axisymmetric interface between two fluids.

The shape of the axisymmetric meniscus can be described by a function,

$$x = f(\sigma). \tag{5.11.2}$$

Working as in Section 5.9 for an axisymmetric meniscus, and requiring that the mean curvature of the interface decays to zero far from the particle, as σ tends to infinity, we derive a system of two first-order differential equations,

$$\frac{\mathrm{d}f}{\mathrm{d}\sigma} = q, \qquad \frac{\mathrm{d}q}{\mathrm{d}\sigma} = (1+q^2)\left(-\frac{q}{\sigma} + \sqrt{1+q^2}\,\frac{f}{\lambda^2}\right), \tag{5.11.3}$$

where $\lambda^2 = \gamma/(\Delta\rho g)$ is the square of the capillary length and $\Delta\rho = \rho_2 - \rho_1$ is the density difference between the lower and upper fluids. A Bond number can be defined in the terms of the capillary length as

$$\mathrm{Bo} = \frac{\Delta\rho g a^2}{\gamma} = \left(\frac{a}{\lambda}\right)^2. \tag{5.11.4}$$

Physically, the Bond number is a measure of the extent of the interfacial deformation around the contact line.

The contact line condition requires that

$$f(\sigma_{\mathrm{cl}}) = x_{\mathrm{cl}}, \qquad q(\sigma_{\mathrm{cl}}) = \tan(\alpha - \beta), \tag{5.11.5}$$

and the far-field condition requires that

$$f(\infty) = 0, \tag{5.11.6}$$

where α is the contact angle, as shown in Figure 5.11.1.

The following MATLAB function entitled *flsphere_ode*, located in directory *flsphere* inside directory *03_hydrostat* of FDLIB, integrates the differential equations (5.11.3) using the fourth-order Runge–Kutta method:

```
function [f,s,q] = flsphere_ode (ndiv,smax,capls,xcl,scl,slope);

%=====================================================
% solve ODEs for a semi-infinite axisymmetric meniscus
% by the RK4 method
%
% scl:  sigma of contact line
%
% will integrate from scl to smax
%=====================================================

dsg = (smax-scl)/ndiv;
dsgh = 0.5*dsg;

s(1) = scl;   % starting point
f(1) = xcl;
q(1) = slope;

%---
% integrate
%---

for i=1:ndiv

  fp = q(i);
  tmp = 1+q(i)*q(i);
  tmg = sqrt(tmp)/capls;
  qp = tmp*(-fp/s(i) + f(i)*tmg);
  fp1 = fp;
  qp1 = qp;

  s(i+1) = s(i)+ dsgh;
  f(i+1) = f(i)+fp*dsgh;
  q(i+1) = q(i)+qp*dsgh;
  fp2 = fp;
  qp2 = qp;

  fp = q(i+1);
  tmp = 1+q(i+1)*q(i+1);
  tmg = sqrt(tmp)/capls;
  qp = tmp*(-fp/s(i+1) + f(i+1)*tmg);
  fp3 = fp;
  qp3 = qp;

  f(i+1) = f(i)+fp*dsgh;
  q(i+1) = q(i)+qp*dsgh;

  fp = q(i+1);
  tmp = 1+q(i+1)*q(i+1);
```

```
  tmg = sqrt(tmp)/capls;
  qp = tmp*(-fp/s(i+1) + f(i+1)*tmg);

  s(i+1) = s(i)+ dsg;
  f(i+1) = f(i)+fp*dsg;
  q(i+1) = q(i)+qp*dsg;

  fp = q(i+1);
  tmp = 1+q(i+1)*q(i+1);
  tmg = sqrt(tmp)/capls;
  qp = tmp*(-fp/s(i+1) + f(i+1)*tmg);
  fp4 = fp;
  qp4 = qp;

  f(i+1) = f(i) + (fp1+2*fp2+2*fp3+fp4)*dsg/6.0;
  q(i+1) = q(i) + (qp1+2*qp2+2*qp3+qp4)*dsg/6.0;

end

%---
% done
%---

return
```

Note that the interfacial slope, $q(\sigma_{\rm cl})$, is provided in the last argument of the input.

Force exerted on the sphere

To compute the force exerted on the sphere, we note that the pressure distribution in the upper or lower fluid is given by

$$p^{(1)}(x) = -\rho_1\, g\, x + \pi_0, \qquad p^{(2)}(x) = -\rho_2\, g\, x + \pi_0, \tag{5.11.7}$$

where π_0 is the interfacial pressure far from the sphere. By symmetry, the y and z components of the buoyancy force exerted on the sphere are identically zero. The x component of the buoyancy force is given by

$$F_x^{\rm buoyancy} = -\iint p\, n_x\, {\rm d}S, \tag{5.11.8}$$

where $n_x = \cos\theta$ is the x component of the unit vector normal to the sphere and θ is the meridional angle defined in Figure 5.11.1. Writing

$${\rm d}S = (\sigma\, {\rm d}\varphi)(a\, {\rm d}\theta), \qquad \sigma = a\sin\theta, \tag{5.11.9}$$

and thus

$${\rm d}S = a^2\, \sin\theta\, {\rm d}\theta\, {\rm d}\varphi, \tag{5.11.10}$$

and integrating with respect to the azimuthal angle, φ, we find that

$$F_x^{\text{buoyancy}} = 2\pi a^2 \Big(\int_0^\beta p^{(1)}(\theta) \cos\theta \, \mathrm{d}\cos\theta + \int_\beta^\pi p^{(2)}(\theta) \cos\theta \, \mathrm{d}\cos\theta \Big). \tag{5.11.11}$$

Next, we substitute the expressions for the pressure, set $x = x_c + a\cos\theta$, and simplify to obtain

$$F_x^{\text{buoyancy}} = -2\pi a^2 g \Big(\rho_1 \int_0^\beta (x_c + a\cos\theta) \cos\theta \, \mathrm{d}\cos\theta + \rho_2 \int_\beta^\pi (x_c + a\cos\theta) \cos\theta \, \mathrm{d}\cos\theta \Big). \tag{5.11.12}$$

As expected on physical grounds, the constant π_0 does not make a net contribution to the force. Carrying out the integration, we find that

$$F_x^{\text{buoyancy}} = -2\pi g a^2 \Big(\rho_1 \, x_c \, \frac{\cos^2\beta - 1}{2} + \rho_1 \, a \, \frac{\cos^3\beta - 1}{3} + \rho_2 \, x_c \, \frac{1 - \cos^2\beta}{2} - \rho_2 \, a \, \frac{1 + \cos^3\beta}{3} \Big). \tag{5.11.13}$$

Rearranging, we obtain

$$F_x^{\text{buoyancy}} = \pi g a^2 \Big(x_c \, \Delta\rho \, (\cos^2\beta - 1) + \tfrac{2}{3} \, a \, \Delta\rho \, \cos^3\beta + \tfrac{4}{3} \, a \, \overline{\rho} \Big), \tag{5.11.14}$$

where

$$\overline{\rho} = \tfrac{1}{2} \, (\rho_1 + \rho_2) \tag{5.11.15}$$

is the mean fluid density. When $\rho_1 = \rho_2 = \overline{\rho}$, only the last term survives, yielding the buoyancy force on a submerged sphere.

Surface tension pulls the sphere tangentially to the interface at the contact line. Integrating the tension along the circular contact line, we derive the resultant x component of the capillary force,

$$F_x^{\text{capillary}} = \gamma \, (2\pi\sigma_{\text{cl}}) \, \sin(\alpha - \beta) = 2\pi a \gamma \, \sin\beta \, \sin(\alpha - \beta), \tag{5.11.16}$$

where $\sigma_{\text{cl}} = a \sin\beta$ is the radius of the circular contact line.

Force equilibrium requires that

$$F_x^{\text{buoyancy}} + F_x^{\text{capillary}} = W, \tag{5.11.17}$$

where W is the weight of the sphere. We may set $W = \frac{4\pi}{3} \, a^3 \rho_s g$, where ρ_s is the actual or effective density of the sphere. Simplifying, we derive a force equilibrium equation,

$$\frac{x_c}{a} \, \sin^2\beta = \tfrac{2}{3} \, \cos^3\beta + \tfrac{2}{3} \, \kappa + 2 \, \frac{\lambda^2}{a^2} \, \sin\beta \, \sin(\alpha - \beta), \tag{5.11.18}$$

where

$$\kappa = 2\,\frac{\overline{\rho} - \rho_s}{\Delta\rho} \tag{5.11.19}$$

is a dimensionless parameter. The limits $\kappa \to -1$ or 1 correspond to $\rho_s = \rho_2$ or ρ_1, where the sphere is neutrally buoyant in the lower or upper fluid.

Far-field meniscus

Far from the sphere, the interfacial slope is small. Linearizing the Laplace–Young equation, we obtain the zeroth-order Bessel equation,

$$f'' = -\frac{f'}{\sigma} + \frac{f}{\lambda^2}. \tag{5.11.20}$$

An acceptable solution that decays at infinity is proportional to the modified Bessel function of zeroth order, K_0,

$$f(\sigma) \simeq \xi\, a\, \mathrm{K}_0(\sigma/\lambda), \tag{5.11.21}$$

where ξ is a dimensionless constant. It is beneficial to eliminate the constant ξ by formulating the ratio between the shape function f and its derivative, finding

$$f(\sigma) + \lambda\,\frac{\mathrm{K}_0(\sigma/\lambda)}{\mathrm{K}_1(\sigma/\lambda)}\,f'(\sigma) \simeq 0, \tag{5.11.22}$$

where K_1 is the first-order modified Bessel function. This condition can be applied at a sufficiently large value of σ in place of the far-field condition (5.11.6) to improve the performance of the numerical methods.

Flat interface solution

In the case of a flat interface, $x_c = -a\cos\beta$, the expression for the buoyancy force simplifies to

$$F_x^{\text{buoyancy,flat}} = \pi g a^3 \Delta\rho\,\cos\beta\,(1 - \tfrac{1}{3}\,\cos^2\beta) + \tfrac{2}{3}\,\pi g a^3\,(\rho_2 + \rho_1). \tag{5.11.23}$$

The contact angle is equal to the contact line aperture, $\alpha = \beta$, the capillary force vanishes, and the trigonometric equation (5.11.18) simplifies to a cubic equation for $\cos\beta$,

$$\cos^3\beta - 3\,\cos\beta - 2\,\kappa = 0. \tag{5.11.24}$$

A solution for $\cos\beta$ in the admissible range $[-1, 1]$ exists only when $|\kappa| < 1$.

Solution algorithm

When $|\kappa| < 1$, equation (5.11.18) and the accompanying Laplace–Young equation admit a solution in a limited range of sufficiently high capillary lengths. A numerical method for computing hydrostatic shapes can be implemented according to the following steps:

1. Begin by considering a flat interface, solve the cubic equation (5.11.24) for $\cos\beta$, and recover an approximation to β.
2. Choose a value for the contact angle, $\alpha \simeq \beta$.
3. Solve equation (5.11.18) for x_c to satisfy the vertical force balance.
4. Integrate the system of differential equations (5.11.3) from $\sigma = \sigma_{\rm cl}$ up to a specified distance, $\sigma = \sigma_{\rm max}$, and check whether $f(\sigma_{\rm max}) = 0$. If not, we adjust β to make it so. The adjustment can be done using the secant or Newton's method.
5. Change the contact angle, α, and return to Step 3 to obtain a new configuration.

The procedure ensures that a good initial guess is available for the shooting method, obtained by parameter continuation.

The numerical method is implemented in a MATLAB function entitled *flsphere*, located in directory *03_hydrostat* of FDLIB:

```
function [s,x,q,beta,alpha,xc,xcl,scl ...
            ,beta_flat,xc_flat ...
            ,al_scan,bt_scan,xc_scan] ...
         ...
       = flsphere(a,capl,rho1,rho2,kappa,alphain ...
       ,smax,ndiv ...
         ,mincut,maxcut ...
         ,iplot_shape)

%=====================================================
% Compute families of floating sphere configurations
%
% alphain:  targeted value of alpha
%         (will stop when alpha = alphain)
%=====================================================

%-----------
% parameters
%-----------

eps = 0.0000001;   % for Newton's method
tol = 0.0000001;   % for Newton's method

%---
% will scan the contact angle space with step dal
% that depends on the capillary length
%---

dal = -0.005;

if(capl<1.5) dal = -0.002; end
```

```
if(capl<0.9) dal = -0.001; end
if(capl<0.8) dal = -0.0005; end

Nmax = 2*abs(floor(pi/dal))   % to prevent run off

%----
% prepare
%---

Drho = rho2-rho1;
Brho = 0.5*(rho1+rho2);     % mean fluid density
rhos = Brho-0.5*kappa*Drho;     % density of the sphere
capls = capl^2;     % square of the capillary number

%----
% flat interface solution
%
% computed by solving a cubic equation using
% the "roots" matlab function (internal)
%---

C(1) = 1.0;
C(2) = 0.0;
C(3) = -3.0;
C(4) = -2*kappa;

cosbeta = roots(C);   % roots() is an internal matlab function

if(abs(cosbeta(1))<1)
  beta = acos(cosbeta(1));
elseif(abs(cosbeta(2))<1)
  beta = acos(cosbeta(2));
elseif(abs(cosbeta(3))<1)
  beta = acos(cosbeta(3));
end

xc = -a*cos(beta);
beta_flat = beta; xc_flat = xc;

%---
% prepare to scan the contact angle (alpha)
%---

Ido = 1;
Iflag = 0;
Icount = 0;   % counter
Jcount = 0;   % counter
Irecord = 1;   % recording flag
alpha = beta;   % flat plate contact angle
```

```
%---
while(Ido==1)     % loop over contact angles
%---

Icount = Icount+1;

itermax = 20;

for iter=1:itermax

%---
% solve for beta using Newton's method
%---

  cs = cos(beta);
  sn = sin(beta);
  amb = alpha-beta;
  xc = (2/3*cs^3 + 2/3*kappa + 2*capls/a^2*sn*sin(amb))/sn^2;
  xcl = xc+a*cs;
  scl = a*sn;
  slope = tan(amb);

  [x,s,q] = flsphere_ode(ndiv,smax,capls,xcl,scl,slope);

%   obj = x(ndiv+1);   % primary far-field
  arg = s(ndiv+1)/capl;   % far-field from asymptotics
  obj = x(ndiv+1) + capl*besselk(0,arg) ...
  /besselk(1,arg)*q(ndiv+1);

  if(abs(obj)<tol) break; end
  beta = beta+eps;
  cs = cos(beta);

  sn = sin(beta);
  amb = alpha-beta;
  xc = (2/3*cs^3 + 2/3*kappa + 2*capls/a^2*sn*sin(amb))/sn^2;
  xcl = xc+a*cs;
  scl = a*sn;

  slope = tan(amb);

  [x1,s1,q1] = flsphere_ode(ndiv,smax,capls,xcl,scl,slope);

%   obj1 = x1(ndiv+1);   % primary far-field
  arg1 = s1(ndiv+1)/capl;   % far-field from asymptotics
  obj1 = x1(ndiv+1) + capl*besselk(0,arg) ...
  /besselk(1,arg)*q1(ndiv+1);
```

```
  beta = beta-eps;   % reset
  der = (obj1-obj)/eps;
  correction = -obj/der;
  beta = beta+correction;

  if(abs(correction)<0.0000001) break; end

end   % of Newton iterations

if(iter==itermax)
  disp("flsphere:  Newton iterations did not converge")
  return
end

cs = cos(beta);
sn = sin(beta);
amb = alpha-beta;
xc = (2/3*cs^3 + 2/3*kappa + 2*capls/a^2*sn*sin(amb))/sn^2;

%==============
% plotting session
%==============

%---
if(iplot_shape==1)
%---

  figure(10)
  hold on
  xlabel('y/a','fontsize',15)
  ylabel('x/a','fontsize',15)

%---
% plot the interface profile
%---

  plot(s,x,'k');
  plot(-s,x,'k');
  axis equal

%---
% plot the particle contour
%---

  ncrc=64;

  for i=1:ncrc+1
    tht = (i-1)*2*pi/ncrc;
    xcrc(i) = xc+a*cos(tht);
```

```
    scrc(i) = a*sin(tht);
  end

  plot(scrc,xcrc,'k');
  patch(scrc,xcrc,'y');
  pause(0.001)

%======
end   % of plotting
%======

if(Irecord==1)
  Jcount = Jcount +1;
  al_scan(Jcount) = alpha/pi;
  bt_scan(Jcount) = beta/pi;
  xc_scan(Jcount) = xc/a;
end

if(Iflag==1)
  break;
end

alpha = alpha+dal;

%-------
% change alpha scanning direction or lock
%-------

if(alpha<0.01*pi)
  dal = abs(dal);
  alpha = alpha + dal;
elseif(alpha>0.99*pi)
  dal = -abs(dal);
  alpha = alpha+dal;
elseif(abs(alpha-alphain)<1.0*abs(dal))   % lock on alphain
  alpha = alphain + 0.00;
  Iflag = 1;
end

if(Icount>Nmax) break; end

%---
end
%---

return
```

Nondimensionalizing lengths by the sphere radius, a, we find that the interfacial profile depends on the ratio of the capillary length to the sphere radius, λ/a, the density difference

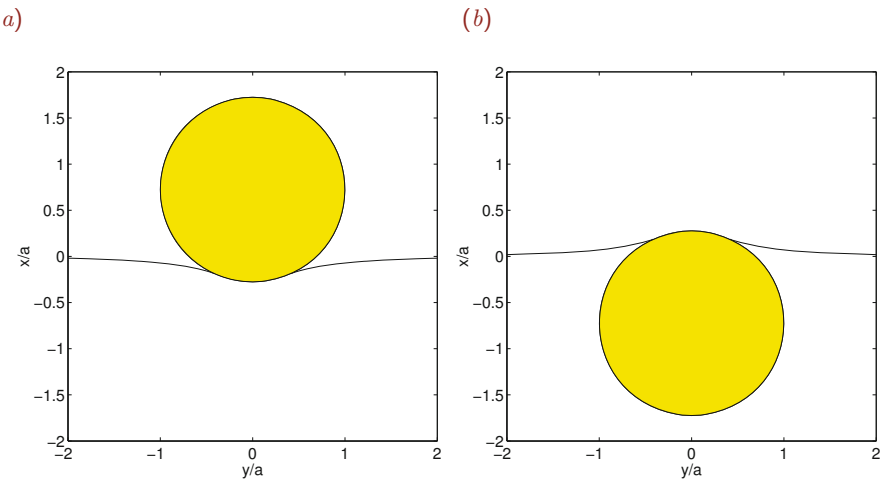

Figure 5.11.2 Axisymmetric interfacial profiles attached to a floating sphere for $\lambda/a = 1$ and (a) $\kappa = 0.5$, $\alpha = 0.98\pi$, or (b) $\kappa = -0.5$, $\alpha = 0.0242\pi$.

ratio, κ, and the contact angle, α. Two interfacial shapes are shown in Figure 5.11.2(a, b). In Figure 5.11.2(a), a heavy hydrophobic particle is kept afloat. In Figure 5.11.2(b), a light hydrophilic particle is held captive.

Graphs of the particle center position against the contact angle, α, are shown in Figure 5.11.3 for $\kappa = 0$ and $\frac{1}{2}$. When $\kappa = 0$ and the contact angle is $\alpha = \frac{1}{2}\pi$, the interface is flat and the particle is divided equally between the upper and lower fluids, independent of the capillary length. When $\kappa = \frac{1}{2}$, the interface is flat at a certain contact angle that is insensitive to the capillary length. The particle center position for $\kappa = -\frac{1}{2}$ is the mirror image of that for $\kappa = \frac{1}{2}$, subject to a reflection in the contact angle. As λ/a increases, the particle center becomes independent of κ and is given by $x_c = -a\cos\alpha$.

Spheroidal particle

As a straightforward generalization, we consider the equilibrium position of a floating spheroidal particle whose axis revolution is parallel to the acceleration of gravity, as shown in Figure 5.11.4. The origin of the x axis is set at the position of the infinite flat interface far from the particle.

The elliptical particle contour in an azimuthal plane is described by the equations

$$x = x_c + a\cos\zeta, \qquad \sigma = b\sin\zeta, \tag{5.11.25}$$

where x_c describes the location of the particle center, a and b are the particle semi-axes, and the parameter ζ varies from 0 at the top of the particle to π at the bottom of the particle, as shown in Figure 5.11.4. The parameter ζ should not be confused with the meridional angle, θ. They are equal only in the case of a spherical particle.

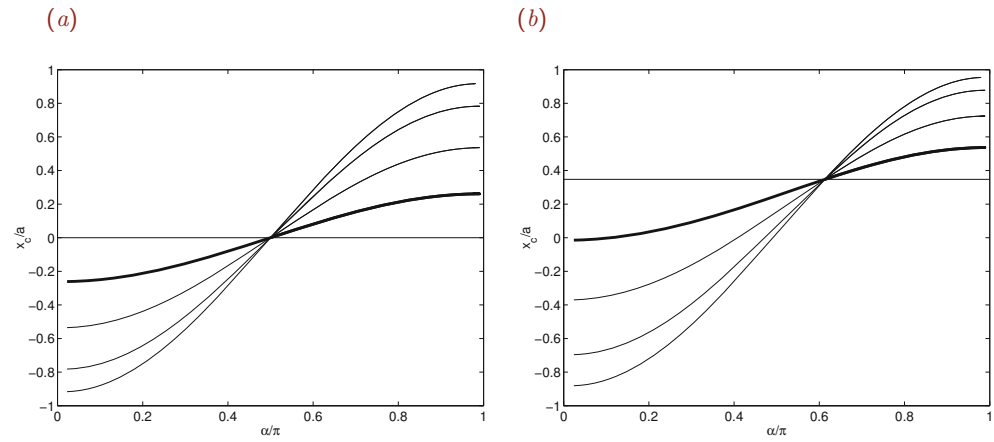

Figure 5.11.3 Floating spherical particle center position for $\lambda/a = 0.5$ (bold lines), 1.0, 2.0, and 4.0, and (a) $\kappa = 0$ or (b) 0.5.

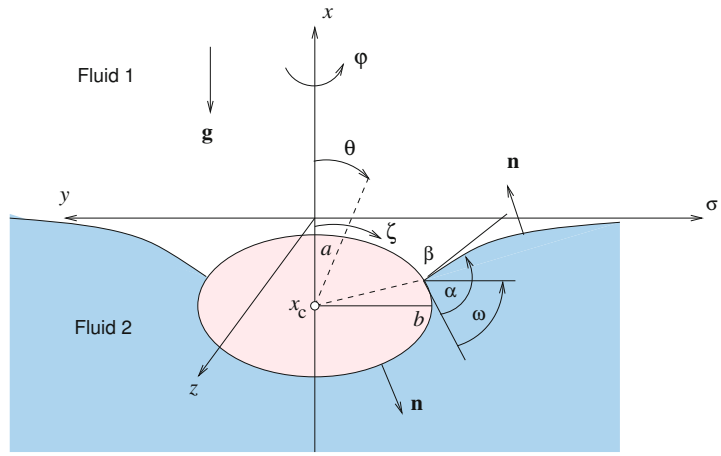

Figure 5.11.4 Illustration of a spheroidal particle floating at the interface between two immiscible fluids. The axis of revolution is normal to the plane of the undisturbed interface.

The circular contact line is located at the axial position

$$x_{\rm cl} = x_c + a\cos\beta \tag{5.11.26}$$

and at the radial position

$$\sigma_{\rm cl} = b\sin\beta, \tag{5.11.27}$$

where the parameter β varies in the range $[0, \pi]$. In the case of a flat interface, $x_{\rm cl} = 0$ and

$x_c = -a\cos\beta$. The shape of the meniscus is governed by the equations described previously in this section for a spherical particle.

Buoyancy force

The vertical component of the force exerted on the spheroidal particle is given in equation (5.11.8),

$$F_x^{\text{buoyancy}} = -\iint p\, n_x \,\mathrm{d}S, \tag{5.11.28}$$

where n_x is the x component of the unit vector normal to the spheroid. Introducing the arc length around the particle contour, ℓ, measured in the direction of increasing parameter ζ, setting

$$\mathrm{d}S = 2\pi\sigma \mathrm{d}\ell, \qquad n_x = \frac{\mathrm{d}\sigma}{\mathrm{d}\ell}, \qquad n_x\,\mathrm{d}S = 2\pi\,\mathrm{d}\sigma, \tag{5.11.29}$$

and performing the integration around the axis of revolution, we derive an expression for the x component of the buoyancy force,

$$F_x^{\text{buoyancy}} = -\pi b^2 \int_0^{\pi} p\,\sin 2\zeta\,\mathrm{d}\zeta. \tag{5.11.30}$$

Now we recall that $\zeta = \beta$ marks the location of the contact line in the two fluids and write

$$F_x^{\text{buoyancy}} = -\pi b^2 \Big(\int_0^{\beta} p^{(1)}\,\sin 2\zeta\,\mathrm{d}\zeta + \int_{\beta}^{\pi} p^{(2)}\,\sin 2\zeta\,\mathrm{d}\zeta \Big). \tag{5.11.31}$$

Substituting the expressions for the pressure, and setting $x = x_c + a\cos\zeta$, we obtain

$$\begin{aligned} F_x^{\text{buoyancy}} = -2\pi b^2 g \,\big(\rho_1 \int_0^{\beta} (x_c + a\cos\zeta)\cos\zeta\,\mathrm{d}\cos\zeta \\ + \rho_2 \int_{\beta}^{\pi} (x_c + a\cos\zeta)\,\cos\zeta\,\mathrm{d}\cos\zeta \,\big). \end{aligned} \tag{5.11.32}$$

Carrying out the integration, we find that

$$\begin{aligned} F_x^{\text{buoyancy}} = 2\pi g b^2 \,\big(\rho_1 x_c \,\frac{\sin^2\beta}{2} - \rho_1 a\,\frac{\cos^3\beta - 1}{3} \\ - \rho_2 x_c\,\frac{\sin^2\beta}{2} + \rho_2 a\,\frac{1+\cos^3\beta}{3}\,\big). \end{aligned} \tag{5.11.33}$$

Rearranging, we obtain

$$F_x^{\text{buoyancy}} = \pi g b^2 \big(-x_c\,\Delta\rho\,\sin^2\beta + \tfrac{2}{3}\,a\,\Delta\rho\,\cos^3\beta + \tfrac{4}{3}\,a\,\overline{\rho}\,\big) \tag{5.11.34}$$

involving the *a priori* unknown particle center position, x_c.

Capillary force

The x component of the capillary force is given by

$$F_x^{\text{capillary}} = \gamma\,(2\pi\sigma_{\text{cl}})\,\sin(\alpha-\omega), \tag{5.11.35}$$

where ω is the angle subtended between the tangent vector and the σ axis at the contact line, as shown in Figure 5.11.4, given by

$$\omega = \arctan\Big(\frac{b}{a}\,\tan\beta\Big). \tag{5.11.36}$$

Substituting $\sigma_{\text{cl}} = b\,\sin\beta$, we obtain

$$F_x^{\text{capillary}} = 2\pi b\gamma\,\sin\beta\,\sin(\alpha-\lambda). \tag{5.11.37}$$

Vertical force balance

Now substituting into the force equilibrium equation

$$F_x^{\text{buoyancy}} + F_x^{\text{capillary}} = W \tag{5.11.38}$$

the expression

$$W = \frac{4\pi}{3} b^2 a \rho_s g \tag{5.11.39}$$

for the particle weight, and simplifying, we obtain the governing equation

$$\frac{x_c}{a}\,\sin^2\beta = \frac{2}{3}\,\cos^3\beta + \frac{2}{3}\,\kappa + 2\,\frac{\lambda^2}{ab}\,\sin\beta\,\sin(\alpha-\lambda). \tag{5.11.40}$$

In the case of a flat interface, $x_c = -a\cos\beta$, the expression for the buoyancy force simplifies to

$$F_x^{\text{buoyancy}} = \pi g b^2 a\,\Delta\rho\,\cos\beta\,\big(1-\tfrac{1}{3}\,\cos^2\beta\big) + \tfrac{4}{3}\pi g b^2\,a\,\overline{\rho}, \tag{5.11.41}$$

the contact angle is equal to the contact line aperture angle, $\alpha = \omega$, the capillary force vanishes, and the trigonometric equation (5.11.40) simplifies to (5.11.24).

The particle position and meniscus shape can be found by a modification of the method discussed previously in this section for a spherical particle (Problem 5.11.3).

Problems

5.11.1 *Flat interface*

Prove that a solution of (5.11.24) for $\cos\beta$ in the admissible range $[-1,1]$ exists only when $|\kappa| < 1$.

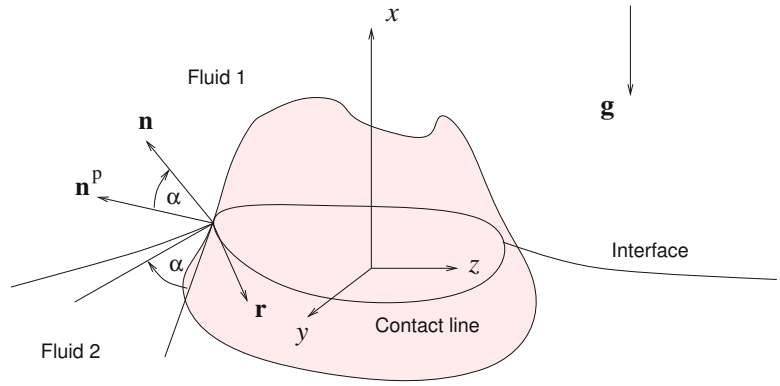

Figure 5.12.1 Illustration of a three-dimensional particle straddling the interface between two immiscible fluids.

5.11.2 *Floating position of a spherical particle*

Prepare the counterparts of the graphs shown in Figure 5.11.3 for $\kappa = 0.1$ and 0.9. Discuss the physical interpretation of the results.

5.11.3 *Spheroidal particle*

Modify the code given in the text for a spherical particle to compute the floating position of a spheroidal particle. Prepare the counterparts of the graphs shown in Figure 5.11.3 for particle aspect ratio $a/b = 0.5$ and 0.1.

5.12 A three-dimensional meniscus

Having discussed two-dimensional and axisymmetric interfacial configurations, now we consider a genuinely three-dimensional configuration with reference to the shape of a meniscus developing around a small particle with an arbitrary shape straddling the interface between two stationary immiscible fluids, as shown in Figure 5.12.1. The upper fluid is labeled 1 and the lower fluid is labeled 2. The fluids are assumed to be stably stratified, that is, $\rho_2 > \rho_1$ or $\Delta\rho \equiv \rho_2 - \rho_1 > 0$.

The interface meets the particle around a closed contact line and becomes horizontal far from the contact line. The contact angle, α, is given by

$$\alpha = \arccos(\mathbf{n}^p \cdot \mathbf{n}), \tag{5.12.1}$$

where $0 < \alpha < \pi$, $\mathbf{n}^p$ is the unit vector normal to the particle, $\mathbf{n}$ is the unit vector normal to the interface, and the left-hand side is evaluated at a point $\mathbf{x}$ around the contact line.

Laplace–Young equation

The working Cartesian system is defined such that the x axis points against the acceleration of gravity and passes through a designated particle center. The shape of the interface can

be described by a function of two variables, y and z, as

$$x = \zeta(y, z). \tag{5.12.2}$$

Far from the particle, as y and z tend to infinity, the function ζ decays to zero, yielding a planar shape. The Laplace–Young equation requires that

$$2\,\kappa_m = -\frac{\zeta}{\lambda^2}, \tag{5.12.3}$$

where $\lambda^2 = \gamma/(\Delta\rho\, g)$ is the square of the capillary length, γ is the surface tension, g is the magnitude of the acceleration of gravity, and κ_m is the mean curvature reckoned to be positive when the interface is downward concave. the absence of a constant on the right-hand side of (5.12.3) guarantees that the mean curvature vanishes far from the contact line where ζ decays to zero.

Substituting into the Laplace–Young equation the expression for the mean curvature given in (4.4.15) with appropriate changes in the notation,

$$2\,\kappa_m = -\frac{(1+\zeta_z^2)\,\zeta_{yy} - 2\,\zeta_y\,\zeta_z\,\zeta_{yz} + (1+\zeta_y^2)\,\zeta_{zz}}{(1+\zeta_y^2+\zeta_z^2)^{3/2}}, \tag{5.12.4}$$

we derive a nonlinear partial differential equation,

$$\nabla^2\zeta + \zeta_z^2\,\zeta_{yy} - 2\,\zeta_y\,\zeta_z\,\zeta_{yz} + \zeta_y^2\,\zeta_{zz} - (1+|\boldsymbol{\nabla}\zeta|^2)^{3/2}\,\frac{\zeta}{\lambda^2} = 0, \tag{5.12.5}$$

where $\boldsymbol{\nabla}$ is the gradient and ∇^2 is the Laplacian operator in the yz plane, a subscript y denotes a partial derivative with respect to y, and a subscript z denotes a partial derivative with respect to z. We will assume that the elevation of the contact line around the contact line is specified in lieu of a Dirichlet boundary condition.

5.12.1 *Elliptic coordinates*

Consider a configuration where the projection of the contact line in the yz plane is an ellipse arising by rotating a circle, as shown in Figure 5.12.2(a). To solve equation (5.12.5) in the exterior of the ellipse, we introduce elliptic coordinates, (u, φ), defined by the conformal mapping function

$$y + \mathrm{i}\,z = A\,\sinh(u + \mathrm{i}\,\varphi), \tag{5.12.6}$$

where i is the imaginary unit, $\mathrm{i}^2 = -1$, and A is a real constant. Resolving the mapping function into its real and imaginary parts, we obtain

$$y = A\,\sinh u\cos\varphi, \qquad z = A\,\cosh u\sin\varphi. \tag{5.12.7}$$

The variable u ranges from a certain value u_0 around the ellipse to infinity far from the ellipse. The variable φ varies in the range $[0, 2\pi]$ around the contact line. Note that φ is *not* the meridional angle measured around the vertical x axis. As u tends to infinity,

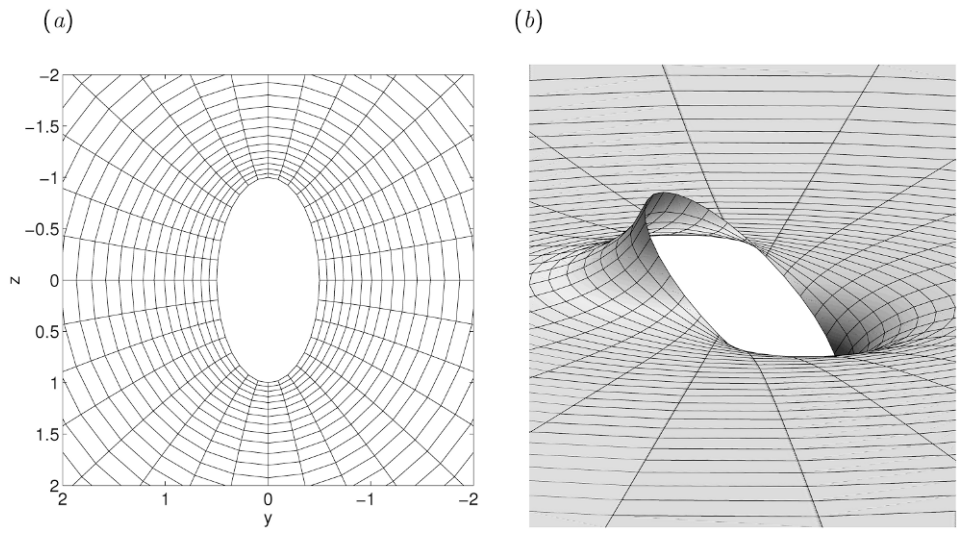

Figure 5.12.2 (*a*) Illustration of grid lines based on orthogonal elliptic coordinates. (*b*) Hydrostatic shape of a meniscus attached to a rotated circle computed in the elliptic coordinates.

the contour lines of constant u tend to become circles, as shown in Figure 5.12.2(*a*). The elliptic coordinates (u, φ) are orthogonal in the yz plane but not over the three-dimensional interface.

To accommodate the elliptical shape of the projection of the contact line onto the yz plane, we set

$$b = A \sinh u_0, \qquad c = A \cosh u_0, \tag{5.12.8}$$

where b and c are the ellipse semi-axes along the y and z axes. Solving for A and u_0, we find that

$$A = \frac{b}{\sinh u_0}, \qquad \tanh u_0 = \frac{b}{c}. \tag{5.12.9}$$

The magnitude of the gradient in the yz plane is given by

$$|\boldsymbol{\nabla}\zeta| = \frac{1}{h}\,|\widehat{\boldsymbol{\nabla}}\zeta| \tag{5.12.10}$$

and the Laplacian is given by

$$\nabla^2\zeta = \frac{1}{h^2}\,\widehat{\nabla}^2\zeta, \tag{5.12.11}$$

where a caret (hat) indicates differentiation with respect to the elliptic coordinates (u, φ), and h is the metric coefficient of the transformation given by

$$h = A\,|\cosh(u + \mathrm{i}\,\varphi)| = A\sqrt{\cosh^2 u - \sin^2 \varphi}. \tag{5.12.12}$$

The Laplace–Young equation (5.12.5) takes the form

$$\frac{1}{h^2}\,\widehat{\nabla}^2\zeta + \zeta_z^2\,\zeta_{yy} - 2\,\zeta_y\,\zeta_z\,\zeta_{yz} + \zeta_y^2\,\zeta_{zz} - (1+|\boldsymbol{\nabla}\zeta|^2)^{3/2}\,\frac{\zeta}{\lambda^2} = 0, \tag{5.12.13}$$

which can be regarded as a nonlinear Poisson-like equation, forced by an *a priori* unknown source term involving the interfacial elevation.

5.12.2 Finite-difference method

The solution of (5.12.13) can be found numerically using a finite-difference method in elliptic coordinates with evenly spaced grid lines. The second-order finite-difference representation of (5.12.13) at the (i,j) interior grid point in the $u\varphi$ plane is

$$\frac{1}{h_{i,j}^2}\left(\frac{\zeta_{i-1,j} - 2\,\zeta_{i,j} + \zeta_{i+1,j}}{\Delta u^2} + \frac{\zeta_{i,j-1} - 2\,\zeta_{i,j} + \zeta_{i,j+1}}{\Delta\varphi^2}\right)$$
$$+\Big(\,\zeta_z^2\,\zeta_{yy} - 2\,\zeta_y\,\zeta_z\,\zeta_{yz} + \zeta_y^2\,\zeta_{zz}\,\Big)_{i,j} - (1+|\nabla\zeta|^2)_{i,j}^{3/2}\,\frac{\zeta_{i,j}}{\lambda^2} = 0. \tag{5.12.14}$$

To implement Gauss–Seidel iterations, we rearrange to obtain

$$\zeta_{i,j} = \frac{1}{G}\left[\,\frac{1}{h_{i,j}^2}\left(\frac{\zeta_{i-1,j} + \zeta_{i+1,j}}{\Delta u^2} + \frac{\zeta_{i,j-1} + \zeta_{i,j+1}}{\Delta\varphi^2}\right)\right.$$
$$\left.+\Big(\,\zeta_z^2\,\zeta_{yy} - 2\,\zeta_y\,\zeta_z\,\zeta_{yz} + \zeta_y^2\,\zeta_{zz}\,\Big)_{i,j}\,\right], \tag{5.12.15}$$

where

$$G = \frac{2}{h_{i,j}^2}\left(\frac{1}{\Delta u^2} + \frac{1}{\Delta\varphi^2}\right) + \frac{1}{\lambda^2}\,(1+|\nabla\zeta|^2)_{i,j}^{3/2}. \tag{5.12.16}$$

The iterations proceed by guessing grid values, and then replacing the guesses with the right-hand side of (5.12.15) at each grid point.

The first derivatives of ζ with respect to y and z can be computed from derivatives with respect to u and φ by solving a system of 2×2 equations arising from the chain rule,

$$\begin{bmatrix} \partial y/\partial u & \partial z/\partial u \\ \partial y/\partial\varphi & \partial z/\partial\varphi \end{bmatrix}\begin{bmatrix} \partial\zeta/\partial y \\ \partial\zeta/\partial z \end{bmatrix} = \begin{bmatrix} \partial\zeta/\partial u \\ \partial\zeta/\partial\varphi \end{bmatrix}. \tag{5.12.17}$$

The derivatives with respect to u and φ on the right-hand side can be computed by numerical differentiation. The second derivatives can be computed by a similar method.

The numerical method is implemented in the following MATLAB code entitled *men_3d*, residing inside directory *03_hydrostat* of FDLIB:

```
%=================
% meniscus in the exterior of an ellipse
```

```
% in the yz plane
%=================

b = 0.5;
c = 1.0;
capl = 0.75;     % capillary length
xcline = 0.5;     % height of the contact line

tol = 0.000001;     % iteration tolerance
Niter = 1000;

%----------
% divisions
%----------

Nu = 32; Nphi = 32;

%---
% prepare
%---

Dphi = 2*pi/Nphi;
capls = capl*capl;
Dphi2 = 2.0*Dphi;
u0 = atanh(b/c);
snhu0 = sinh(u0);
cshu0 = cosh(u0);
A = b/snhu0;
umax = log(32.0*b/A);
Du = (umax-u0)/Nu;
Du2 = 2.0*Du;

%---
% grid
%---

for i=1:Nu+1
  u(i) = u0+(i-1)*Du;
  snhu(i) = sinh(u(i));
  cshu(i) = cosh(u(i));
  for j=1:Nphi+1
    phi(j) = (j-1)*Dphi;
    csphi(j) = cos(phi(j));
    snphi(j) = sin(phi(j));
    y(i,j) = A*snhu(i)*csphi(j);
    z(i,j) = A*cshu(i)*snphi(j);
    h(i,j) = A*sqrt(cshu(i)^2-snphi(j)^2);
  end
end
```

```
%---
% plot the grid
%---

figure(1)
hold on
axis square
axis([-2 2 -2 2 -2 2])
view(140,30)
xlabel('y','fontsize',15);
ylabel('z','fontsize',15);
zlabel('x','fontsize',15);
set(gca,'fontsize',15)

for i=1:Nu+1
  plot(y(i,:),z(i,:),'k')
end
for j=1:Nphi
  plot(y(:,j),z(:,j),'k')
end


%---
% initialize the interfacial elevation
%---

for i=1:Nu+1
  for j=1:Nphi+2
    x(i,j) = 0.0;
  end
end

%---
% boundary conditions
%---

for j=1:Nphi+1
  x(1,j) = xcline*y(1,j);
  x(Nu+1,j) = 0.0;
end

x(1,Nphi+2) = x(1,2);
x(Nu+1,Nphi+2) = 0.0;

%---
% iterations
%---
```

```
for iterations=1:Niter

%---
% compute the first derivatives:  dx/dy and dx/dz
%---

% interior nodes:

for i=2:Nu
  for j=2:Nphi+1
    MAT(1,1) = A*cshu(i)*csphi(j);
    MAT(1,2) = A*snhu(i)*snphi(j);
    MAT(2,1) = -A*snhu(i)*snphi(j);
    MAT(2,2) = A*cshu(i)*csphi(j);
    RHS(1) = (x(i+1,j)-x(i-1,j))/Du2;
    RHS(2) = (x(i,j+1)-x(i,j-1))/Dphi2;
    SOL = RHS/MAT';
    dxdy(i,j) = SOL(1);
    dxdz(i,j) = SOL(2);
  end
  dxdy(i,1) = dxdy(i,Nphi+1);
  dxdz(i,1) = dxdz(i,Nphi+1);
  dxdy(i,Nphi+2) = dxdy(i,2);
  dxdz(i,Nphi+2) = dxdz(i,2);
end

% boundary nodes by one-sided differences:

for j=1:Nphi+2
  dxdy(1,j) = 2.0*dxdy(2,j)-dxdy(3,j);
  dxdy(Nu+1,j) = 2.0*dxdy(Nu,j)-dxdy(Nu-1,j);
  dxdz(1,j) = 2.0*dxdz(2,j)-dxdz(3,j);
  dxdz(Nu+1,j) = 2.0*dxdz(Nu,j)-dxdz(Nu-1,j);
end

%---
% compute the second derivatives
%---

for i=2:Nu
  for j=2:Nphi+1
    MAT(1,1) = A*cshu(i)*csphi(j);
    MAT(1,2) = A*snhu(i)*snphi(j);
    MAT(2,1) = -A*snhu(i)*snphi(j);
    MAT(2,2) = A*cshu(i)*csphi(j);
    RHS(1) = (dxdy(i+1,j)-dxdy(i-1,j))/Du2;
    RHS(2) = (dxdy(i,j+1)-dxdy(i,j-1))/Dphi2;
      SOL = RHS/MAT';
    dxdyy(i,j) = SOL(1);
```

```
    dxdyz(i,j) = SOL(2);
    RHS(1) = (dxdz(i+1,j)-dxdz(i-1,j))/Du2;
    RHS(2) = (dxdy(i,j+1)-dxdy(i,j-1))/Dphi2;
      SOL = RHS/MAT';
    dxdyy(i,j) = SOL(1);
    dxdyz(i,j) = SOL(2);
    RHS(1) = (dxdz(i+1,j)-dxdz(i-1,j))/Du2;
    RHS(2) = (dxdz(i,j+1)-dxdz(i,j-1))/Dphi2;
      SOL = RHS/MAT';
    dxdzy(i,j) = SOL(1);
    dxdzz(i,j) = SOL(2);
  end
end

%------
% scan the grid points
%------

errr = 0.0;

for i=2:Nu
  for j=2:Nphi+1
    H = h(i,j); HS = H*H;
    tmp = 1.0+dxdy(i,j)^2+dxdz(i,j)^2;
    G = 2.0*(1.0/Du^2+1.0/Dphi^2)/HS + tmp^(3/2)/capls;
    xnew = (x(i+1,j)+x(i-1,j))/(HS*Du^2) ...
      +(x(i,j+1)+x(i,j-1))/(HS*Dphi^2);
    xnew = xnew + dxdz(i,j)^2 * dxdyy(i,j);
    xnew = xnew - 2.0*dxdy(i,j)*dxdz(i,j)*dxdyz(i,j);
    xnew = xnew + dxdy(i,j)^2 * dxdzz(i,j);
    xnew=xnew/G;
    corr = abs(xnew-x(i,j));
    x(i,j) = xnew;
    if(corr>errr) errr = corr; end
  end
end

for i=2:Nu+1
  x(i,1) = x(i,Nphi+1);
  x(i,Nphi+2) = x(i,2);
end

if(errr<tol) break; end

%--
end     % of iterations
%--

if(errr>tol)
```

```
  disp('the iterations did not converge')
  errr
  return
end

%---
% plotting
%---

figure(2)
hold on
xlabel('y','fontsize',15);
ylabel('z','fontsize',15);
zlabel('x','fontsize',15);
axis square
axis([-1 1 -1 1 -1 1])
view(162, 12)

for i=1:Nu
  for j=1:Nphi
    patch([y(i,j), y(i,j+1), y(i+1,j+1), y(i+1,j)], ...
      [z(i,j), z(i,j+1), z(i+1,j+1), z(i+1,j)], ...
      [x(i,j), x(i,j+1), x(i+1,j+1), x(i+1,j)], ...
      [x(i,j), x(i,j+1), x(i+1,j+1), x(i+1,j)]);
  end
end
```

A solution subject to the boundary condition for the contact angle elevation implemented in the code, reflecting a rotating circle, is shown in Figure 5.12.2(b).

5.12.3 Capillary force and torque

Surface tension pulls the particle around the contact line in a direction that is tangential to the interface and lies in a plane that is normal to the contact line at each point. The resultant capillary force is given by

$$\mathbf{F}^{\text{capillary}} = \gamma \oint \mathbf{r} \times \mathbf{n} \, \mathrm{d}\ell, \tag{5.12.18}$$

where $\mathbf{n}$ is the unit vector normal to the interface given by

$$\mathbf{n} = \frac{1}{\left| \dfrac{\partial \mathbf{x}}{\partial u} \times \dfrac{\partial \mathbf{x}}{\partial \varphi} \right|} \frac{\partial \mathbf{x}}{\partial u} \times \frac{\partial \mathbf{x}}{\partial \varphi}, \tag{5.12.19}$$

$\mathbf{r}$ is the unit vector tangential to the contact line, as shown in Figure 5.12.1, ℓ is the arc length around the contact line, and the integration is performed around the contact line.

The resultant capillary torque with respect to an arbitrary point, $\mathbf{x}_0$, is given by

$$\mathbf{T}^{\text{capillary}} = \gamma \oint (\mathbf{x} - \mathbf{x}_0) \times (\mathbf{r} \times \mathbf{n}) \, \mathrm{d}\ell. \tag{5.12.20}$$

Using a vector identity, we may express the capillary torque in the form

$$\mathbf{T}^{\text{capillary}} = \gamma \oint \Big([\,(\mathbf{x} - \mathbf{x}_0) \cdot \mathbf{n}\,]\,\mathbf{r} - [\,(\mathbf{x} - \mathbf{x}_0) \cdot \mathbf{r}\,]\,\mathbf{n} \Big) \, \mathrm{d}\ell. \tag{5.12.21}$$

Once the computation of the meniscus shape has been concluded, the capillary force and torque can be obtained using the following module:

```
%---
% compute dxdu, dxdphi,
% the surface normal and tension vector
% around the contact line
%---

x0 = 0.0; y0 = 0.0; z0 = 0.0;

for j=1:Nphi+1

  dxdu(j) = (-x(3,j)+4.0*x(2,j)-3.0*x(1,j))/Du2;
  dydu(j) = A*cshu0*csphi(j);
  dzdu(j) = A*snhu0*snphi(j);
  dmdu(j) = sqrt(dxdu(j)^2+dydu(j)^2+dzdu(j)^2);

  if(j==1)
    dxdphi(j) = (x(1,2)-x(1,Nphi))/Dphi2;
  else
    dxdphi(j) = (x(1,j+1)-x(1,j-1))/Dphi2;
  end

  dydphi(j) =-A*snhu0*snphi(j);
  dzdphi(j) = A*cshu0*csphi(j);
  dmdphi(j) = sqrt(dxdphi(j)^2+dydphi(j)^2+dzdphi(j)^2);
  vnx(j) = dydu(j)*dzdphi(j)-dzdu(j)*dydphi(j);
  vny(j) = dzdu(j)*dxdphi(j)-dxdu(j)*dzdphi(j);
  vnz(j) = dxdu(j)*dydphi(j)-dydu(j)*dxdphi(j);
  vnm(j) = sqrt(vnx(j)^2+ vny(j)^2+vnz(j)^2);
  vnx(j) = vnx(j)/vnm(j); vny(j) = vny(j)/vnm(j);
  vnz(j) = vnz(j)/vnm(j);
  tngx(j) = dydphi(j)*vnz(j)-dzdphi(j)*vny(j);
  tngy(j) = dzdphi(j)*vnx(j)-dxdphi(j)*vnz(j);
  tngz(j) = dxdphi(j)*vny(j)-dydphi(j)*vnx(j);
  crsx(j) = (y(1,j)-y0)*tngz(j)-(z(1,j)-z0)*tngy(j);
  crsy(j) = (z(1,j)-z0)*tngx(j)-(x(1,j)-x0)*tngz(j);
  crsz(j) = (x(1,j)-x0)*tngy(j)-(y(1,j)-y0)*tngx(j);
```

```
end

%---
% force and torque
%---

forcex = 0.0; forcey = 0.0; forcez = 0.0;
torqux = 0.0; torquy = 0.0; torquz = 0.0;

for j=1:Nphi
  forcex = forcex+tngx(j);
  forcey = forcey+tngy(j);
  forcez = forcez+tngz(j);
  torqux = torqux+crsx(j);
  torquy = torquy+crsy(j);
  torquz = torquz+crsz(j);
end

forcex = forcex*Dphi;
forcey = forcey*Dphi;
forcez = forcez*Dphi;
torqux = torqux*Dphi;
torquy = torquy*Dphi;
torquz = torquz*Dphi;
```

Problem

5.12.1 *Convergence of iterations*

Consider a meniscus originating from a horizontal elliptical contact line. Study the shape of the meniscus for several contact line elevations and capillary lengths. Investigate the convergence of the Gauss–Seidel iterations.